CHARACTERIZATION OF GAIT DEFICITS IN A MOUSE MODEL OF MULTIPLE SCLEROSIS

by

Maximillian D.J. Fiander

Submitted in partial fulfilment of the requirements
for the degree of Master of Science

at

Dalhousie University
Halifax, Nova Scotia
July 2016

Dedicated to my parents.

TABLE OF CONTENTS

LIST OF TABLES

LIST OF FIGURES

ABSTRACT

Neurological deficits in mice subjected to experimental autoimmune encephalomyelitis (EAE) are typically scored using a clinical scale (CS) with 5-10 levels of ascending paralysis and impaired gait. However, CS scoring is limited by yielding only ordinal data. This study therefore sought to characterize gait changes in EAE mice by kinematic gait analysis. Analysis of sagittal joint angles (hip, knee and ankle) during walking in EAE mice was performed. In general, there was a reduced range of motion and decreased average angle at the hip and knee joints. Deviation from normal gait was then quantified by calculating the root mean square (RMS) difference. Behavioural and kinematic parameters were then correlated with white matter loss in the lumbar spinal cord, revealing a remarkable correlation between ankle RMS difference and white matter loss ($r=0.96$). These findings indicate kinematic gait analysis is extremely sensitive to CNS histopathology and neurological deficits in EAE mice.

LIST OF ABBREVIATIONS AND SYMBOLS USED

ALS	Amyotrophic lateral sclerosis
ANOVA	Analysis of variance
CFA	Complete Freund's adjuvant
cm	Centimetre
CNS	Central nervous system
cm/s	Centimetres per second
CS	Clinical score
d	Difference
DPI	Days post-immunization
EAE	Experimental autoimmune encephalomyelitis
EDSS	Expanded disability status scale
GPS	Gait profile score
L2	Lumbar spinal cord vertebrae 2
L3	Lumbar spinal cord vertebrae 3
L4	Lumbar spinal cord vertebrae 4
L5	Lumbar spinal cord vertebrae 5
MBP	Myelin basic protein
mg	Milligram
ml	Millilitre
mm	millimetre
MOG	Myelin oligodendrocyte glycoprotein
MS	Multiple sclerosis
n	Sample size
NF	Normalized frame

ng	Nanogram
PBS	phosphate buffered saline
PFA	Paraformaldehyde
PLP	Proteolipid protein
PPMS	Primary progressive multiple sclerosis
PPV	Positive predictive value
PRMS	Progressive relapsing multiple sclerosis
PTX	Pertussis toxin
r	Pearson product-moment correlation coefficient
R^2	coefficient of determination
RMS	Root mean square difference
rpm	Rotations per minute
RR	Rotarod
RRMS	Relapse-remitting multiple sclerosis
s	Seconds
s.c.	Subcutaneous
SD	Standard deviation
SPMS	Secondary progressive multiple sclerosis
ug	Microgram
ul	Microlitre
WM	White matter
α	Type I error rate
ρ	Spearman's rank correlation coefficient
%	Percent
~	Approximately

↓	Decrease
↑	Increase

ACKNOWLEDGEMENTS

I owe so much to so many people that it's hard to fit it all in and to make sure no one is forgotten. First and foremost, thank you to my supervisor Dr. George Robertson. George— your passion and enthusiasm for science have inspired me. I deeply appreciate your dedication and generosity with your time for your students and I look forward to continuing our relationship over the coming years. I will never cease to be impressed by your intellectual rigor…or your abilities with PowerPoint animations. I have learned so much from you. Elizabeth—you were right, the acknowledgements are the hardest part. Thank you for teaching me when I dabbled in molecular and cell biology and thank you for your kindness and friendship. I will miss our Walking Dead discussions every Monday. Matt N.—thank you for being the go-to guy in the lab and for your willingness to help others. I'm always impressed by your encyclopedic knowledge of all things science and your work ethic. I've been fortunate to have you to look up to around the lab and I'm fortunate to call you a friend. Arul— we started at the lab together and I'm so glad we got to know one another. Thank you for sacrificing your holidays to help me with my experiments (…oh boy). Wishing you and Selva and baby Vetri (!) all the best. Jin—thanks you're your kindness and generosity. Good luck with your new job! To Dr. Turgay Akay, thank you for your willingness to collaborate and teach me. I have learned a lot from you and admire the thoughtful way that you approach science and also see the beauty in it. Having you tell me that my graphs made sense after my first couple of kinematic experiments is something that I am still proud of. Thanks also to the other members of the Akay lab, Brenda, Lauren, and William for equal parts putting up with me using your stuff, teaching me how to use your stuff, and for being friends. Jordan— I remember you going over the EAE protocol with me when I first started, and me getting totally lost. I'm very happy that that was just the beginning of our relationship. I admire your scientific mind, collaborative spirit, and fun-loving-ness. Thank you for being a friend/collaborator/mentor. We'll always have St. John's. On that note, thank you to Matty C., Alix, and A.C. for your friendship, teaching me some stuff, lending me a book, and for being chill friends I can always talk to. I'm looking forward to seeing the work you guys do. Thanks also to Scott and Elena for their help with my project. Thank you to Purnima for being patient with the whole Robertson lab and for your wisdom, kindness, and friendship. Thank you to the members of my advisory committee, Dr. Eileen Denovan-Wright and Dr. Jana Sawynok—I greatly value your advice and our conversations. Thank you to the members of my thesis committee, Dr. Turgay Akay and Dr. Jason McDougall. Thanks to all the members of the Pharmacology department. Your friendship and guidance have been so valuable to me during the course of my degree—thanks especially to Dr. Kishore Pasumarthi and Ms. Luisa Vaughn. Thank you to everybody that I'm fortunate enough to call a friend.

Most importantly, I would like to thank my family. Mom and dad, you have done so much to provide for me and support my efforts at school. Thank you for everything. To my siblings, I have enjoyed growing up with you and watching you grow up. I'm proud of you all and I'm so glad that we are friends. Siobhan, you have been my partner, confidante, and best friend. Thank you for your unwavering support and sacrifices you have made on my behalf. Thanks also for listening to me talk about oligodendrocytes and reading this thesis.

Finally, thanks to all of the mice that were used in my experiments. I hope there is lots of DietGel ™ in mouse heaven.

CHAPTER 1: INTRODUCTION

Multiple sclerosis (MS) is characterized by autoimmune-mediated demyelination in the central nervous system (CNS) resulting in fatigue, pain, vision problems, cognitive deficits, depression and debilitating motor impairments [1]. The most common mouse model of MS is experimental autoimmune encephalomyelitis (EAE). EAE has been used extensively to gain insights into MS disease mechanisms that have enabled the approval of several therapeutic treatments for this neurodegenerative disorder [2;3]. The primary behavioural measure of EAE disease severity is clinical scoring, a system that is based on the expanded disability status scale (EDSS) used to measure clinical disabilities in MS. However, the ordinal level of data yielded by clinical scoring and the potential for rater bias limit the value of this scale for accurately assessing EAE severity [3]. One recently suggested alternative is testing motor coordination in EAE mice by rotarod performance, a commonly used behavioural test for general motor function [4]. Gait deficits are one of the most common and disabling symptoms of MS that have been frequently studied to better understand the neurological bases for impaired locomotion in this neurodegenerative disorder [5]. Although gait analysis has been performed extensively in MS, these techniques have not been rigorously applied to the study of gait deficits in EAE mice. The aims of the present study were therefore to complete the following goals: (1) examine the relationship between clinical scores and rotarod performance, (2) characterize the gait deficits that occur longitudinally, (3) determine how gait changes with increasing clinical severity, and (4) assess which behavioural measures best correlate with spinal cord lesion volume in female C57Bl/6 mice subjected to EAE.

1.1 MULTIPLE SCLEROSIS INTRODUCTION AND PATHOPHYSIOLOGY

As of 2013, there were 2.3 million people with MS worldwide and the median global prevalence was 33 per 100,000. North America and parts of northern Europe have by far the highest prevalence, ranging from 100-400 per 100,000 [6]. At diagnosis, 85% of people have a form of MS that is characterized by acute attacks of increased inflammation and neurological impairment, or relapses, which are followed by resolution and decreased neurological impairments [7]. This form of MS is termed relapse-remitting MS (RRMS). Although there is a degree of recovery between relapses, over time the cumulative effect of the relapses is an increasing level of disability in RRMS [7]. Approximately 80% of people with RRMS eventually transition into secondary progressive MS (SPMS), a disease state that is characterized by a continuous and unrelenting increase of neurological disability despite the absence of relapses [8]. An estimated 15% of people diagnosed with MS have primary progressive (PPMS) or progressive relapsing (PRMS) forms of the disease which are characterized by steady functional decline from the outset either in the absence (PPMS) or presence (PRMS) or relapses [7].

There are currently 11 drugs approved by Health Canada for the treatment of RRMS. Although the mechanisms of action vary, all of these drugs target clinical relapses and can be classified as immunomodulatory or immunosuppressive [9]. Current MS drugs are effective at reducing relapse rate and accumulation of disability, however, the long-term benefits of first generation treatments like interferon-β and glatiramer acetate are modest and treatment compliance is often compromised by adverse side effects [10;11]. It is now clear that disease progression still occurs despite a reduction in relapses with these therapies [11;12]. This is likely because such immune-based therapies are unable

to halt the neurodegeneration mechanisms initiated by autoimmune-mediated demyelination that cause axonal loss and neuronal cell death resulting in permanent clinical disabilities [13]. As a result, the identification of compounds that prevent myelin loss, axonal injury and promote remyelination are of intense therapeutic interest in not only for MS but also in other demyelinating disorders [14].

Developing better therapeutic treatments for MS will be facilitated by an improved understanding of the neural-immune events responsible for demyelination, axonal damage and subsequent CNS repair. It is known that MS is a multi-factorial disease that likely results from complex genetic and environmental interactions, but precisely how these factors come together to cause MS is not clearly understood [15]. Similarly, the exact pathogenesis of MS is unknown but some basic mechanisms are agreed upon. The first event is infiltration of autoreactive lymphocytes and macrophages into the CNS by traversing the blood brain barrier [8]. These infiltrating cells form perivascular cuffs in the CNS parenchyma where they release destructive pro-inflammatory cytokines as well as reactive oxygen and nitrogen species that cause demyelination, axonal transection, gliosis and microglial activation [8]. The functional consequence of these lesions is impaired action potential propagation that decreases signal fidelity in many neural networks implicated in movement, sensation, affect and cognition, for example [16].

1.2 EXPERIMENTAL AUTOIMMUNE ENCEPHALOMYELITIS (EAE)

EAE has become the most widely used animal model for MS since it was described by Rivers et al. in 1933 [17]. It is an experimentally-induced inflammatory demyelinating disease that shares many of the mechanistic and pathological hallmarks of MS [3]. EAE is induced by immunization with a CNS antigen that results in an immune

response against the CNS. EAE is most commonly induced in mice using myelin antigens like myelin oligodendrocyte glycoprotein (MOG), myelin basic protein (MBP) or proteolipid protein (PLP) [18]. Depending on the mouse strain and antigen, the clinical and histopathological phenotype varies substantially and can be used to study different aspects of MS. Immunization of C57Bl/6 mice with MOG residues 35-55 (MOG_{35-55}), for example, results in a monophasic autoimmune attack that is characterized by an ascending paralysis that progresses from the tail to the hindlimbs and then to the forelimbs in the most severe of cases resulting in pronounced locomotor deficits that recover to a limited degree [18]. By contrast, clinical scores suggest that immunization of SJL mice with PLP residues 139-151 results in a relapse-remitting disease course in which near complete recovery occurs after the first disease episode (relapse) [18]. EAE in C57Bl/6 mice induced with MOG_{35-55} is the most commonly used strain-antigen combination because of the availability of transgenic mice on this genetic background [18].

The EAE model has played an important role in the development and validation of several currently approved treatments for MS: glatiramer acetate, mitoxantrone, natalizumab, and fingolimod [2;17;19]. However, there have been criticisms of EAE as a model for MS. Most of these criticisms are based on differences in some aspects of the immunological mechanisms in EAE and MS, as well as in the discrepancy between the vast number of compounds that have been shown to reduce EAE disease severity and the relative dearth of drugs that actually show clinical efficacy in treatment of this complex neurodegenerative disorder [3;20]. One point that has been addressed in only a limited fashion is how well EAE recapitulates behavioural, or symptomatic, aspects of MS.

1.3 ASSESSING NEUROLOGICAL DISABILITY IN EAE: THE NEED FOR QUANTITATIVE MEASURES OF MOTOR DYSFUNCTION

MS has an extremely variable disease course and clinical presentation that may reflect the random dissemination of lesions within the CNS [21]. Clinical disability in people with MS is typically assessed using the EDSS, which is a scale ranging from 0 to 10, with increasing EDSS scores being indicative of greater levels of disability [22]. Each EDSS level is based on the symptoms presented and their severity. Similarly, the primary experimental outcomes of most EAE studies are clinical scores assigned to mice by the experimenter. Clinical scoring of EAE mice is analogous to the use of the EDSS in MS. Clinical scoring systems for EAE vary between groups but the most common is a 6 point scale that ranges from 0 to 5, with 0 being a mouse with no signs of EAE and 5 being a mouse that is moribund, or dying from the disease [3]. Many groups, including ours, have developed a more detailed scale (11 points) based on the same principles, with the intent of increasing the sensitivity of the scale [23-25]. Clinical scoring is quick and convenient, and thus can be done daily to monitor disease severity in each animal.

However, the practice of scoring mice for neurological disability in this manner has several important limitations. First, the clinical scoring scales are ordinal in nature, meaning that although the intervals on the scale are not numerically equivalent (i.e. 2,3,4), thus the biological differences between the symptoms that characterize each clinical score are unknown and not necessarily equivalent [26]. The ordinal nature of the data also means that it must be handled differently from ratio data, an important point that is often overlooked in the statistical analysis of clinical scores [26]. A second limitation to clinical scoring is that it provides only qualitative descriptions of the mice, based on either the presence or absence of certain symptoms, meaning that it lacks the

necessary sensitivity to detect subtle changes. Finally, rater subjectivity and lack of standardization between laboratories may contribute to variations in clinical scoring using the same EAE model. One meta-analysis examining 126 papers that were studying the effects of putative therapeutic interventions in EAE, found 82 unique scoring systems [20;26]. This lack of standardization makes comparisons of clinical score data between studies difficult. It also raises the possibility that if suboptimal scoring systems are being utilized, important information about disease severity may be missed.

Despite these limitations, clinical scoring is often the only behavioural measure in most EAE studies. Of the approximately 11,000 scientific papers published on EAE in PubMed, only a handful addressed the animals' behaviour beyond clinical scores. This is not the case with other mouse models of neurological diseases that result in motor deficits. Extensive analysis of motor deficits has been performed using mouse models of Parkinson's disease, Huntington's disease, amyotrophic lateral sclerosis (ALS), Alzheimer's disease, stroke and spinal cord injury. [27-32]. The application of more sophisticated behavioural analysis to the EAE field offers three main benefits: (1) a better understanding of the relationship between functional deficits and the underlying CNS lesion, (2) more sensitivity in the detection and description of functional recovery or neurological worsening, and (3) a surrogate measure for the fidelity of neural networks that mediate behaviour [33]. Quantitative ways to assess various aspects of motor and sensory function in EAE mice would therefore offer substantial improvements over clinical scoring.

1.4 THE APPLICATION AND LIMITATIONS OF ROTAROD IN EAE STUDIES

The most commonly used behavioural test to measure motor disability in EAE besides clinical scoring is the rotarod, which has been gaining popularity in the EAE field over the last number of years [34]. It is a widely used behavioural test that assesses general motor function in which mice are placed on a rotating rod and the latency to fall off the rod is recorded [35;36]. The inference is that the longer the mouse stays on the rod, the better its motor function. Rotarod performance is sensitive to deficits in motor coordination, motor learning, fatigue, sensation, cardiopulmonary endurance and lesions to motor areas of the CNS such as the spinal cord, basal ganglia, cerebellum and motor cortex [37-39]. Rotarod testing offers several advantages over clinical scoring including its objectivity and the fact that this behavioural assay yields ratio level data. In the EAE field, rotarod testing has been employed to validate new EAE models [40], to examine basic disease mechanisms [41], and to examine the behavioural impact of various pharmacological interventions [42-48].

Recently, van den Berg et al. characterized rotarod performance in C57Bl/6 mice immunized with MOG_{35-55} and advocated for more widespread usage of the rotarod in EAE studies, citing its correlation with clinical scores and histopathology [4]. One finding was that rotarod performance declined rapidly over a small range of clinical scores ranging from 1.5 to 2.5 (out of 5.0). One of the implications of this finding that was not discussed by the authors was that rotarod test is only sensitive to alterations in performance within a small range of clinical scores. This suggests that changes in motor co-ordination for mildly and severely sick animals may not be detected with this test.

A general limitation of the rotarod is that there are a number of determinants of performance on this test including fatigue, muscle weakness, lack of motor coordination, impairments in motor learning and memory, and sensory and vestibular impairment. Consequently, it is difficult to attribute changes in rotarod performance to a specific CNS mechanism. For example, a mouse with paralyzed hindlimbs but strong forelimbs may be able to stay on the rod for a similar amount of time as an animal with severe vestibular problems. The test is also limited by non-physiological test conditions; rotarod impairment does not necessarily translate to functional impairment for a mouse [49]. Finally, motivational factors can confound attempts to measure motor performance [49]. In conclusion, although rotarod is a valuable tool in assessing motor dysfunction in EAE animals, a more precise description of how the animals are actually moving could be more sensitive to subtle changes at all levels of clinical disability.

1.5 GAIT CHANGES AS MARKERS OF CNS DAMAGE IN EAE

Compared to other behavioural measures used in animal studies, gait analysis is unique in that gait is a fundamental physiological mechanism of movement, generated by specific neural circuits, known to be impaired in MS [49]. Gait analysis has been widely employed in mouse and rat models of neurological disease to understand the spinal control of gait. Traditionally, gait analysis has focused on foot placements either by analyzing paw prints made on paper or with ventral plane videos, despite evidence that the kinematic analysis of limb movements in the sagittal plane is a more sensitive and reliable method for detecting changes in gait [49-52].

Impaired walking ability and the resultant decrease in mobility is the most common and disabling symptoms of MS, occurring in 75% of people with MS over the

course of their disease [53;54]. Many of the moderate to high EDSS scores are biased towards mobility impairment, with 4.0 representing the onset of significant gait deficits, 6.0 representing an inability to walk without assistance, and 7.0 indicating that the person is wheelchair-bound. However, like clinical scoring, the EDSS provides very limited information about how gait is actually changing [22]. Changes in gait are important because they may be clinically relevant to patients (i.e. by increasing the risk of falls, decreasing walking speed and endurance, etc.) and may also reflect changes in disease state. Consequently, gait analysis in MS has been used to detect pre-clinical changes in gait, determine the efficacy of interventions intended to improve gait (e.g. pharmacological, orthotic braces, stretching, exercise), and to help healthcare providers identify impairments and target treatments to areas of the body requiring support [5;55].

Gait analysis in EAE studies, on the other hand, is extremely rare. One group published two papers in the mid-1990s that employed inked footprint analysis of EAE induced in Lewis rats [56;57]. Since then gait analysis has been largely ignored in the EAE field, even in discussions of behavioural testing strategies in EAE studies [3]. With the recent growth in EAE behavioural studies, three papers have addressed some aspects of gait abnormalities in EAE mice [58-60]. However, gait analysis performed in EAE studies to date has been very limited. These studies have shown the following: First, stride length is decreased in Lewis rats passively induced with EAE, C57Bl/6 mice immunized with MOG_{35-55}, and SJL mice immunized with $PLP_{139-151}$ in remission [45;56-59]. Second, paw contact area with the ground and gait regularity are decreased, while the hindlimb base of support is increased in C57Bl/6 mice immunized with MOG_{35-55} [45;60]. Third, the distance from the tip of the tail to the ground is reduced in SJL mice immunized with $PLP_{139-151}$ in remission [58]. Therefore, there is currently very little information about how gait changes in animals with EAE. Most of the information

described in the literature corresponds to spatio-temporal parameters of gait and there is no information on limb kinematics in the sagittal plane.

1.6 RATIONALE

Improved behavioural testing strategies in EAE research have the potential to improve the translation of findings from EAE studies to help people with MS. Rotarod has been used with increasing frequency and has utility as a general measure of motor function but has limitations. Gait analysis techniques have been applied to study walking deficits in people with MS but the knowledge of gait impairment in EAE mice is extremely limited. Furthermore, there are no descriptions of changes in kinematic gait analysis in the sagittal plane in EAE mice in the literature. A better understanding of gait changes in EAE animals could: (1) improve our understanding of EAE as a model for MS by enabling comparison of gait changes in the two diseases, (2) facilitate the discovery of new therapeutic targets by yielding insights into the mechanisms of motor dysfunction in EAE and MS, (3) enhance sensitivity to detect the effects of putative new therapeutics or other interventions, and (4) allow the assessment of symptomatic treatments designed to improve gait without treating the underlying disease.

The aims of the present study were fourfold. First, the study aimed to examine the relationship between clinical scores and rotarod performance. Rotarod performance has recently been characterized in C57Bl/6-MOG_{35-55} EAE mice and put forth as a new standard behavioural test in EAE studies [4]. The first experiment attempted to replicate these findings and examine how rotarod performance correlated with clinical scores at different stages of disease. The second and third aims of this study were to characterize the gait deficits that occur in EAE mice over time and to define changes in gait according

to clinical score. To this end, mildly and severely sick EAE mice were recorded walking on a treadmill and analyzed at weekly time points. Changes in gait kinematics were assessed longitudinally over the course of the experiment and according to clinical score to assess how gait changes with increasing disease severity. The last aim was to assess which behavioural measures best correlated with histopathological changes in this model of EAE. This was done by correlating the behavioural measures obtained at the last experimental time point with white matter loss in the spinal cord.

Although the present experiments were largely exploratory, I hypothesized that (1) kinematic gait analysis would yield more detailed and precise information about the nature of motor disabilities in EAE mice than rotarod testing or clinical scores, and that (2) changes in kinematic gait parameters would better correlate with histopathology in the spinal cord.

CHAPTER 2: MATERIALS AND METHODS

2.1 ANIMAL CARE

All experiments were done in accordance with the Canadian Council on Animal Care guidelines and were approved by the Dalhousie University Committee on Laboratory Animals. Mice were housed in the Life Science Research Institute Animal Care Facility on a 12-hour light/dark cycle (light from 07:00 to 19:00). Food and water was provided ad libitum.

2.2 EXPERIMENTAL AUTOIMMUNE ENCEPHALOMYELITIS

C57BL/6 mice were obtained from Charles River Canada (St. Constant, QC) and were allowed to habituate to the facility for seven days before experiments commenced. Ten week-old female mice were either immunized with amino acids 35 to 55 (MEVGWYRSPFSRVVHLYRNGK) of myelin oligodendrocyte glycoprotein (MOG_{35-55}) to induce EAE (EAE condition), or were given a sham immunization with complete Freund's adjuvant (CFA; CFA condition). The mice in the CFA condition did not develop EAE and served as antigen controls. Mice were randomly assigned to either the CFA or EAE condition. The average weight and rotarod performance (described below) prior to immunization were the same for the CFA and EAE groups.

To induce EAE, MOG_{35-55} (Gen Script, Piscataway, NJ, USA) was dissolved in sterile phosphate buffered saline (PBS; pH = 7.4) at a concentration of 3 mg/ml and emulsified in a 1:1 ratio with complete Freund's adjuvant (CFA). CFA was made by mixing incomplete Freund's adjuvant (Difco Laboratories, Detroit, MI, USA) with heat-

killed Mycobacterium tuberculosis H37RA (Difco Laboratories, Detroit, MI, USA) at a 10 mg/ml concentration. On day 0 of experiments, the MOG_{35-55}/CFA emulsion was delivered via two subcutaneous (s.c.) injections (100 µl/ injection) on both sides of the base of the tail so that each mouse received a total of 300 µg MOG_{35-55}. The mice that received this treatment developed EAE are henceforth designated as EAE mice. For the sham immunization, PBS and CFA were emulsified in a 1:1 ratio and this mixture was delivered via s.c. injection in the same manner as described above for the EAE mice. The mice that received CFA without antigen did not develop EAE and are hereafter referred to as CFA mice.

Additionally, all mice were dosed with pertussis toxin (PTX; Sigma, St. Louis, MO, USA) on the day of immunization (day 0) and 2 days post-immunization (DPI). Each injection consisted of a 200 µl intraperitoneal injection of PTX (1.5 µg/ml) such that each mouse received 300 ng PTX per injection.

2.3 CLINICAL SCORING

Beginning on DPI 7, mice were weighed and scored daily for clinical signs of EAE. The following 11-point ordinal scale was used by two trained experimenters, blind to experimental conditions, to assess motor deficits: 0, no motor deficits; 0.5, hooked tail; 1.0, fully flaccid tail; 1.5, hindlimb splay; 2.0, minor walking deficits characterized by general weakness in the lower body, mild loss of coordination (manifest in an uneven gait or waddling); 2.5, major walking deficits characterized by extreme weakness and swaying of the lower body as well as paraparesis; 3.0, dropped pelvis characterized by an inability of the hindlimbs to raise the pelvis from the ground; 3.5, unilateral hindlimb

paralysis; 4.0, bilateral hindlimb paralysis; 4.5, forelimb paralysis; and 5.0, moribund (Table 1).

2.4 CARE OF EAE MICE

Upon disease onset, all mice were given access to mash and Dietgel Recovery (ClearH2O, Westbrook, ME, USA**)**. Handfeeding with DietGel Boost (ClearH2O) and s.c. injection of 0.9% sodium chloride solution were performed as necessary. A humane end-point was reached when: 1) weight loss exceeded 20% of a mouse's starting weight, 2) if a mouse reached a clinical score of 5, 3) if a mouse was unable to right itself, or 4) exhibited total loss of ability to access food and water for 24 hours.

2.5 ASSESSMENT OF ROTAROD PERFORMANCE

All rotarod testing was performed by an experimenter blind to experimental conditions. The rotarod apparatus (Ugo Basile, VA. Italy) consisted of a rod (3cm in diameter) with 6 flanges at intervals allowing up to 5 mice to be tested simultaneously. The speed of the rod accelerated in a linear manner from 4 to 40 rotations per minute (rpm) over 300 seconds (s). The latency for each mouse to fall off the rod was recorded in seconds. A mouse that did not fall from the rotating rod during this interval was assigned a latency of 300 s. A mouse that was completely unable to balance on the rod due to severe paralysis was assigned a latency of 0 s. It has been reported that mice will sometimes hold on to the bar without walking as it rotates, i.e. passively rotate for long durations, thereby introducing a confound to the experiment; however, this phenomenon was not observed in the present experiments. All testing sessions were done at the

Table 1: EAE clinical scoring scale. Mice were assessed daily for clinical scores.

Clinical Score	Description
0.0	No motor deficits
0.5	**Hooked tail**
1.0	Fully flaccid tail or partially flaccid tail with splay
1.5	**Hindlimb splay with fully flaccid tail**
2.0	Minor walking deficits characterized by general weakness in the lower body, mild loss of coordination (manifest in an uneven gait or waddling);
2.5	**Major walking deficits characterized by extreme weakness and swaying of the lower body as well as paraparesis**
3.0	Dropped pelvis characterized by an inability of the hindlimbs to raise the pelvis from the ground
3.5	**Unilateral hindlimb paralysis**
4.0	Bilateral hindlimb paralysis
4.5	**Forelimb paralysis;**
5.0	Moribund

same time of day, and prior to each rotarod session, mice were habituated to the room containing the rotarod for 20 minutes. For each day of rotarod testing or training, mice were given 3 trials on the rotarod separated by an inter-trial interval of 30 minutes to minimize the effect of fatigue. The mean of the three trials was taken as the mouse's latency for that day and used in analysis. All mice were pre-trained for four consecutive days prior to DPI 0 in order for their performance to reach a baseline that was near-maximal latency. Subsequently, mice were tested weekly on the rotarod beginning on DPI 9 until the end of the experiment.

2.6 TREADMILL RECORDING

Mice were recorded walking on a treadmill to measure the kinematic parameters of their gait. Two baseline recording sessions were performed prior to any immunization procedures to establish inter-session variability. Following immunization, mice were recorded while walking on the treadmill at weekly intervals within 24 hours of rotarod testing (i.e. DPI 9, 16, 23, etc.) until the end of the experiment. To track the movements of the various segments of the leg during walking, reflective markers were attached to the right hind limb as described previously [61]. Mice were first anaesthetized with 2% isoflurane and the right hindlimb was shaved. Next, custom-made three-dimensional markers (2 mm diameter) were attached to the shaved skin at five points on the leg with super glue (Lepage): the iliac crest, the femoral head (hip joint), the ankle joint, the metatarsophalangeal joint (paw), and the tip of the fourth digit (Figure 1A). As markers placed over the knee joint are inaccurate due to skin slippage, the location of the knee was triangulated at later stages of data analysis based on the positions of the hip and ankle joint markers and using the lengths of the femur and tibia, which were measured for each mouse.

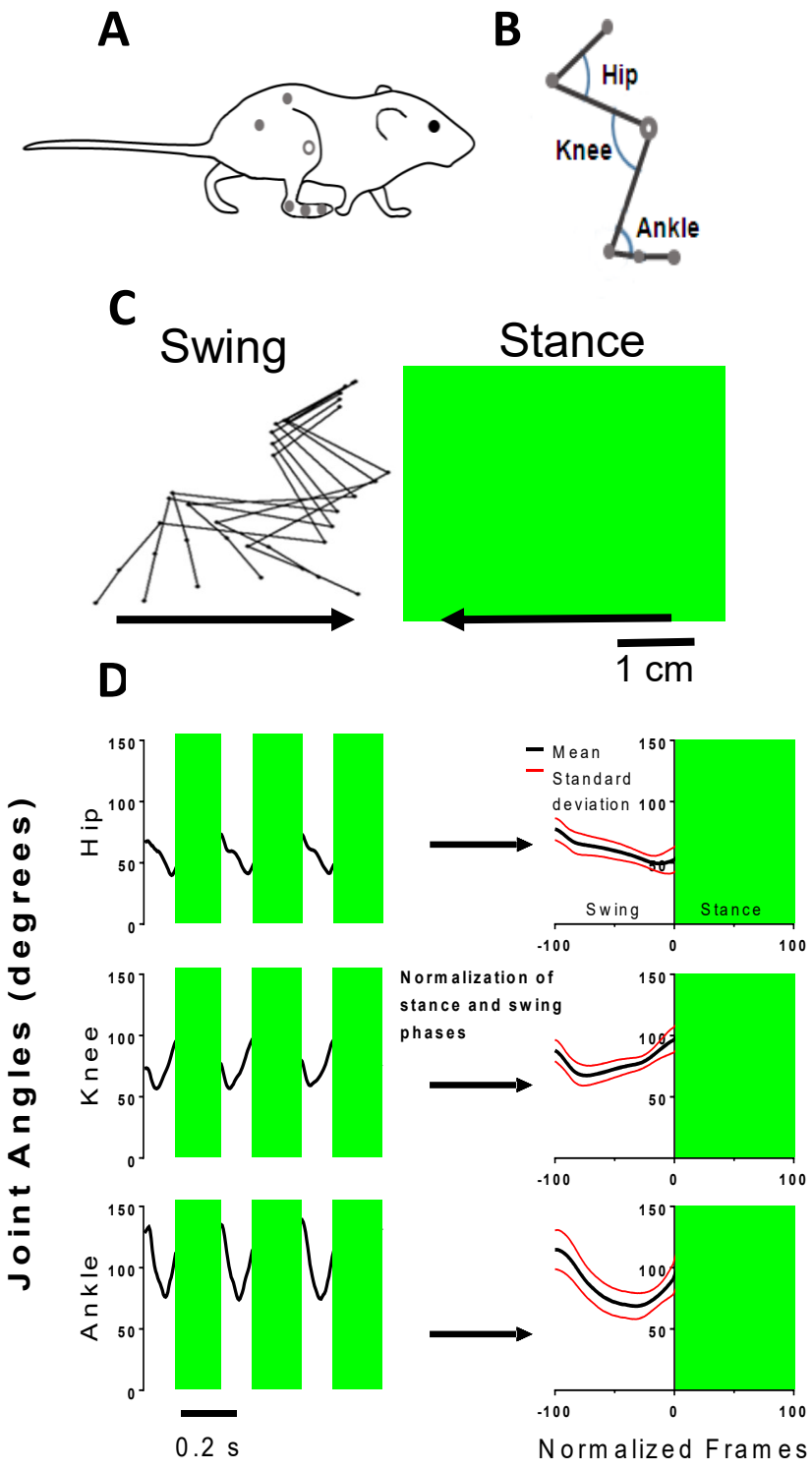
A
B
Hip
Knee
Ankle
C
Swing
Stance
1 cm
D
Joint Angles (degrees)
Hip
Knee
Ankle
150
100
50
0
Mean
Standard deviation
Swing
Stance
-100
0
100
Normalization of stance and swing phases
0.2 s
Normalized Frames

Figure 1: Basis for kinematic recording and data analysis. **(A)** Reflective markers were attached to five anatomical points on each mouse: the iliac crest, hip joint, ankle joint, metatarsophalangeal joint, and tip of the second digit. The markers were tracked to obtain X,Y coordinates for the recording. The location of the knee joint was calculated by triangulation from the hip and ankle markers. **(B)** X,Y coordinates of the six points used to construct a stick model of the leg from which the joint angles and other kinematic data that was extracted. **(C)** Stick models of the leg during swing (white background) and stance phases (green background) of the step cycle. **(D)** Representative angular movements for the hip, knee and ankle joints over three step cycles for one mouse. Swing and stance phases are shown with white and green backgrounds, respectively. Data from multiple step cycles were normalized such that the duration of each phase is 100 normalized frames (NF) and the total step cycle is 200 NF. The average values for all swing and stance phases were calculated, yielding average waveforms of the step cycle of each mouse which were the basis for further analysis.

The mice were then placed on a treadmill (University of Cologne) and given 5 minutes to recover from anaesthesia. Once the animals had recovered, they were required to walk at a speed imposed by the treadmill belt. A high-speed camera (250 frames per second; Fastec IL3-100, San Diego, CA, USA) was used to record the animals from the side while they were walking steadily for 10-12 step cycles.

As the quality of the recordings varied depending on the speed imposed by the treadmill and the health status of the animals, several different treadmill speeds were used in this study. Only video recordings of optimal quality were used in data analysis, and optimal recordings were ones that featured mice that walked steadily. Behaviours such as (1) lagging to the back of the treadmill, followed by running back to the front, only to lag to the back again, (2) rearing on hindlimbs, and (3) swaying from side to side on the treadmill belt can reduce the quality of the data, and render interpretation difficult or impossible. Healthy C57BL/6 mice walked most steadily at a speed of 20 centimetres per second (cm/s) and at lower speeds displayed behaviours reduced recording quality much more frequently. Therefore healthy mice were recorded walking at 20 cm/s. Mice with EAE, on the other hand, were often unable to keep up with the treadmill at 20 cm/s and were therefore assessed at lower treadmill speeds of 15 or 10 cm/s. Treadmill speeds lower than 10 cm/s were used, albeit very rarely. The use of different speeds was incorporated because although spatio-temporal parameters of gait like stride length and time spent in stance phase are highly dependent on walking speed, the kinematic parameters measured in this study are only weakly correlated with speed [62;63].

2.7 ANALYSIS OF TREADMILL RECORDINGS

2.7.1 DIGITIZING MARKER MOVEMENTS

The videos of the mice walking were analyzed using scripts for ImageJ (KinemaJ) and R (KinemaR) developed by Dr. Nicolas Stifani for the purpose of analyzing kinematic experiments [64;65]. Videos were digitized by KinemaJ. Briefly, the intensity threshold was adjusted for each video so that only the reflective markers were visible. This resulted in a video in which only the five markers on the animal's leg were visible in each frame. The X and Y coordinates, in pixels, of these markers were then tracked frame by frame for the duration of the recording, allowing stick model reconstructions of the leg to be made (Figure 1B,C).

2.7.2 DATA TRANSFORMATION AND EXTRACTION OF KINEMATIC DATA

After digitizing the videos, the data was processed using KinemaR. Pixel values were transformed to centimeter (cm) values to avoid variations in measurements resulting from differences in the position and angle of the camera relative to the treadmill for each recording. This was done by recording brief (~ 1 second) videos of four reflective markers arranged in a rectangle 4 cm in height by 7 cm in width under the same conditions as those used to record mouse walking. These calibration videos were taken on each day of recording. In analysis, KinemaJ was used to calculate the conversion coefficient for the transformation of pixels to cm. KinemaR then transformed the data to cm based on the conversion coefficient derived from the calibration videos. From the transformed coordinates of the five markers on the mouse's leg, the location of the knee joint was triangulated based on the measured lengths of the femur and tibia.

The kinematic data describing the angular excursions of the hip, knee and ankle joints as well as the two-dimensional coordinates of each marker were also extracted (Figure 1D, left side).

2.7.3 PHASE DETECTION

The swing and stance phases of the step cycle were then detected by KinemaR based on the movements of the toe marker along the X-axis. Since the mice were walking on a treadmill, the stance phase was defined by movement in a negative direction as the treadmill belt carried the limb back. Swing phase was characterized by movement in the positive direction as the animal moved the hind leg forward. The onset of the swing phase was therefore defined as the transition from movement in a negative direction to movement in a positive direction, or the time at which a local minimum on the X-axis is reached. The converse logic was used to define the stance phase, which was defined as when a local maximum on the X-axis was reached, marking the transition from movement in the positive direction to movement in a negative direction. The duration of each detected phase was calculated based on the number of frames, where each frame of the 250 Hz recording represented 4 milliseconds.

2.7.4 NORMALIZATION OF PHASE DURATION

In order to account for the differences in animal walking speeds and to calculate the average step cycle (described below), the swing and stance phases of each step cycle were normalized to 100 frames respectively by KinemaR. Swing phases were labelled with normalized frame (NF) numbers ranging from -100 to -1, and stance

phases were labelled with NF numbers from 1 to 100. Each normalized step cycle was therefore 200 NF.

2.7.5 WAVEFORM AVERAGES OF STEP CYCLES

Averaging the 10-12 steps in each recording yields an average step cycle that is representative of how the mouse walked in that recording. Using normalized data is necessary as slight differences in the duration of step cycles can confound attempts to average step cycles. Therefore, for each video, a waveform average of the step cycle and the component stance and swing phases was calculated by KinemaR using the phase normalized data. The average and standard deviation were calculated for joint angles and X and Y coordinates at each of the 200 NF of each step cycle (Figure 1D, right side). For example, if a mouse took 10 steps in a recording, the values of the kinematic parameter at NF -100 for each of the 10 steps were averaged to calculate the value seen at -100 in the average step cycle. The same process was repeated for NF -99, -98, etc. The average step cycles for each video were thus generated and used as the basis for further analysis.

2.8 HISTOLOGY

All mice were anaesthetized with Euthansol (200µl, intraperitoneal, 34 mg/ml; Schering Canada, Pointe-Claire, Quebec) and transcardially perfused with PBS (5ml) and 4% paraformaldehyde (PFA; 5ml). Spinal cords were dissected and post-fixed in 4% PFA for 24 hours before being cryoprotected in 30% sucrose for 48 hours. Three spinal cord segments from the second to fifth lumbar vertebrae (L2, L3-4, and L5) were dissected and frozen in optimum cutting temperature tissue-tek (Sakura Finetek, USA).

The frozen spinal cord segments were serially cut into 30 μm coronal sections using a cryostat (Leica CM1950). For histochemical staining, all sections underwent serial rehydration by being passed through xylene, followed by descending concentrations of ethanol (100% to 75%) before being incubated in a water bath. They were then stained with eriochrome cyanine (Sigma Aldrich) for 15 minutes and differentiated for 3 s in a 1% ammonium hydroxide solution. The sections were then counterstained with neutral red (Acros Organics) for 2 minutes and dehydrated in an ascending ethanol series, followed by two washes in xylene.

2.9 QUANTITATIVE IMAGE ANALYSIS

Slides were imaged using Aperio AT2 (Leica Biosystems, Ontario, Canada) slide scanner and analyzed using Aperio ImageScope (Leica Biosystems). White matter lesion area were defined as loss of eriochrome cyanine staining, with or without the presence of cellular infiltrates shown by neutral red [4]. White matter lesions were traced by an observer blind to experimental conditions and the area was calculated for two representative sections from each lumbar segment (i.e. L2, L3-4, and L5); overall, six lumbar sections were analyzed per mouse. For each section, the summed lesion area was divided by the total white matter area and multiplied by 100 to yield a percent of white matter affected by lesions. The average percent white matter loss of the six sections was calculated and used in data analysis.

2.10 DATA ANALYSES

Both statistical analysis and figure production were completed using Graph Pad Prism 6.07 (GraphPad Software, San Diego, CA). Excel (Microsoft), Aperio Imagescope

(Leica), ImageJ, and R were also used in the processing, analysis, and management of data. An α level of 0.05 was used as the threshold for significance on all statistical tests. All results are reported as mean ± SD, unless otherwise indicated. Differences between clinical scores of CFA and EAE groups were statistically analyzed using the non-parametric Wilcoxon matched-pairs signed rank test. The effect of experimental condition, time, and an interaction between those two factors on rotarod performance was analyzed using a two-way repeated measures analysis of variance (ANOVA). Sidak's multiple comparisons test was used for post hoc analyses of differences between experimental conditions at each time point. Linear relationships between continuous variables were assessed by performing Pearson product-moment correlations, yielding Pearson's r (r). Because clinical scoring produces ordinal data, the non-parametric Spearman's rank-order correlation was performed and Spearman's rho (ρ) was calculated. Correlation significance was assessed by the p value and correlation strength was assessed by the correlation coefficients according to the levels proposed by Evans: $r < 0.2$ = very weak; $0.2 \leq r > 0.4$ = weak; $0.4 \leq r > 0.6$ = moderate; $0.6 \leq r > 0.8$ = strong; and $0.8 \leq r$ = very strong [66]. Mice were classified according to their clinical scores and rotarod performance as described by van den Berg et al. as either asymptomatic, moderately sick, or severely sick (Table 2) [4]. Changes in the kinematic parameters of average hip height, average toe height during swing phase, average angle, and range of motion were analyzed using repeated measures one-way ANOVA with Holm-Sidak's multiple comparisons test to compare all time points to DPI -2 (baseline). In the case of affected parameters, the difference between peak change to that at the last measurement (DPI 44) was also tested to assess whether recovery occurred. Root mean square (RMS) differences (explained in Chapter 3) differences for each joint were compared to baseline RMS differences established in Figure 9D using one-sample *t*-tests and differences between time points were assessed using one-way

repeated measures ANOVA with Holm-Sidak multiple comparisons post-hoc test to assess recovery as described above. For all tests, p values were reported as exact values unless they were less than 0.0001, which is the smallest value Graphpad Prism reports. In case that the p value was less than 0.0001, it was reported as $p = <0.0001$.

CHAPTER 3: RESULTS

3.1 CORRELATING CLINICAL SCORES AND ROTAROD PERFORMANCE

In order to assess the relationship between rotarod performance and clinical scores in EAE, sixty-three 10 week old female C57Bl/6 mice were pre-trained on the rotarod for four consecutive days to establish baseline performance. Mice were then randomized into one of two conditions, EAE or CFA. There were no differences between the two groups with respect to weight or rotarod performance after training. The 33 mice in the EAE condition were immunized on DPI 0 with MOG_{35-55}-CFA, while the 30 mice in the CFA condition received PBS-CFA (CFA mice) and served as control mice. All mice received pertussis toxin on DPI 0 and 2. Mice were weighed and monitored daily beginning DPI 7 and rotarod behavioural testing was performed weekly, beginning DPI 7. Mice were humanely sacrificed on DPI 31.

3.1.1 CLINICAL SCORES AND ROTAROD PERFORMANCE

All of the mice in the EAE condition developed clinical signs of EAE (100% incidence) beginning DPI 10-13 (Figure 2A). EAE mice had significantly higher clinical scores than CFA mice which did not develop clinical signs ($p = <0.0001$). For the rotarod, there was a significant interaction between DPI and experimental condition [$F(3,183) = 40.92$, $p = <0.0001$], with CFA animals performing maximally throughout the experiment while EAE mice displayed significant deficits on DPI 16, 23, and 30 ($p = <0.0001$; Figure 2B).

3.1.2 CLINICAL SCORES CORRELATE WELL WITH ROTAROD AT EARLY BUT NOT LATER TIME POINTS IN EAE

To better understand the relationship between clinical scores and rotarod, the Spearman's rank correlation coefficients (ρ) were calculated for clinical scores and rotarod latencies at three time points: DPI 16, 23, and 30 (Figure 2C-E). Clinical scores were strongly correlated with rotarod performance at DPI 16 ($\rho = -0.7682$, $n = 33$, $p = <0.0001$). However, at later time points this correlation decreased in strength. At DPI 23 and 30, clinical scores and rotarod correlated weakly ($\rho = -0.4207$, $n = 33$, $p = 0.0286$) and moderately ($\rho = -0.5298$, $n = 33$, $p = 0.0095$), respectively.

3.1.3 CLINICAL SCORES PREDICT ROTAROD PERFORMANCE WELL FOR ASYMPTOMATIC AND SEVERELY SICK ANIMALS BUT NOT MODERATELY SICK ANIMALS

The weaker ρ values for clinical scores and rotarod latencies resulted in further statistical analyses to determine how well clinical scores actually predicted rotarod performance at each of the time points following immunization (Figure 2F). Animals were classified according to clinical scores or rotarod performance into one of three categories (asymptomatic, moderately sick or severely sick; Table 2). The positive predictive values (PPV) for each of these 3 disease levels of clinical scores for comparable rotarod performance were calculated. When mice were classified as asymptomatic (clinical score = 0) there was 84% agreement with the same category

Table 2: Disease severity classification. Definitions of asymptomatic, moderate and severe disease severity according to clinical score and rotarod performance. Adapted from van den Berg et al. (2016).

Category	Clinical Score	Rotarod (s)
Asymptomatic	0	> 250
Moderate	0.5-2.5	150-250
Severe	>2.5	< 150

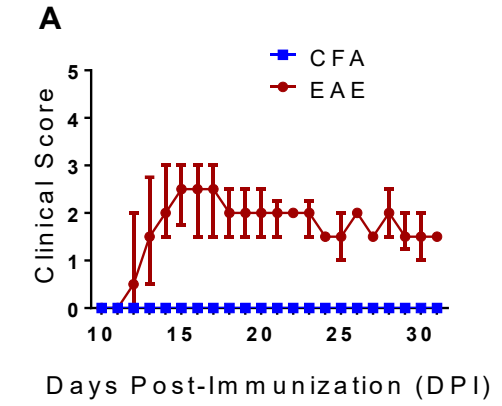

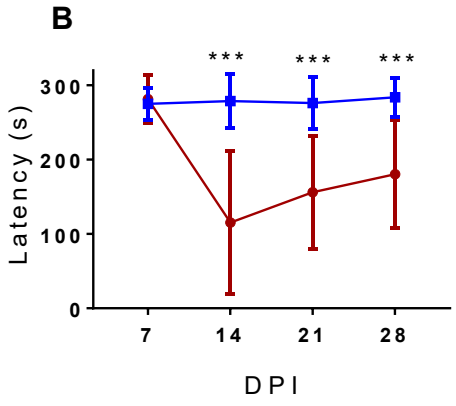

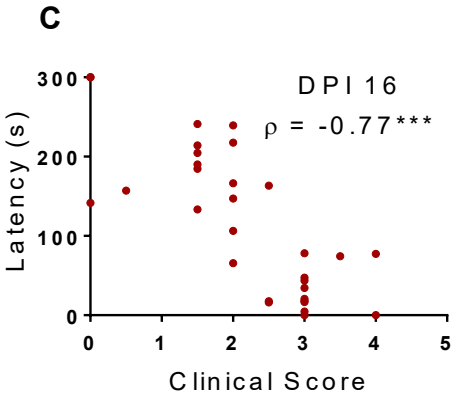

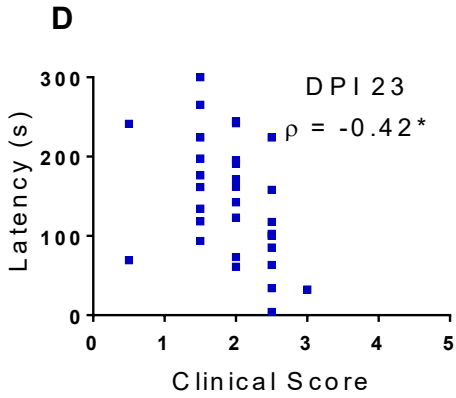

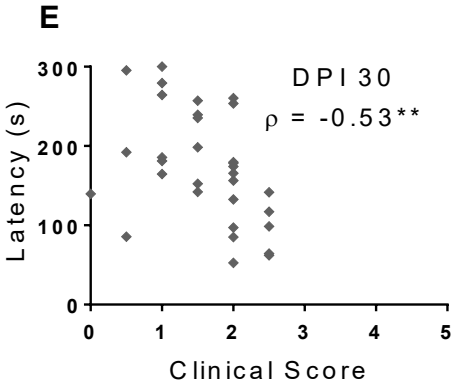

F

Rotarod	Clinical Score: Asymptomatic	Moderate	Severe
Asymptomatic	31	9	0
Moderate	4	37	0
Severe	2	34	15
Total	**37**	**80**	**15**
Positive predictive value	0.84	0.46	1.00

Figure 2: Clinical scores strongly predicted rotarod latency when animals are severely sick (CS < 2.5) but the predictive power was much lower for moderately sick animals (CS 0.5 – 2.5). **(A)** EAE animals exhibited clinical signs starting on DPI 11 and had a higher degree of motor impairment than CFA animals which exhibited no clinical signs of EAE (***). Data are expressed as median +/- interquartile range and were analyzed using a Wilcoxon matched-pairs signed rank test. CFA n = 30, EAE n = 33. **(B)** Rotarod performance generally corresponded with clinical scores and was significantly decreased in EAE animals relative to CFA at DPI 14, 21 and 28. Data are expressed as mean +/- SD and were analyzed using a 2-way repeated measures ANOVA with post-hoc Sidak's multiple comparisons test to assess differences between EAE and CFA groups. CFA n = 30, EAE n = 33. **(C-E)** Clinical scores plotted against rotarod performance at three time points. Spearman's rho (ρ) is shown. n = 33. **(C)** Clinical scores correlate strongly with rotarod performance at DPI 16. n = 33. **(D)** Clinical scores correlate weakly with rotarod performance at DPI 23. n = 33. **(E)** Clinical scores correlate moderately with rotarod performance at DPI 30. n = 33. **(F)** Table showing the agreement between clinical scores and rotarod classification of animals as either "asymptomatic", "moderately sick", or "severely sick" from DPI 9, 16, 23 and 30. The positive predictive value (PPV) of each clinical score category to predict rotarod classification was calculated. Classification of animals based on clinical scores predicted rotarod performance well for both asymptomatic and severely sick animals (PPV = 0.84 and 1.00, respectively), but not for moderately sick animals (PPV = 0.49). n = 132. * $p < 0.05$, ** $p < 0.01$, *** $p < 0.001$.

for rotarod latencies (≥250 s). Similarly, when mice were classified as severely sick by clinical scores, 100% of them were also severely sick according to rotarod latencies (<150 s). However, clinical scores predicted with only 46% accuracy rotarod performance (150-249 s) for moderately sick animals.

3.2 KINEMATIC GAIT ANALYSIS TO ASSESS WALKING DEFICITS IN EAE MICE

The low predictive power of clinical scores for the rotarod performance of moderately sick EAE mice led me to examine whether kinematic parameters of gait were more accurate and informative measures of motor disabilities in EAE mice. To accomplish this, 24 female C57Bl/6 mice each, were randomized into either CFA or EAE conditions as described above. The experiment was done with two cohorts, each with CFA (n = 4) and EAE mice (n = 8). In both experiments, CFA mice were tested at three points: two days before sham immunization (DPI -2), DPI 16, and DPI 30. CFA mice were humanely sacrificed on DPI 31 and their spinal cords were harvested for histology. All EAE mice underwent the same immunization procedures as described previously. The EAE disease course varied substantially between the two cohorts (Table 3). The first cohort, designated severe EAE (n = 8) had relatively severe clinical scores and rotarod impairment, while the second cohort had a much milder disease course with respect to clinical scores and rotarod. The two cohorts also experienced peak disease at different times, with severe EAE mice experiencing peak at DPI 23 and mild EAE experiencing peak at DPI 16. Both cohorts were followed for three weeks after their respective peaks to assess recovery, so severe EAE animals were followed until DPI 44 and mild EAE animals were followed until DPI 37 before their spinal cords were harvested for histological analyses. All EAE mice were recorded walking on the treadmill weekly beginning at DPI -2 until the end of the experiment. The recordings from DPI -2

Table 3: Summary of clinical scores and rotarod performance for CFA, mild and severe EAE groups at peak and chronic stages of disease.

		CFA	EAE (mild)	EAE (severe)
Clinical score *Median (range)*	Peak [a]	0	0.5 (0.0 – 2.0)	2.5 (2.0 – 3.5)
	Chronic [b]	0	0.25 (0.0 – 2.5)	2.25 (2.0 – 3.0)
Rotarod *Mean +/- SD (s)*	Peak	279 +/- 36	211 +/- 70	56 +/- 69
	Chronic	282 +/- 32	201 +/- 101	37 +/- 31

[a] Peak stage of disease for CFA and mild EAE is DPI 16 and for severe EAE is DPI 23

[b] Chronic phase of experiment for CFA is DPI 30, mild EAE is DPI 37, and severe EAE is DPI 44

were used as the baseline measures for statistical comparisons. A subsection of mice from each cohort were also tested at DPI -9 in addition to DPI -2 and these recordings were used to assess inter-session variability (Section 3.3).

3.2.1 CHANGES IN HIP AND TOE HEIGHT OVER TIME IN EAE MICE

Since a severe clinical disease course results in ascending paralysis that eventually involves the hindlimbs, it was predicted that decreases in hip and toe height during walking would occur in EAE mice. Hip height indicates how high the animal carries its body while toe height measures how high the mouse lifts its foot during the swing phase of a step cycle.

As expected, hip height was unchanged in CFA animals at all time points (Figure 3A and B) [$F(2,7) = 0.01705$, $p = 0.9694$]. Similarly, hip height was unchanged in mild EAE mice at all time points (Figure 3C and D) [$F(5,7) = 2.061$, $p = 0.1362$]. By contrast, severe EAE mice were unable to support their body with their hindlimbs when walking, resulting in much lower hip heights than at baseline (Figure 3E). When compared to DPI -2 mice (Figure 3D), the hip heights for EAE mice were significantly decreased [$F(6,7) = 10.46$, $p = <0.0001$] at DPI 16 ($p = 0.0282$), 23 ($p = 0.0096$), 30 ($p = 0.0083$), 37 ($p = 0.0096$), and 44 ($p = 0.0284$). The maximal decrease in hip height was observed at DPI 23 and the hip height appeared to trend positively upwards at DPI 44, but the difference between DPI 23 and DPI 44 was not significant ($p = 0.192$).

CFA animals showed no obvious changes in toe height during swing (Figure 4A) and showed no statistically significant changes in average toe height at any time point (Figure 4B) [$F(2,7) = 1.026$, $p = 0.3765$]. Conversely, both groups of EAE mice showed

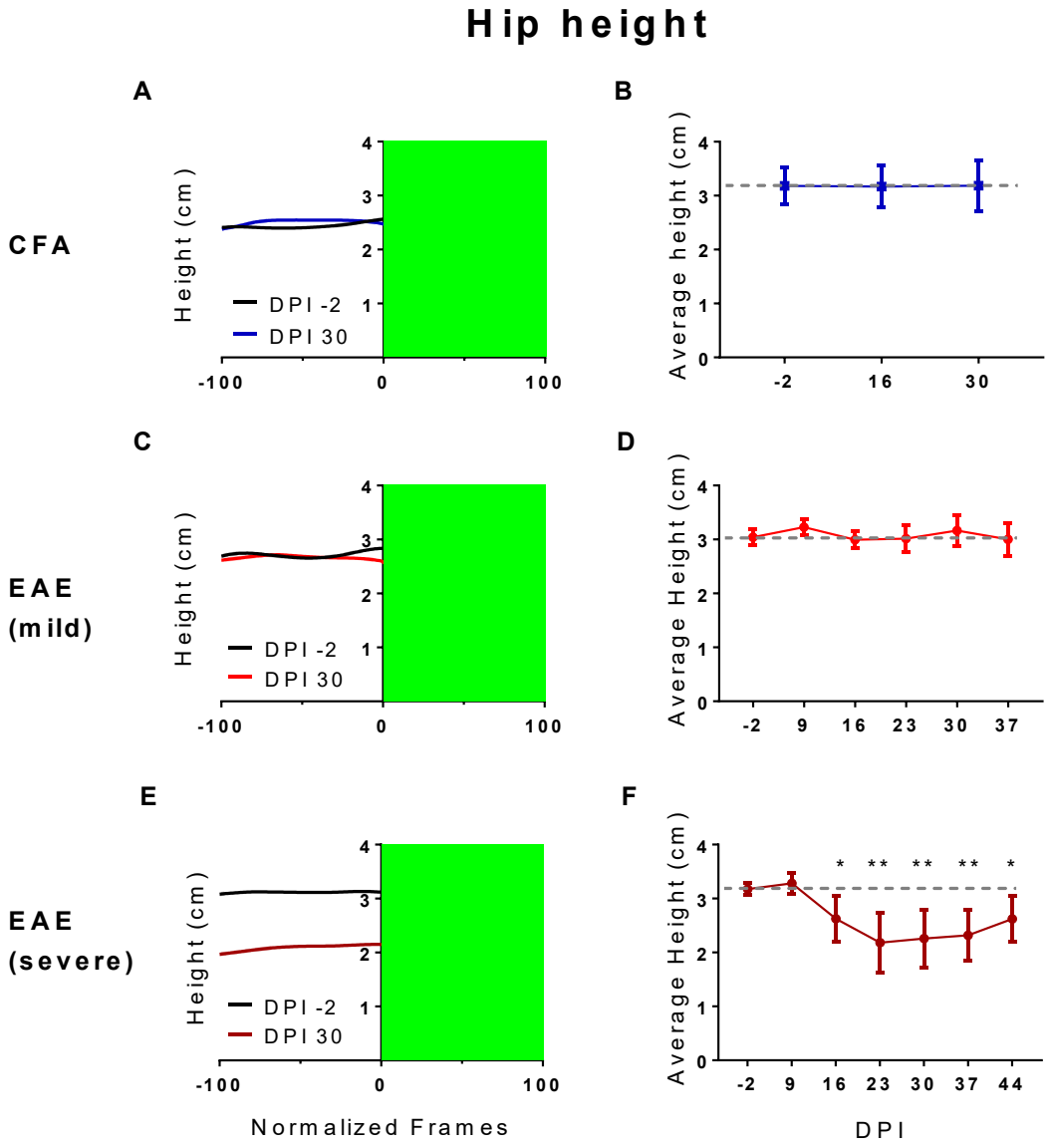

Figure 3: Hip height was decreased in severe EAE but not in mild EAE. **(A,C,E)** Representative step cycles for hip height in CFA **(A)**, severe EAE **(C)**, and mild EAE mice **(E)**. **(B,D,F)** Average hip height at multiple time points. Data are expressed as mean +/- SD and were analyzed using one-way repeated measures ANOVA with Holm-Sidak's multiple comparisons test to compare all time points to baseline (DPI -2) and to assess recovery when applicable. CFA n = 8, severe EAE n = 8, mild EAE (n = 8). **(B)** Hip height did not change for CFA animals. **(D)** Hip height was unchanged for mild EAE animals. **(F)** Hip height decreased with EAE onset at DPI 16 and at DPI 23, 30, 37 and 44 but not DPI 9. There was not significant recovery in hip height at DPI 44 relative to the lowest hip height at DPI 23. * $p < 0.05$, ** $p < 0.01$, *** $p < 0.001$ difference from DPI -2. Grey line represents the average hip height at value at DPI -2.

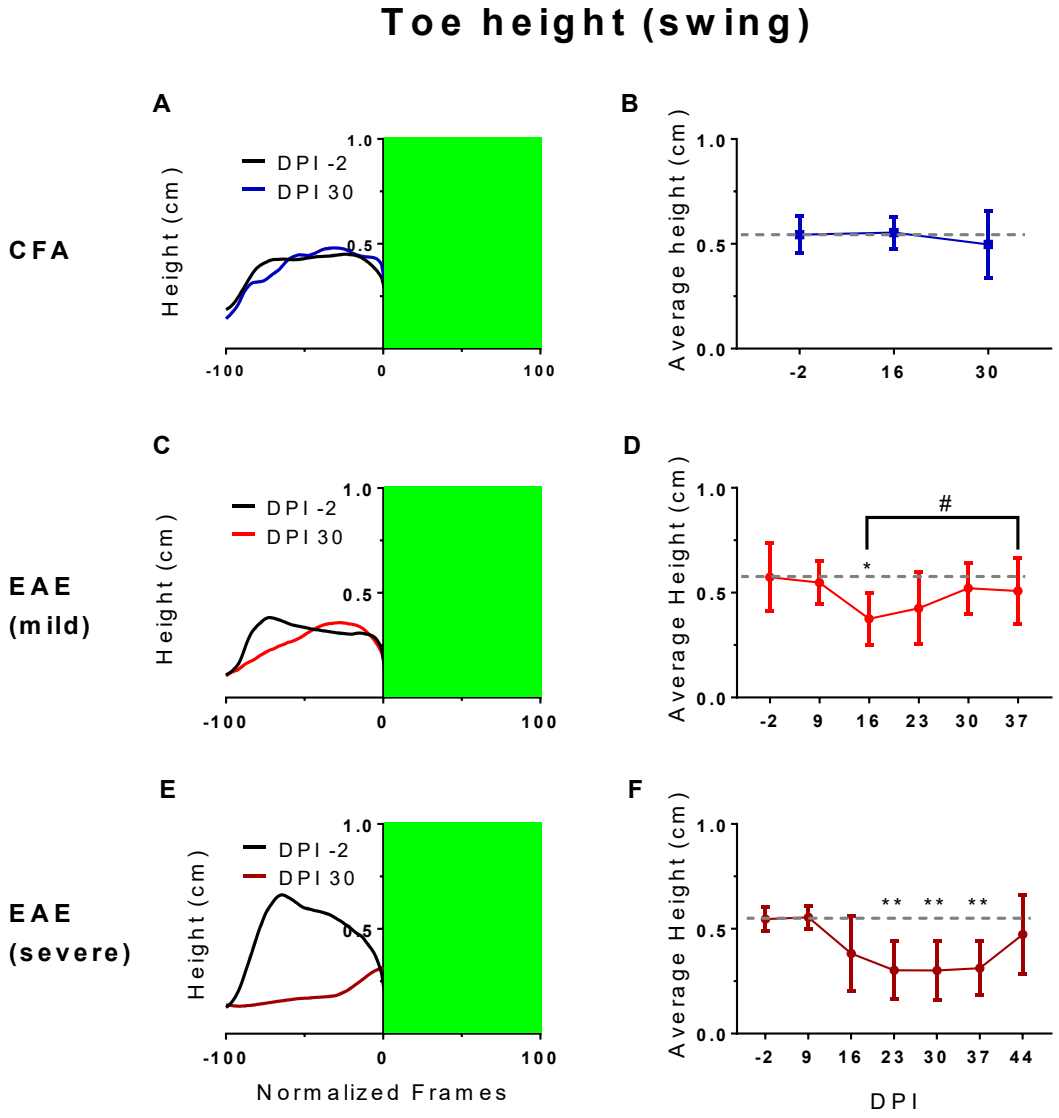

Figure 4: Toe height during swing decreased in mild and severe EAE. **(A,C,E)** Representative step cycles for toe height in CFA **(A)** mild EAE **(C)**, and severe EAE **(E)** mice. **(B,D,F)** Average toe height at multiple time points. Data are expressed as mean +/- SD and were analyzed using one-way repeated measures ANOVA with Holm-Sidak's multiple comparisons test to compare all time points to baseline (DPI -2) and to assess recovery when applicable. CFA n = 8, severe EAE n = 8, mild EAE (n = 8). **(B)** Toe height did not change in CFA animals. **(D)** Average toe height in during swing decreased in mild EAE animals at DPI 16 and recovered by DPI 37. **(E)** In severe EAE animals, average toe height during swing phase was significantly decreased at DPI 23, 30, AND 37. There was a trend towards recovery from the lowest toe y value at DPI 30 and DPI 44 but this did not reach significance. * $p < 0.05$, ** $p < 0.01$, *** $p < 0.001$ difference from DPI -2. Grey line represents the average toe height during swing at DPI -2.

changes in toe movement during swing. Mild EAE mice were still able to lift their toes to the same height as they did at baseline, but they appeared to lift the toe more slowly, as indicated by the fact that the toe did not reach its peak height until the last half of the swing phase (Figure 4C). Average toe height during swing, therefore, was found to be decreased in mild EAE mice (Figure 4D) [F5,7) = 5.782, p = 0.0063] at DPI 16 (p = 0.0181). This measure trended towards recovery at later time points and was significantly higher at DPI 37 relative to DPI 16 (p = 0.0116). Severe EAE mice exhibited a more severe change and were only able to lift the toe from the treadmill belt very slightly at very end of the swing phase, indicating that the toe was largely dragged on the ground (Figure 4E). Unsurprisingly, the average toe height during swing was decreased in severe EAE mice (Figure 4F) [F(6,7) = 8.178, p = 0.0009] at DPI 23 (p = 0.0090), 30 (p = 0.0043), and 37 (p = 0.0090). However, there was a trend towards recovery from the lowest toe height at DPI 30 to DPI 44 that nearly reached statistical significance (p = 0.0752).

3.2.2 CORRELATIONS BETWEEN HEIGHT PARAMETERS AND CLINICAL SCORES

Average hip height and average toe height during swing phase were pooled from both cohorts according to clinical score in order to examine how each parameter changed with clinical scores. Average hip height was strongly correlated with clinical scores Figure 5) (ρ = -0.6452, n = 108, p = <0.0001). There was a significant decrease in hip height from CS = 0.0 [(F(6,101) = 38.91, p = <0.0001] at CS = 2.5 (p = <0.0001), and a further decrease at CS = 3.0 (p = <0.0001). Average toe height during swing phase was also strongly correlated with clinical scores (Figure 6) (ρ = -0.7072, n = 108, p = <0.0001). There was an initial decrease from CS = 0.0 [F(6,101) = 22.89, p = <0.0001] at CS = 1.0 (p = 0.0067) and a further decrease at CS = 3.0 (p = 0.0499).

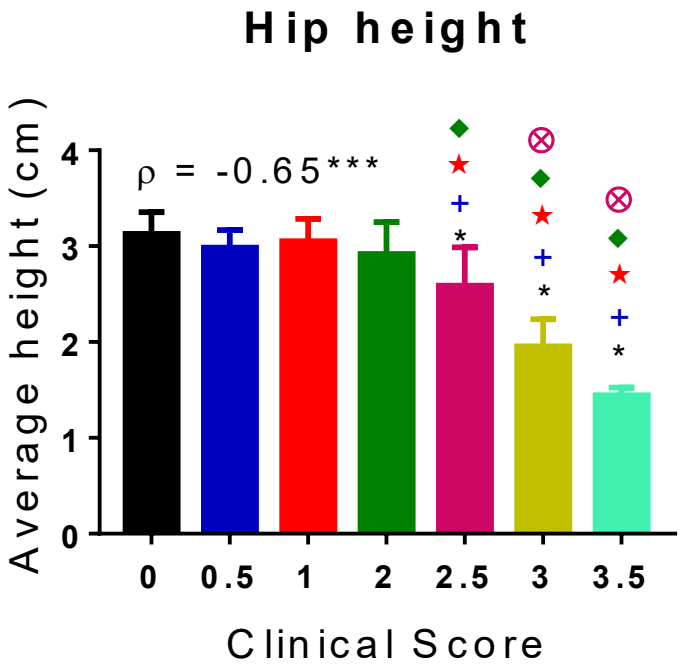

Figure 5: Average hip height strongly correlated with clinical scores. Hip height from all EAE animals pooled according to clinical score. Hip height strongly correlated with clinical score and decreased at CS = 2.5 and CS = 3.0. Data are expressed as mean +/- SD and were analyzed by performing Spearman's rank order correlation as well as one-way ANOVA with Holm-Sidak's multiple comparisons test used to test for differences between every pair of clinical scores. For Spearman's rho (ρ), * $p < 0.05$, ** $p < 0.01$, *** $p < 0.001$. For bar graph, symbols indicate statistical significance at a level of 0.05 from designated clinical score: * CS = 0.0, + CS = 0.5, ☆ CS = 1.0, ◆ CS = 2.0, ⊗ CS = 2.5, # CS = 3.0.

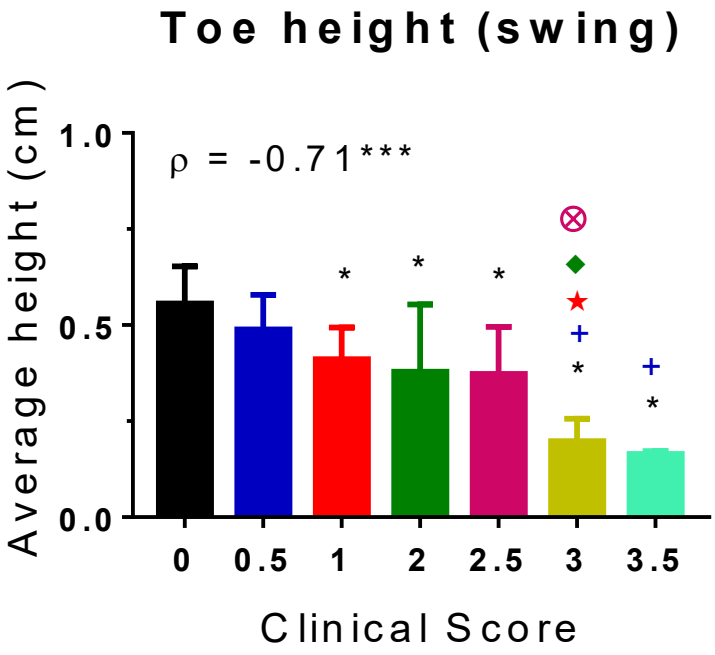

Figure 6: Average toe height in swing phase strongly correlated with clinical scores. Average toe height during swing phase from all EAE animals pooled according to clinical score. Toe height strongly correlated with clinical score and decreased at CS = 1.0 and CS = 3.0. Data are expressed as mean +/- SD and were analyzed by performing Spearman's rank order correlation as well as one-way ANOVA with Holm-Sidak's multiple comparisons test used to test for differences between every pair of clinical scores. For Spearman's rho (ρ), * $p < 0.05$, ** $p < 0.01$, *** $p < 0.001$. For bar graph, symbols indicate statistical significance at a level of 0.05 from a certain clinical score: * CS = 0.0, + CS = 0.5, ☆ CS = 1.0, ◆ CS = 2.0, ⊗ CS = 2.5, # CS = 3.0.

3.2.3 CHANGES IN HIP JOINT KINEMATICS OVER TIME IN EAE

Hip height and toe height during swing can be considered the end products of the movements that occur during locomotion. To understand the changes in gait underlying changes in these end products are achieved, two additional parameters were quantified for each of the primary joints of the leg, the hip, knee and ankle. The average angle provides a general sense of how flexed (smaller angles) or extended (larger angles) the joint is while walking (Figure 7A). Range of motion, simply describes the difference between the peak extension of the joint (largest angle reached) and the peak flexion (smallest angle reached) during the average step cycle (Figure 7B). Combined, the average angle and range of motion of the hip, knee and ankle joints give a good description of how EAE perturbs normal movement of the hindlimbs.

Sham immunization of mice in the CFA condition did not alter movement at the hip (Figure 8A). For the average hip angle (Figure 9A), despite significance in a one-way repeated measures ANOVA [$F(2,7) = 4.313$, $p = 0.0394$], Holm-Sidak multiple comparison tests indicated no significant changes from the baseline recordings at DPI 16 ($p = 0.1174$) or 30 ($p = 0.4087$), nor was there a difference between DPI 16 and 30 ($p = 0.1207$). Similarly, there was no change in hip range of motion for CFA mice [$F(2,7) = 0.01165$, $p = 0.9867$] (Figure 7B).

By comparison, mild EAE mice, exhibited less extension of the hip joint throughout the step cycle (Figure 8B). This was reflected by decreases in the average hip angle and range of motion. Average hip angle was decreased (Figure 9C) [$F(5,7) = 7.205$, $p = 0.0019$] at all time points (DPI 9, $p = 0.0119$; DPI 16, $p = 0.0206$; DPI 23, $p = 0.0086$; DPI 30, $p = 0.0206$; DPI 37, $p = 0.0119$). There was no recovery in average hip

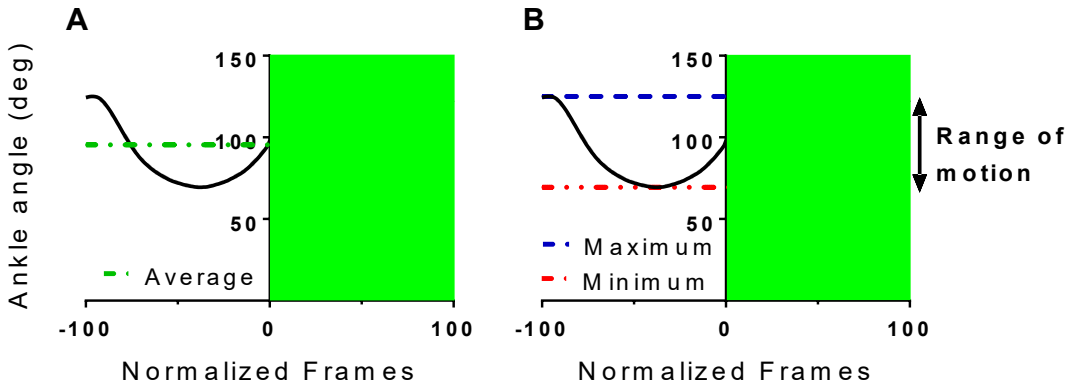

Figure 7: Derivation of kinematic parameters from waveform average step cycles. **(A)** The average angle (or height) was calculated for the whole step cycle or an individual phase. **(B)** The range of motion of a joint was determined by calculating the difference between the maximum and minimum angles across the entire step cycle.

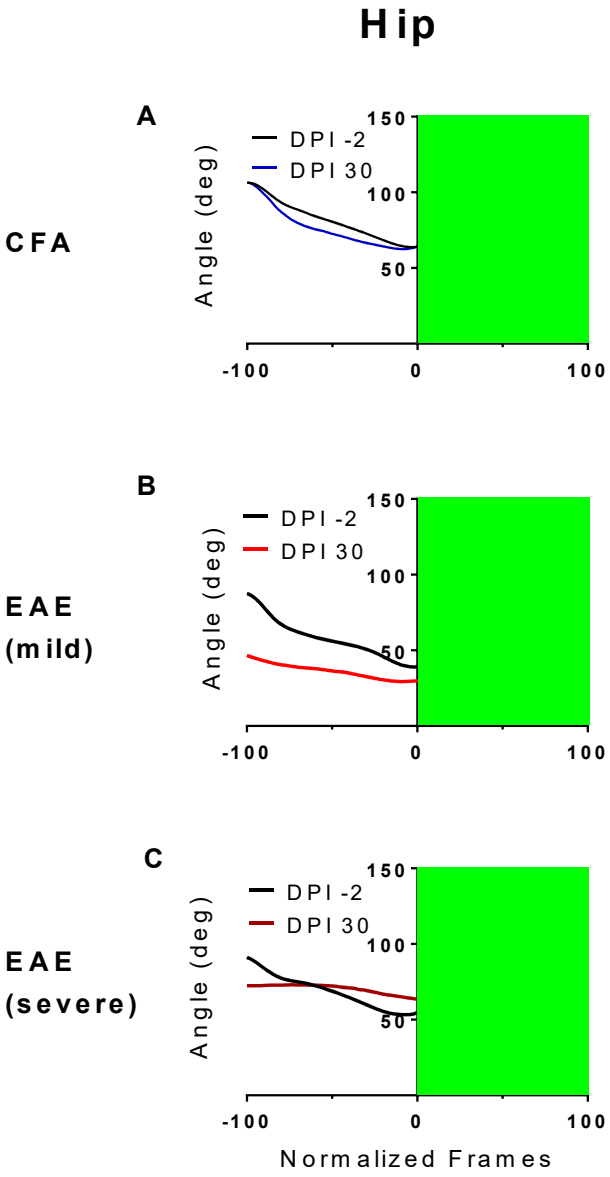

Figure 8: Representative step cycles of hip joint angle in CFA, mild and severe EAE mice. Representative step cycles from (A) CFA, (B) mild EAE, and (C) severe EAE mice.

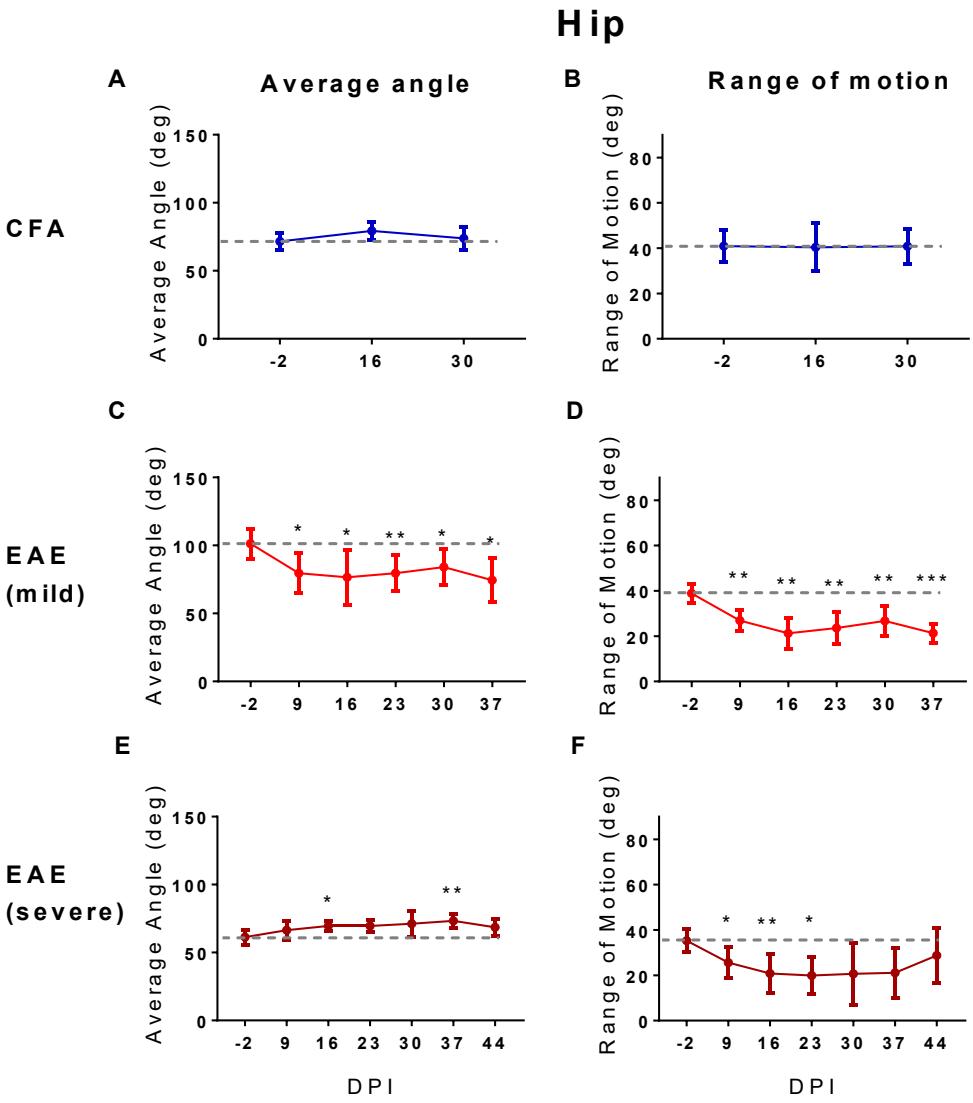

Figure 9: Hip average angle and range of motion changed most robustly in mild EAE and changed to a lesser degree in severe EAE. Average hip angle and hip range of motion at multiple time points for CFA **(A,B)**, mild EAE **(C,D)**, and severe EAE mice **(E,F)**. Data are expressed as mean +/- SD and were analyzed using one-way repeated measures ANOVA with Holm-Sidak's multiple comparisons test to compare all time points to baseline (DPI -2) and to assess recovery. CFA n = 8, mild EAE n = 8, severe EAE n = 8. **(A)** The average hip angle for CFA animals did not change. **(B)** Hip range of motion did not change in CFA animals. **(C)** For mild EAE mice, the average hip angle was decreased relative to baseline (DPI -2) at all time points. **(D)** Hip range of motion was decreased at all time points except for DPI 9 in mild EAE mice. **(E)** For severe EAE mice, the average angle of the hip joint did not change in in standard. **(F)** The angular range of the hip joint decreased in severe EAE mice, on DPI 9, 16, and 23. There was a trend towards recovery at DPI 44 relative to DPI 23. * $p < 0.05$, ** $p < 0.01$, *** $p < 0.001$ difference from DPI -2. Grey line represents average hip angle and range of motion at DPI -2 for each group.

angle at DPI 37 relative to DPI 16 ($p = 0.6917$). Range of motion was decreased (Figure 7D) [$F(5,7) = 15.09$, $p = <0.0001$] all time points relative to DPI -2 (DPI 9, $p = 0.0013$; DPI 16, $p = 0.0013$; DPI 23, $p = 0.0027$; DPI 30, $p = 0.0027$; DPI 37, $p = 0.0006$) and no recovery was observed from DPI 23 to DPI 37 ($p = 0.2439$).

Changes in the hip kinematics for severe EAE mice were more subtle (Figure 8C). There were slight increases in the average hip angle (Figure 7E) [$F(6,7) = 3.487$, $p = 0.0307$] at DPI 16 ($p = 0.0428$) and DPI 37 ($p = 0.0099$). Range of motion was decreased (Figure 9E) [$F(6,7) = 5.221$, $p = 0.0071$], with significantly reduced range of motion relative to baseline at DPI 9 ($p = 0.0237$) that became more pronounced at DPI 16 ($p = 0.0054$) and DPI 23 ($p = 0.0138$). There was a trend towards recovery from DPI 23 to DPI 44 that nearly reached statistical significance ($p = 0.0564$).

3.2.4 CORRELATIONS BETWEEN HIP KINEMATIC PARAMETERS AND CLINICAL SCORES

As with average hip height and toe height during swing, changes in hip average angle and range of motion were pooled between the two cohorts according to clinical score to assess change as a function of clinical scores (Figure 10). Average hip angle was weakly correlated with clinical scores (Figure 10A) ($\rho = -0.3145$, $n = 108$, $p = 0.0009$) and the only significant changes observed [$F6,101) = 5.079$, $p = 0.0001$] small decreases relative to CS = 0.0 at CS = 2.0 ($p = 0.0493$) and 2.5 ($p = 0.0052$). Hip range of motion correlated moderately with clinical scores (Figure 10B) ($\rho = -0.5307$, $n = 108$, $p = <0.0001$). There was a significant decrease in hip range of motion [$F6,101) = 10.21$, $p = <0.0001$] relative to CS = 0.0 at CS = 3.0 ($p = <0.0001$).

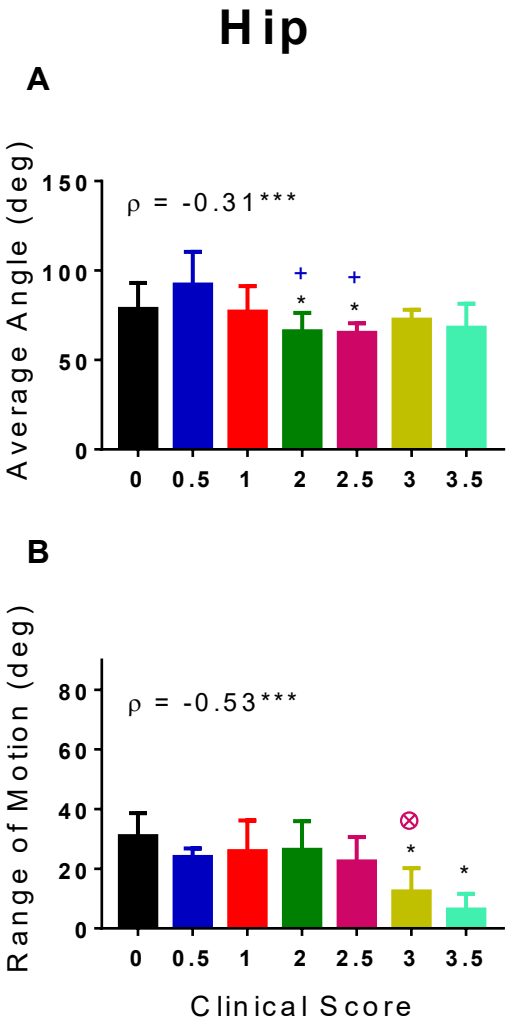

Figure 10: Hip average angle and range of motion correlated with clinical scores weakly to moderately. Average hip height **(A)** and hip range of motion **(B)** from all EAE animals pooled according to clinical score. (A) Average hip angle correlated weakly with clinical score and was decreased at CS = 2.0 and 2.5. (B) Hip range of motion correlated moderately with clinical score and was decreased at CS = 3.0 and 3.5. Data are expressed as mean +/- SD and were analyzed by performing Spearman's rank order correlation as well as one-way ANOVA with Holm-Sidak's multiple comparisons test used to test for differences between every pair of clinical scores. For Spearman's rho (ρ), * $p < 0.05$, ** $p < 0.01$, *** $p < 0.001$. For bar graph, symbols indicate statistical significance at a level of 0.05 from a certain clinical score: * CS = 0.0, + CS = 0.5, ⊗ CS = 2.5.

3.2.5 CHANGES IN KNEE JOINT KINEMATICS IN EAE MICE

As with the hip joint, there were no overt changes in knee kinematics in CFA mice (11A). Average knee angle did not change (Figure 12A) [$F(2,7) = 0.1926$, $p = 0.7751$], but the range of motion slightly increased [$F(2,7) = 10.28$, $p = 0.0083$] at DPI 16 ($p = 0.0006$) and 30 ($p = 0.0328$) relative to baseline (Figure 12B).

For mild EAE mice, subtle changes were observed, with less knee extension at the end of stance phase and the beginning of swing phase (Figure 11B). This was reflected by a decrease in the average knee angle (Figure 12C) at DPI 9 ($p = 0.0326$), DPI 16 ($p = 0.0237$), and DPI 23 ($p = 0.0330$) although the one-way repeated measures ANOVA for average knee angle did not reach significance [$F(5,7) = 3.499$, $p = 0.0619$]. There was no significant improvement from DPI 16 by DPI 37 ($p = 0.9270$). In contrast, knee range of motion did not change in mild EAE mice (Figure 12D) [$F(5,7) = 2.246$, $p = 0.1020$].

By contrast, severe EAE mice displayed profound changes in knee joint angles (Figure 11C). The average angle of the knee joint was decreased dramatically relative to baseline (Figure 12E) [$F(6,7) = 11.08$, $p < 0.0001$] at all time points except DPI 9: DPI 16 ($p = 0.0119$), 23 ($p = 0.0072$), 30 ($p = 0.0119$), 37 ($p = 0.0111$), and 44 ($p = 0.0092$). There was also a clear trend towards recovery of knee range of motion from the lowest point (DPI 23) to DPI 44 ($p = 0.0502$). Similarly, the range of motion at the knee joint was substantially reduced (Figure 12F) [$F(6,7) = 14.42$, $p < 0.0001$] at all time points after clinical onset, DPI 16 ($p = 0.0181$), 23 ($p = 0.0063$), 30 ($p = 0.0063$), 37 ($p = 0.0005$), and 44 ($p = 0.0063$). However, there was no recovery of knee range of motion from the lowest point (DPI 37) to DPI 44 ($p = 0.1224$).

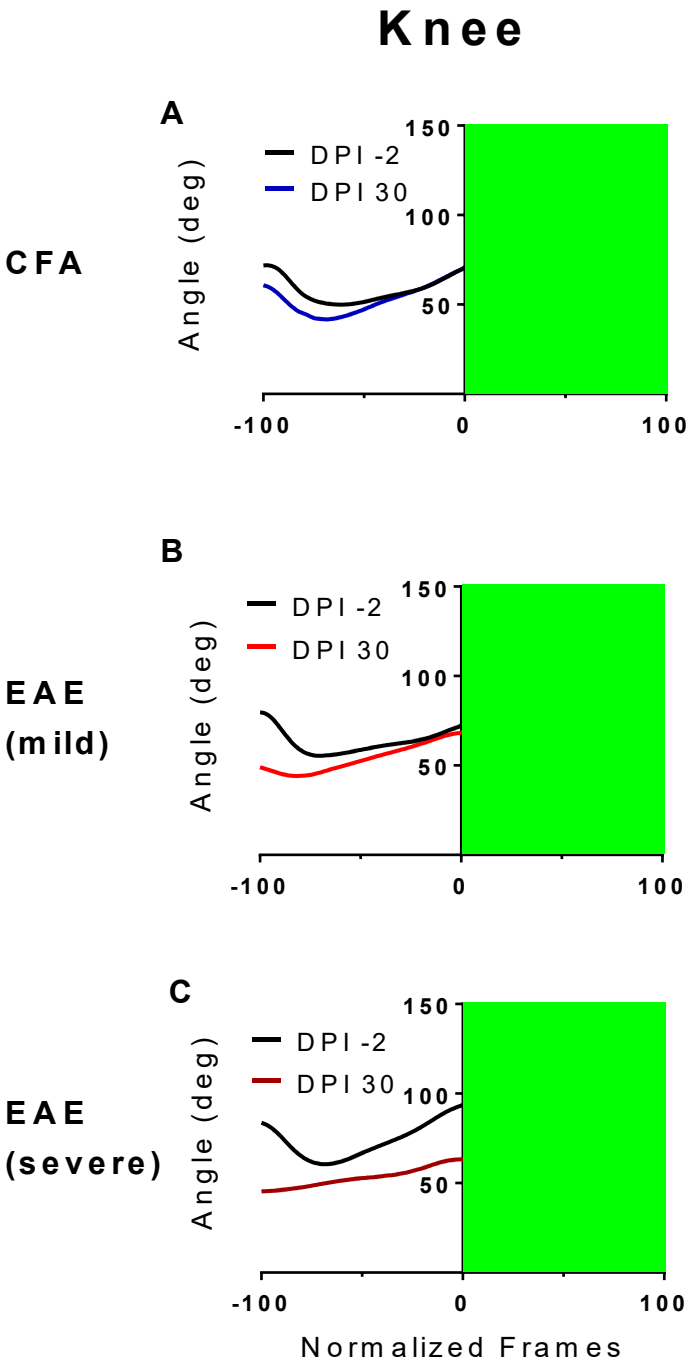

Figure 11: Representative step cycles of knee joint angle in CFA, mild and severe EAE mice. Representative step cycles from (A) CFA, (B) mild EAE, and (C) severe EAE mice.

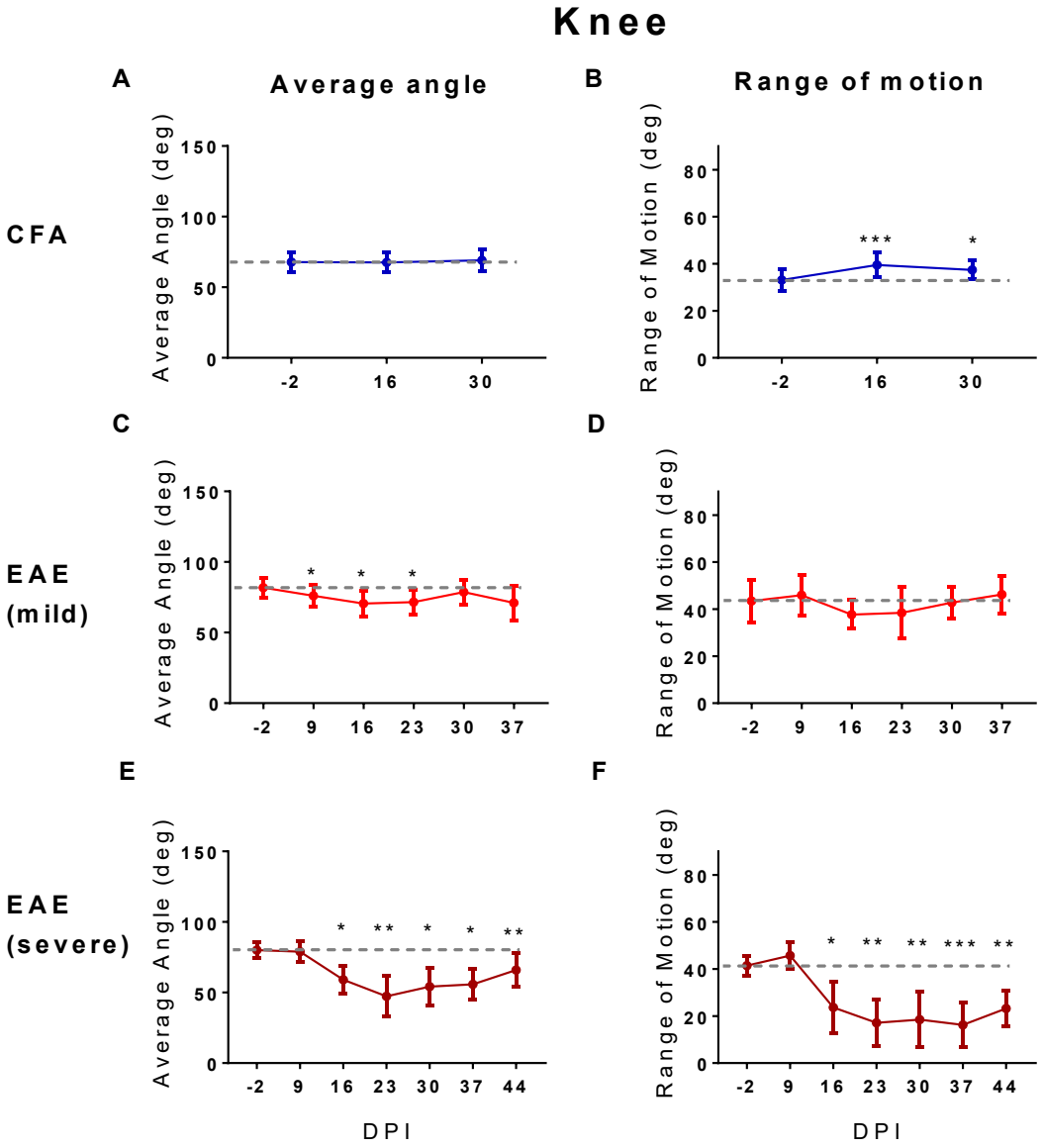

Figure 12: Average angle and range of motion at the knee were decreased with EAE disease severity. Average angle and range of motion of the knee at multiple time points for CFA **(A,B)**, mild EAE **(C,D)**, and severe EAE mice **(E,F)**. Data are expressed as mean +/- SD and were analyzed using one-way repeated measures ANOVA with Holm-Sidak's multiple comparisons test to compare all time points to baseline (DPI -2) and to assess recovery. CFA n = 8, mild EAE n = 8, severe EAE n = 8. **(A)** The average knee angle for CFA animals did not change. **(B)** Knee range of motion increased in CFA animals at DPI 16 and DPI 30 relative to DPI -2. **(C)** For mild EAE mice, the average knee angle was decreased relative to baseline (DPI -2) at DPI 9, 16 and 23. **(D)** Knee range of motion was unchanged in mild EAE mice. **(E)** Knee average angle decreased for severe EAE mice, at DPI 16, 23, 30, 37 and 44. There was a trend but no significant recovery from DPI 23 to DPI 44. **(F)** Knee range of motion was also decreased in severe EAE mice at DPI 16, 23, 30, 37, and 44 with no evidence of recovery. * $p < 0.05$, ** $p < 0.01$, *** $p < 0.001$ difference from DPI -2. Grey line represents average knee angle and range of motion at DPI -2 for each group.

3.2.6 CORRELATIONS BETWEEN KNEE KINEMATIC PARAMETERS AND CLINICAL SCORES

Knee average angle was strongly correlated with clinical score (Figure 13A) (ρ = -0.7732, n = 108, p = <0.0001). Average angle was significantly decreased [$F(6,101) = 43.98$, p = <0.0001] at CS = 2.0 relative to CS = 0.0 (p = <0.0001) and there was a further decrease at CS = 3.0 (p = <0.0001). Knee range of motion similarly correlated (Figure 13B) (ρ = -0.7438, n = 108, p <0.0001) with clinical scores in a negative manner [$F(6,101) = 49.35$, p = <0.0001]. The first decrease from CS = 0.0 occurred at CS = 2.0 (p = <0.0001). There was another decrease in knee range of motion between CS = 2.0 to 2.5 (p = 0.0196) and another decrease between CS = 2.5 and 3.0 (p = <0.0001).

3.2.7 CHANGES IN ANKLE KINEMATICS OVER TIME IN EAE MICE

CFA mice did not have any obvious changes in ankle kinematics (Figure 14A). No differences between either the average angle (Figure 15A) [$F(2,7) = 0.3051$, p = 0.7359] or the range of motion of the ankle (Figure 15B) [$F(2,7) = 0.8578$, p = 0.4375) were detected.

Similar to the knee joint, only subtle changes in ankle kinematics were observed in mild EAE (Figure 14B). There were no changes in average ankle angle (Figure 15C) [$F(5,7) = 1.648$, p = 0.2306], and for range of motion, one-way repeated measures ANOVA did not reach significance (Figure 15D) [$F(5,7) = 2.853$, p = 0.0745], but post hoc testing revealed significant decreases in this parameter at DPI 16 (p = 0.0077) and DPI 37 (p = 0.0377), with a significant decrease of ankle range of motion at DPI 37 relative to DPI 16 (p = 0.0484).

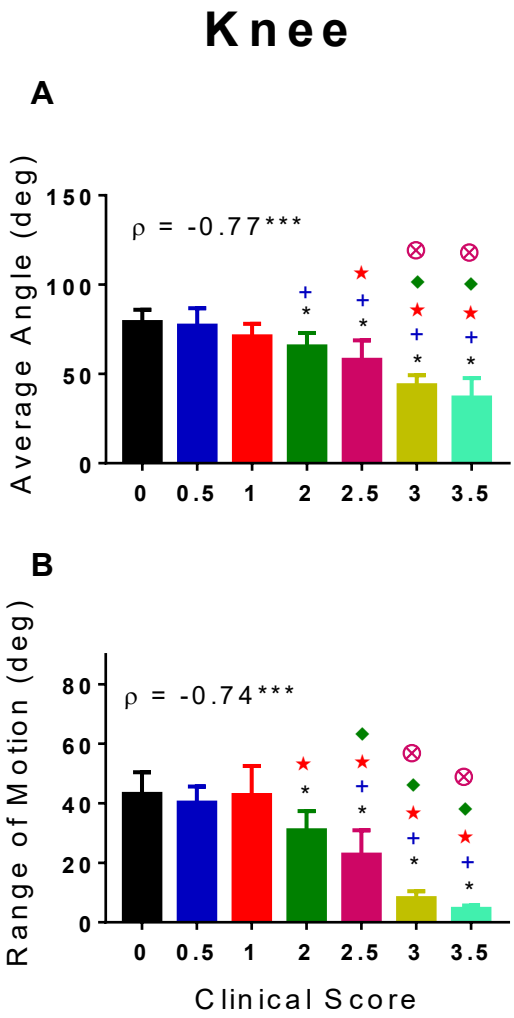

Figure 13: Knee average angle and range of motion strongly correlated with clinical scores. Average knee angle **(A)** and range of motion **(B)** from all EAE animals pooled according to clinical score. **(A)** Average knee angle correlated strongly with clinical score and was decreased at CS = 2.0 followed by another decrease at CS = 3.0. **(B)** Knee range of motion also correlated strongly with clinical score and decreased at CS = 2.0, 2.5 and 3.0. Data are expressed as mean +/- SD and were analyzed by performing Spearman's rank order correlation as well as one-way ANOVA with Holm-Sidak's multiple comparisons test used to test for differences between every pair of clinical scores. For Spearman's rho (ρ), * $p < 0.05$, ** $p < 0.01$, *** $p < 0.001$. For bar graph, symbols indicate statistical significance at a level of 0.05 from a certain clinical score: * CS = 0.0, + CS = 0.5, ☆ CS = 1.0, ◆ CS = 2.0, ⊗ CS = 2.5, # CS = 3.0.

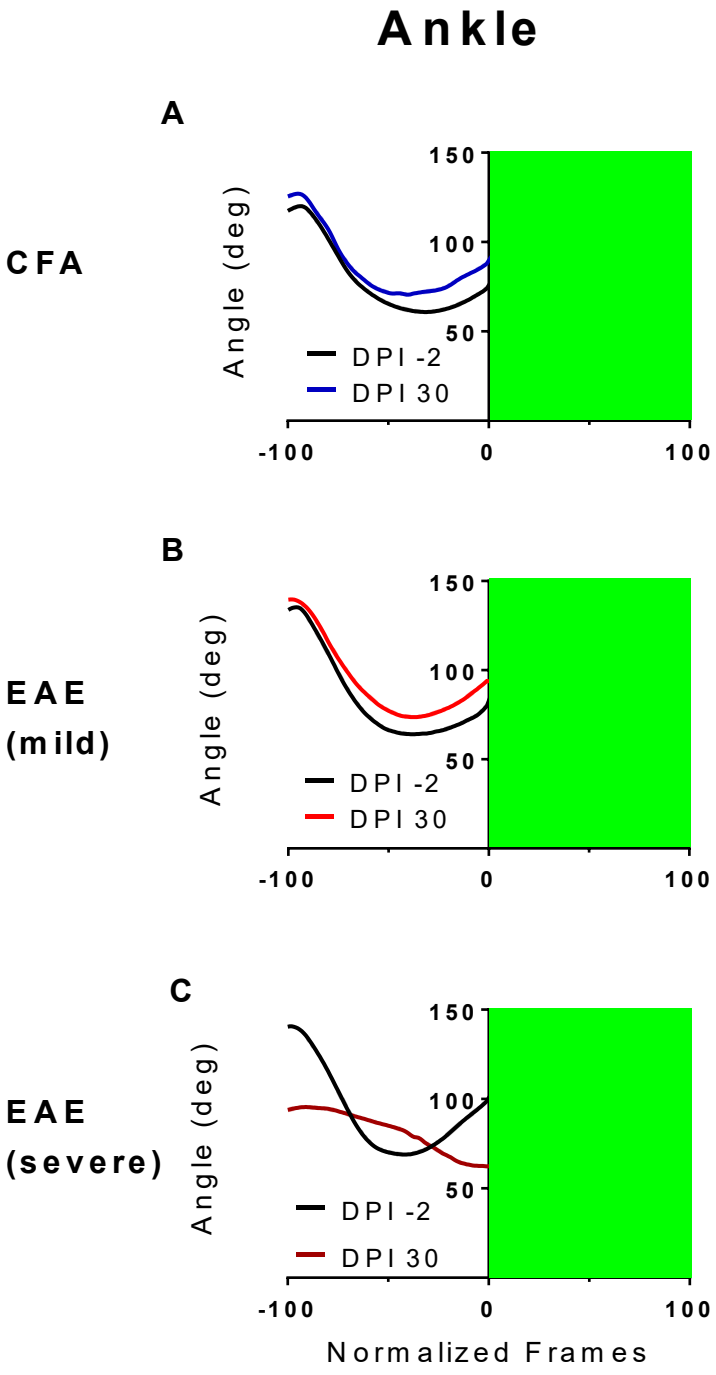

Figure 14: Representative step cycles of ankle joint angle in CFA, mild and severe EAE mice. Representative step cycles from (A) CFA, (B) mild EAE, and (C) severe EAE mice.

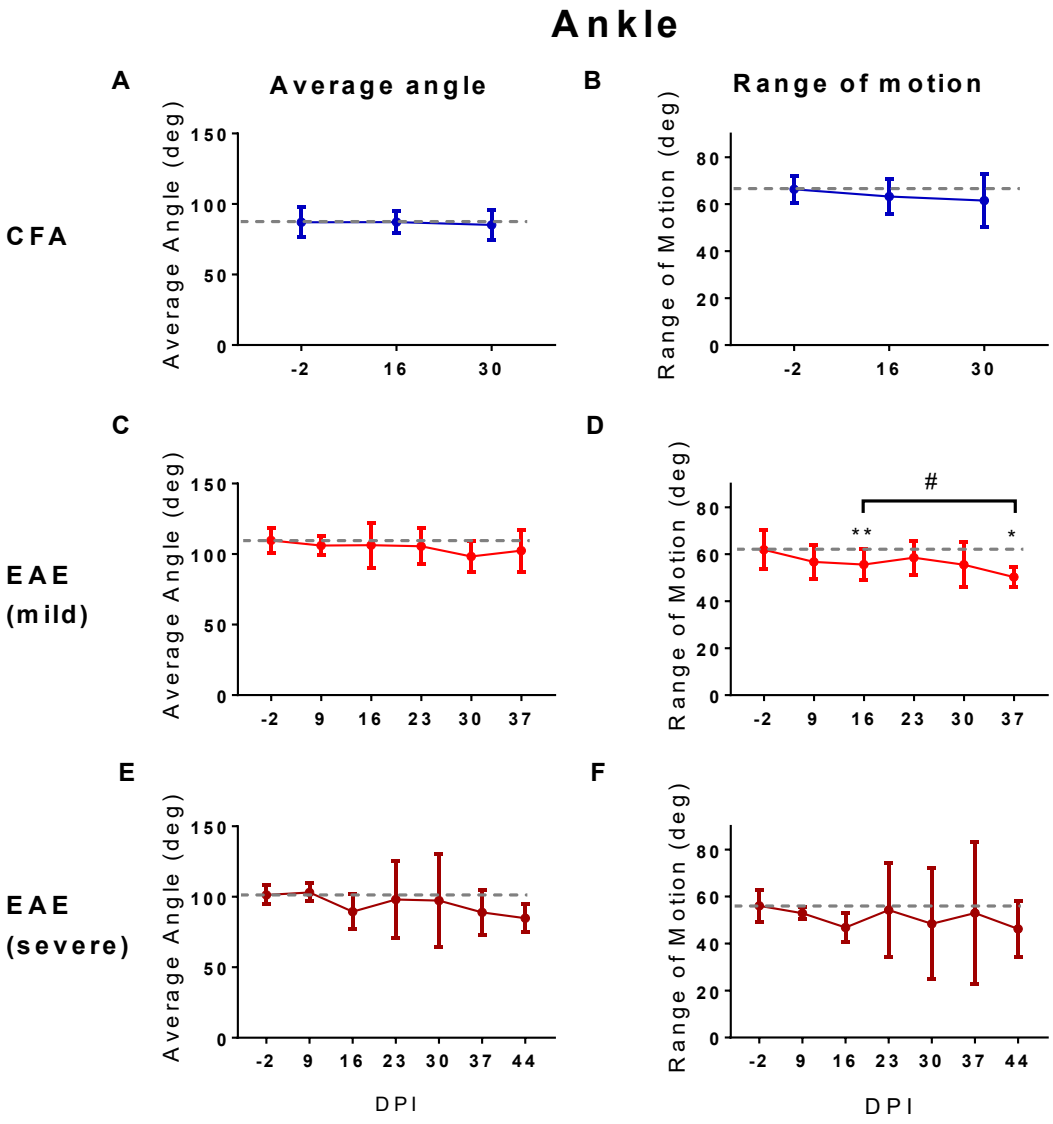

Figure 15: Average angle and range of motion for the ankle were highly variably in severe EAE mice and range of motion slightly decreased in mild EAE mice. Average ankle angle and range of motion at multiple time points for CFA **(A,B)**, mild EAE **(C,D)**, and severe EAE mice **(E,F)**. Data are expressed as mean +/- SD and were analyzed using one-way repeated measures ANOVA with Holm-Sidak's multiple comparisons test to compare all time points to baseline (DPI -2) and to assess recovery. CFA n = 8, mild EAE n = 8, severe EAE n = 8. **(A)** The average ankle angle did not change in CFA animals **(B)** The range of motion did not change in CFA animals. **(C)** For mild EAE mice, the average ankle angle was unchanged. **(D)** Range of motion at the ankle was slightly decreased in mild EAE mice at DPI 16 and DPI 37, with a significant decrease occurring from DPI 16 to 37. **(E)** In severe EAE mice, ankle average angle was unchanged but had very high variability. **(F)** Ankle range of motion in severe EAE mice was similarly unchanged with high variability.* $p < 0.05$, ** $p < 0.01$, *** $p < 0.001$ difference from DPI -2. Grey line represents average ankle angle and range of motion at DPI -2 for each group.

In severe EAE mice, there were obvious perturbations in ankle joint kinematics over a step cycle, but these differences were more complex and variable than the changes observed at the knee and hip joints (Figure 14C). For instance, the large standard deviations at 23 and 30 DPI for ankle angle suggested that EAE impacted movement of this joint (Figure 15E). These changes in ankle angles, however, were highly variable between mice, and no statistical differences were detected [$F(6,7) = 1.02$, $p = 0.3848$). A similar increase in standard deviations for the range of motion (Figure 15F) at DPI 23, 30, and 37 also obscured the detection of significant changes in this measure for EAE mice [$F(6,7) = 0.3987$, $p = 0.8763$]. The results of kinematic gait analysis of CFA, severe and mild EAE mice are summarized in Table 4.

3.2.8 CORRELATIONS BETWEEN ANKLE KINEMATIC PARAMETERS AND CLINICAL SCORES

Average ankle angle did not significantly correlate with clinical scores (Figure 16A) ($\rho = -0.1742$, $n = 108$, $p = 0.0714$). There was an increase in average angle [$F(6,101) = 11.09$, $p = <0.0001$] at CS = 2.0 relative to 0.0, but CS = 2.5 and 3.0 were not different from CS 0.0. Average angle also increased significantly at CS = 3.5. Ankle range of motion correlated weakly with clinical scores (Figure 16B) ($\rho = -0.2441$, $n = 108$, $p = 0.0109$). The only change between clinical scores [$F(6,101) = 7.266$, $p = <0.0001$] from CS = 0.0 was at CS = 3.0 ($p = 0.0418$) and 3.5 ($p = <0.0001$).

Table 4: Summary of kinematic data from CFA, standard EAE and mild EAE mice. ↑ indicate an increase in a parameter and ↓ indicate a decrease. For average height, average angle, and range of motion, increase or decrease of ≤ 20 % is represented by "↓" or "↑", 21-40 % is represented by "↓↓" or "↑↑", and decrease of ≥ 41 % is represented by "↓↓↓" or "↑↑↑". For RMS values, increases from baseline of ≤ 75% are represented by "↑", 76-150% are represented by "↑↑" and increase ≥ 151 are represented by "↑↑↑". Unchanged values are represented by "-".

		CFA			EAE (Mild)			EAE (Severe)		
Joint	Parameter	Pre-clinical [a]	Peak [b]	Chronic [c]	Pre-clinical	Peak [f]	Chronic [g]	Pre-clinical	Peak [d]	Chronic [e]
Hip	Avg height	NA	-	-	-	-	-	-	↓↓	↓↓
	Avg angle	NA	-	-	↓	↓	↓↓	-	-	-
	R.O.M	NA	-	-	↓↓	↓↓↓	↓↓↓	↓↓	↓↓↓	-
	RMS	NA	-	-	-	-	↑	-	-	-
Knee	Avg angle	NA	-	-	↓	↓	-	-	↓↓	↓↓
	R.O.M.	NA	↑	↑	-	-	-	-	↓↓↓	↓↓↓
	RMS	NA	-	-	-	↑	-	-	↑↑↑	↑↑
Ankle	Avg angle	NA	-	-	-	-	-	-	-	-
	R.O.M.	NA	-	-	-	↓	↓	-	-	-
	RMS	NA	-	-	-	-	-	↑	↑↑↑	↑↑↑
Toe	Avg height (sw)	NA	-	-	-	↓↓	-	-	↓↓	-

[a] Pre-clinical is DPI 9 for all conditions.
[b] Peak for CFA animals is DPI 16
[c] Chronic phase for CFA animals is DPI 30
[d] Peak for severe EAE is DPI 23
[e] Chronic for severe EAE is DPI 44
[f] Peak for mild EAE is DPI 16
[g] Chronic for mild EAE is DPI 37

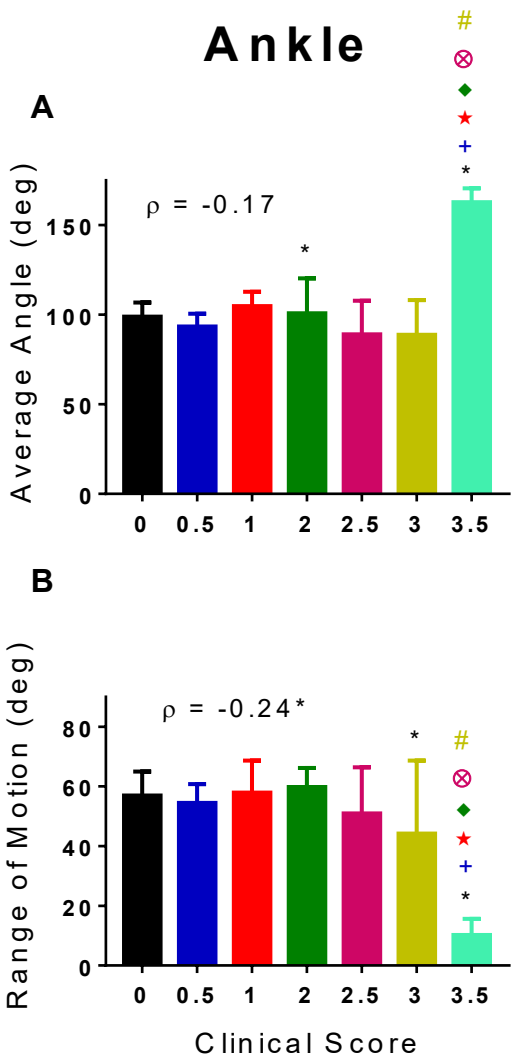

Figure 16: Ankle average angle did not correlate and ankle range of motion weakly correlated with clinical scores. Ankle average angle **(A)** and range of motion **(B)** from all EAE animals pooled according to clinical score. **(A)** Average ankle angle did not correlate with clinical scores and only increased at CS = 3.5. **(B)** Ankle range of motion correlated weakly with clinical score and decreased at CS = 3.5. Data are expressed as mean +/- SD and were analyzed by performing Spearman's rank order correlation as well as one-way ANOVA with Holm-Sidak's multiple comparisons test used to test for differences between every pair of clinical scores. For Spearman's rho (ρ), * $p < 0.05$, ** $p < 0.01$, *** $p < 0.001$. For bar graph, symbols indicate statistical significance at a level of 0.05 from a certain clinical score: * CS = 0.0, + CS = 0.5, ☆ CS = 1.0, ◆ CS = 2.0, ⊗ CS = 2.5, # CS = 3.0.

3.3 CALCULATING THE ROOT MEAN SQUARE (RMS) OF THE DIFFERENCE BETWEEN TWO STEP CYCLES IS A SIMPLE WAY TO QUANTIFY PATHOLOGICAL GAIT CHANGES

When the changes in gait kinematics are complicated or highly variable between animals, as in the case of ankle angle changes in severe EAE mice, it can be difficult to quantify how gait changes. Additionally, because the data provided by kinematic gait analysis is so detailed, it can be hard to describe all of the components of gait using only a few parameters, like average angle and range of motion. To overcome these limitations, I adapted the Gait Profile Score (GPS) which has been used to quantify pathological gait deviations in humans [62]. The basis of the GPS is calculating the root mean square (RMS) difference between a normal step cycle and a pathological one for nine gait variables, including ankle, knee and hip angles [62]. Figure 17 explains the calculation and utility of calculating the RMS difference. Figure 17A shows representative step cycles from one mouse at two time points, baseline and DPI 30, when the mouse shows signs of EAE. The two step cycles are obviously different but have very similar average angles and ranges of motion. The orange arrows indicate the difference (d) in degrees between the two lines at each normalized frame of the step cycle. The graph of difference (d) between the two lines, as calculated using the formula in (Figure 17Ci) is shown (Figure 17B). If the average of the difference (d) is calculated, the value is close to zero because the difference between the two lines encompasses both positive and negative values which cancel out (black line hashed line; 17B). Alternatively, if the root mean square of the difference between these two lines is calculated (Figure 17Cii), the output is more representative of the actual average difference between the two graphs. The RMS difference between two step cycles takes into account all of the details of that step cycle, including the shape of the line, which

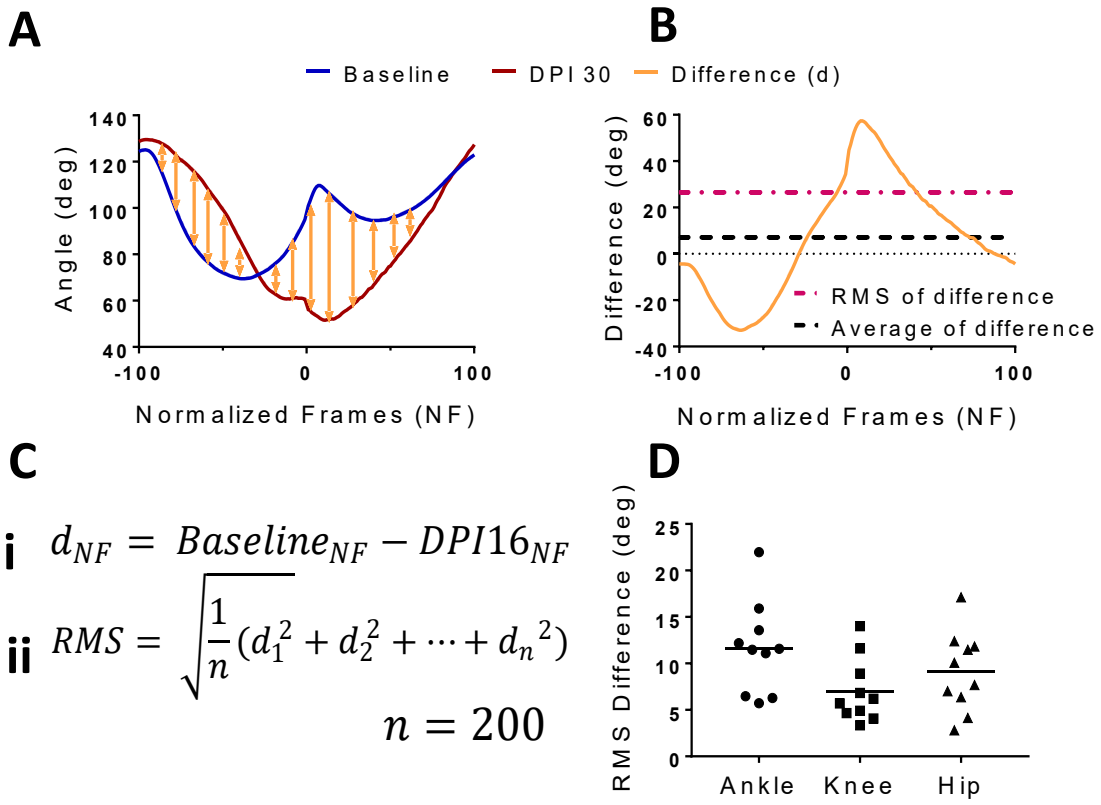

Figure 17: Calculation of root mean square (RMS) of the difference between baseline and later time points. **(A)** An example of repeated measures testing of a mouse at Baseline and at DPI 30. The difference in degrees between the two lines was calculated at each normalized frame (NF) **(C i)**.The resultant graph of the difference (d) between Baseline and DPI 16 is shown in **(B)**. When the average value of d was calculated, positive and negative values cancelled out and the average was close to zero. In contrast, calculation of the RMS difference by **(C ii)** yielded a number that more closely reflected the average degree of difference between the two lines. **(D)** RMS difference for standard EAE animals at DPI -9 and DPI -2. Data are expressed as individual values and mean. Hip RMS difference mean = 11.62, knee RMS difference mean = 7.022, ankle RMS difference mean = 9.086. These values were used as a baseline threshold for statistical analyses of RMS differences.

makes it a useful way to capture all of the changes occurring in pathological gait. The RMS differences for the hip, knee and ankle joints for a subsection of eight animals prior to immunization (DPI -9 and -2) were calculated to assess inter-recording variability (Figure 17D). The mean RMS differences for the hip, knee and ankle joints in naïve animals recorded two weeks apart were 11.62, 7.022, and 9.086 degrees, respectively. These average values were used as thresholds for each joint to assess deviations from normal variability between recording sessions.

3.3.1 RMS DIFFERENCES FOR THE HIP, KNEE AND ANKLE JOINTS OVER TIME IN CFA, MILD AND SEVERE EAE ANIMALS

The RMS differences for the hip, knee and ankle joints were calculated for CFA and EAE animals at all time points relative to the baseline values established above. RMS difference values for CFA animals did not exceed threshold variability for hip, knee or ankle joints (Figure 18A-C).

Mild EAE mice exhibited only subtle and transient increases in RMS difference values. For the hip joint, RMS difference was slightly elevated at DPI 37 relative to threshold (Figure 19A) [$t(7) = 2.37$, $p = 0.0496$]. Repeated measures one-way ANOVA, however, revealed no statistically significant difference between time points [$F(4,7) = 1.974$, $p = 0.1665$]. There was also a small increase in knee RMS difference at DPI 16 (Figure 19C) [$t(7) = 2.938$, $p = 0.0215$], but there were no significant differences between time points [$F(4,7) = 2.065$, $p = 0.1683$]. Lastly, there were no changes in ankle RMS difference above threshold or between time points in mild EAE (Figure 19E) [$F(4,7) = 0.4209$, $p = 0.6802$].

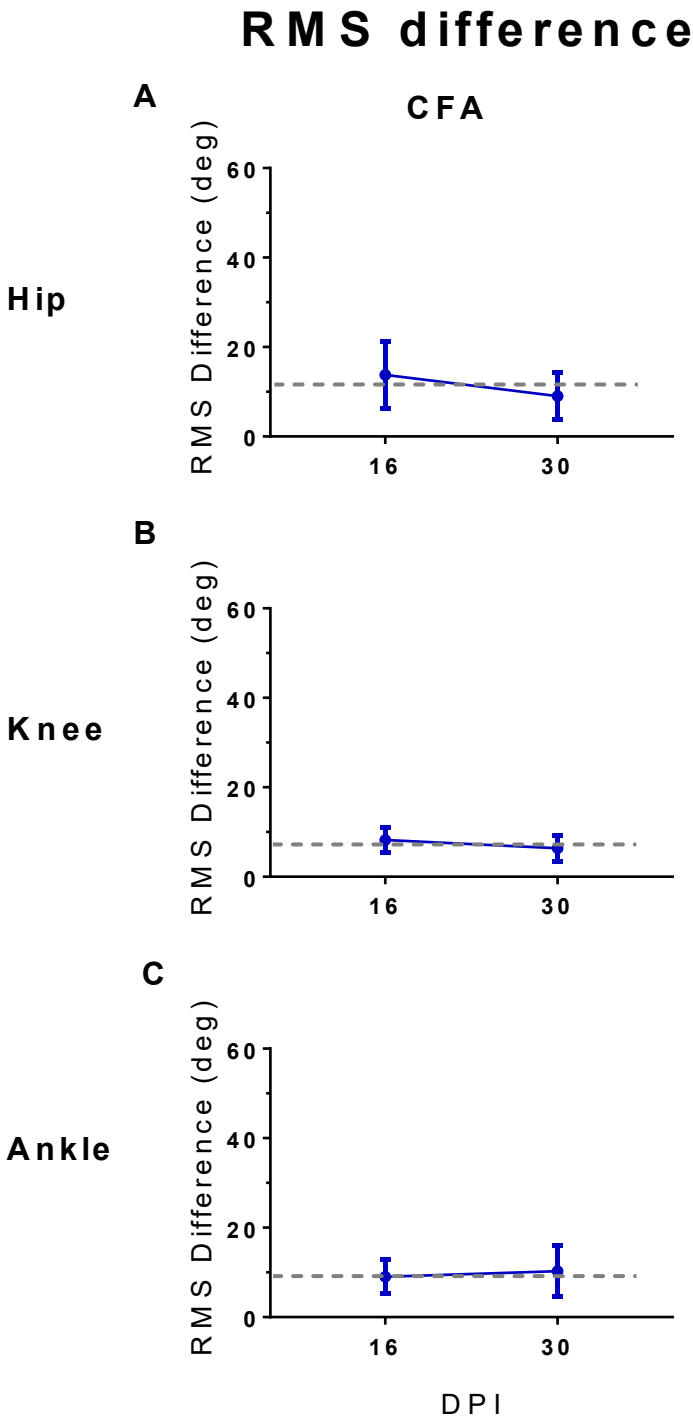

Figure 18: RMS differences were unchanged in CFA mice. **(A,B,C)** RMS difference values were not significantly higher than threshold for the hip, knee, or ankle in CFA animals at any time point. Data are expressed as mean +/- SD and were analyzed using one sample t-tests to compare RMS differences to the threshold values of the relevant joint. n = 8. * $p < 0.05$, ** $p < 0.01$, *** $p < 0.001$ difference from threshold. Grey line represents threshold value for each joint, hip = 11.62, knee = 7.022, ankle = 9.086.

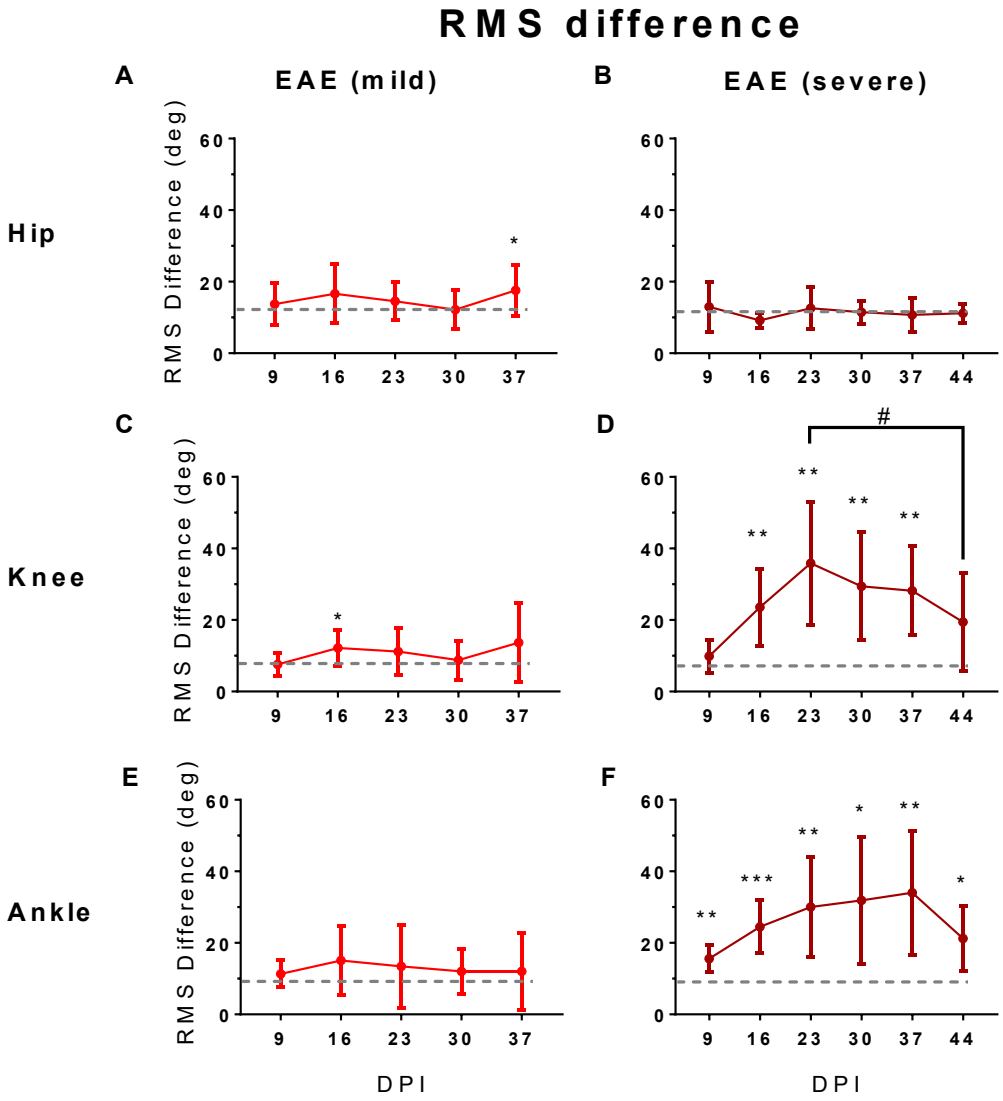

Figure 19: RMS differences were mostly unchanged in mild EAE but were significantly elevated in mild EAE for both ankle and knee joints. RMS differences at multiple time points for mild and severe EAE mice for the hip **(A,B)**, knee **(C,D)**, and ankle joints **(E,F)**. **(A)** Hip RMS difference in mild EAE mice was increased slightly at DPI 37 relative to threshold. **(B)** Hip RMS difference was not increase in severe EAE mice. **(C)** Knee RMS difference was slightly increased at DPI 16 compared to threshold in mild EAE mice. **(D)** For severe EAE mice, knee RMS difference was highly elevated above threshold at DPI 16, 23, 30, 37, and 44. There was a significant degree of recovery from DPI 23 to DPI 44. **(E)** Ankle RMS difference was unchanged in mild EAE mice. **(F)** Ankle RMS difference was highly increased above threshold at all time points in severe EAE mice. There was a trend towards recovery from DPI 37 to DPI 44, but this was not significant. Data are expressed as mean +/- SD and were analyzed using one sample t-tests to compare RMS differences to the threshold values of the relevant joint. n = 8. * $p < 0.05$, ** $p < 0.01$, *** $p < 0.001$ difference from threshold. # $p < 0.05$ difference between peak and final time points. Grey line represents threshold value for each joint, hip = 11.62, knee = 7.022, ankle = 9.086.

In severe EAE there were no increases beyond basal RMS for the hip joint in EAE animals at each time point nor any differences between different time points (Figure 19B) [$F(5,7) = 0.8758$, $p = 0.4532$]. There were however, large increases in RMS difference for both the knee and ankle joints. For the knee joint, the RMS difference increased from threshold (Figure 19D) at DPI 16 [$t(7) = 3.566$, $p = 0.0091$], 23 [$t(7) = 4.245$, $p = 0.0038$], 30 [$t(7) = 3.634$, $p = 0.0084$], and 37 [$t(7) = 4.134$, $p = 0.0044$]. There were differences between time points [$F(5,7) = 6.25$, $p = 0.0027$], and there was a significant degree of recovery from the peak RMS difference at DPI 23 to DPI 44 ($p = 0.0168$). In stark contrast to average angle and range of motion at the knee joint, the ankle RMS difference was significantly increased above threshold at all time points for severe EAE animals (Figure 19F), DPI 9 ($p = 0.0042$), 16 ($p = 0.0009$), 23 ($p = 0.0050$), 30 ($p = 0.0103$), 37 ($p = 0.0058$) and 44 ($p = 0.0099$). There was a trend toward significant differences between time points but this did not quite reach statistical significance [$F(5,7) = 3.014$, $p = 0.0501$] and there was no significant recovery from peak ankle RMS difference at DPI 37 to DPI 44 ($p = 0.1258$). The kinematic changes, including RMS differences in CFA, mild and severe EAE mice are summarized in Table 4.

3.3.2 CORRELATIONS BETWEEN RMS DIFFERENCES AND CLINICAL SCORES

Hip RMS difference did not correlate with clinical score (Figure 20A) ($\rho = 0.02134$, $n = 92$, $p = 0.8339$). Knee RMS difference, however, was strongly correlated with clinical scores (Figure 20B) ($\rho = 0.7639$, $n = 92$, $p = <0.0001$). Knee RMS increased across clinical score [$F(6,85) = 51.43$, $p = <0.0001$] with first increase occurring at CS = 2.5 ($p = <0.0001$). There was a further increase from CS = 2.5 to 3.0 ($p = <0.0001$). Lastly, ankle RMS difference was also strongly correlated with clinical scores (Figure

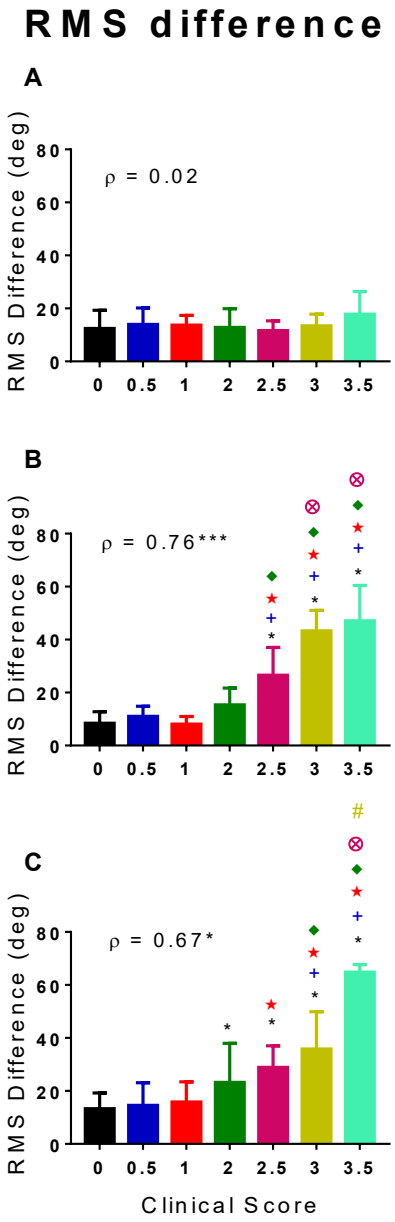

Figure 20: Knee and ankle RMS differences were strongly correlated with clinical scores. RMS differences for the hip **(A)**, knee **(B)**, and ankle **(C)** from all EAE animals pooled according to clinical score. **(A)** Hip RMS difference did not correlate with clinical scores. **(B)** Knee RMS difference was strongly correlated clinical scores and increased at CS = 2.5 and 3.0. **(C)** Ankle RMS difference also strongly correlated with clinical scores and increased at CS = 2.0, 3.0 and 3.5. Data are expressed as mean +/- SD and were analyzed by performing Spearman's rank order correlation as well as one-way ANOVA with Holm-Sidak's multiple comparisons test used to test for differences between every pair of clinical scores. For Spearman's rho (ρ), * $p < 0.05$, ** $p < 0.01$, *** $p < 0.001$. For bar graph, symbols indicate statistical significance at a level of 0.05 from a certain clinical score: * CS = 0.0, + CS = 0.5, ☆ CS = 1.0, ◆ CS = 2.0, ⊗ CS = 2.5, # CS = 3.0.

20C) ($\rho = 0.6691$, $n = 92$, $p = <0.0001$). Ankle RMS difference increased across clinical scores [$F(6,85) = 19.38$, $p = <0.0001$] and first increased relative to CS = 0.0 at CS = 2.0 ($p = 0.0146$). There were further increases from CS = 2.0 to 3.0 ($p = 0.0210$) and from CS = 3.0 to 3.5 ($p = 0.0013$).

3.4 PRE-CLINICAL GAIT CHANGES IN EAE

Between both severe and mild EAE experiments, there were changes in kinematics at DPI 9 for four parameters: hip range of motion and average angle, knee average angle, and ankle RMS. Of these, only hip range of motion changes in both experiments. To determine how robust these changes were, data from standard and mild EAE were pooled for DPI -2 and DPI 9. Average hip angle trended towards decreasing on DPI 9 (Figure 21A) ($p = 0.0573$). Average knee angle did significantly decrease at DPI 9 relative to DPI -2 (Figure 21B) ($p = 0.0101$). Hip range of motion also significantly decreased at DPI 9 (Figure 21C) ($p = <0.0001$) and lastly, ankle RMS difference was slightly higher than the baseline level of 9.082 (Figure 21D) ($p = 0.0010$). All of these changes were relatively small, with the exception of the change in hip range of motion, which constituted an almost 30% decrease. Changes in kinematic parameters across clinical scores are summarized in Figure 22, which illustrates the clinical scores at which specific gait deficits first occur (including pre-clinical changes) and Table 5, which shows the kinematic changes that characterize each clinical score from the previous one.

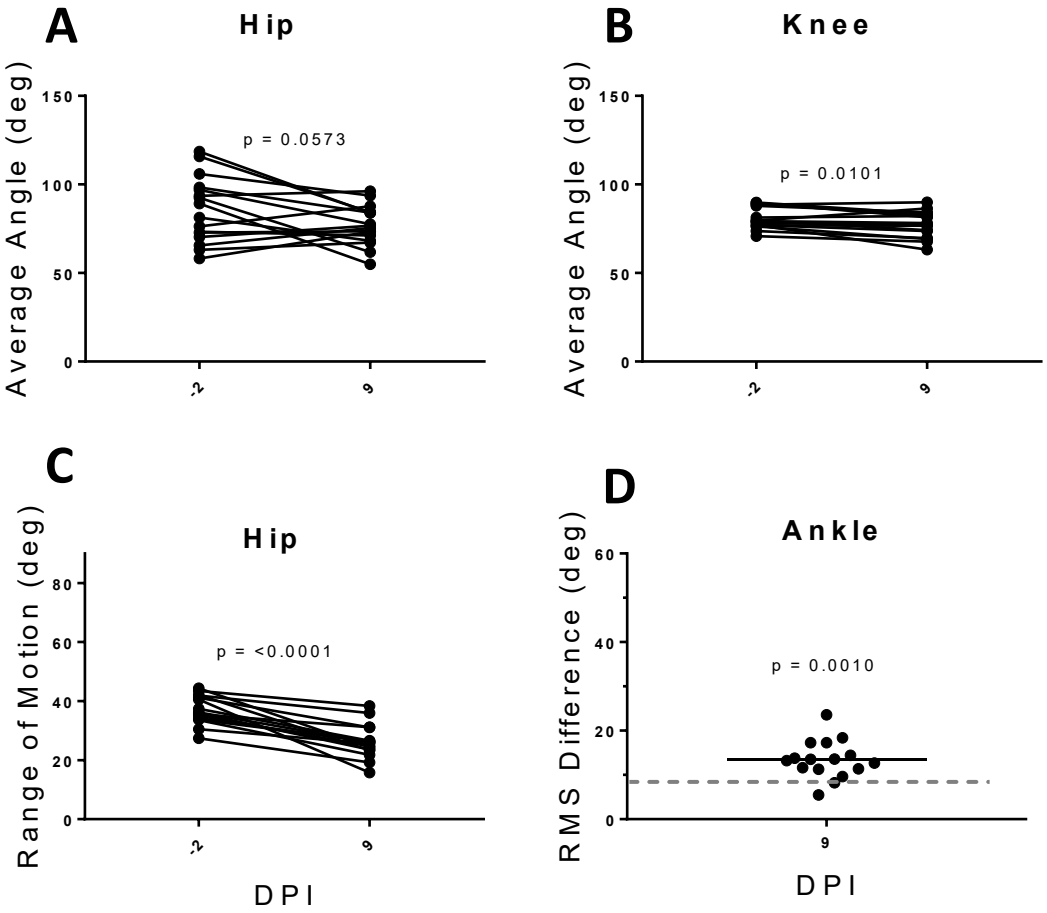

Figure 21: There were subtle changes in gait in preclinical changes in EAE mice at DPI 9. Pooled data from both mild and severe EAE mice for (A) average hip angle, **(B)** average knee angle, **(C)** hip range of motion, and **(D)** ankle RMS difference. **(A)** The average hip angle trended towards decreasing in pre-clinical EAE mice. **(B)** The average knee angle decreased slightly in EAE animals at DPI 9 relative to DPI -2. **(C)** The range of motion at the hip decreased at DPI 9 relative to DPI -2. **(D)** The ankle RMS was significantly higher than the threshold. For A-C, data are expressed as individual values, with lines connecting repeated measures and paired t-tests were used to assess statistical differences. For D, data are expressed as individual values with mean and one-sample t-test was used to test statistical difference from threshold. Data are expressed as individual values and mean (solid horizontal line) with the baseline RMS value shown as the hashed grey line. The grey line represents threshold value for the ankle = 9.086.

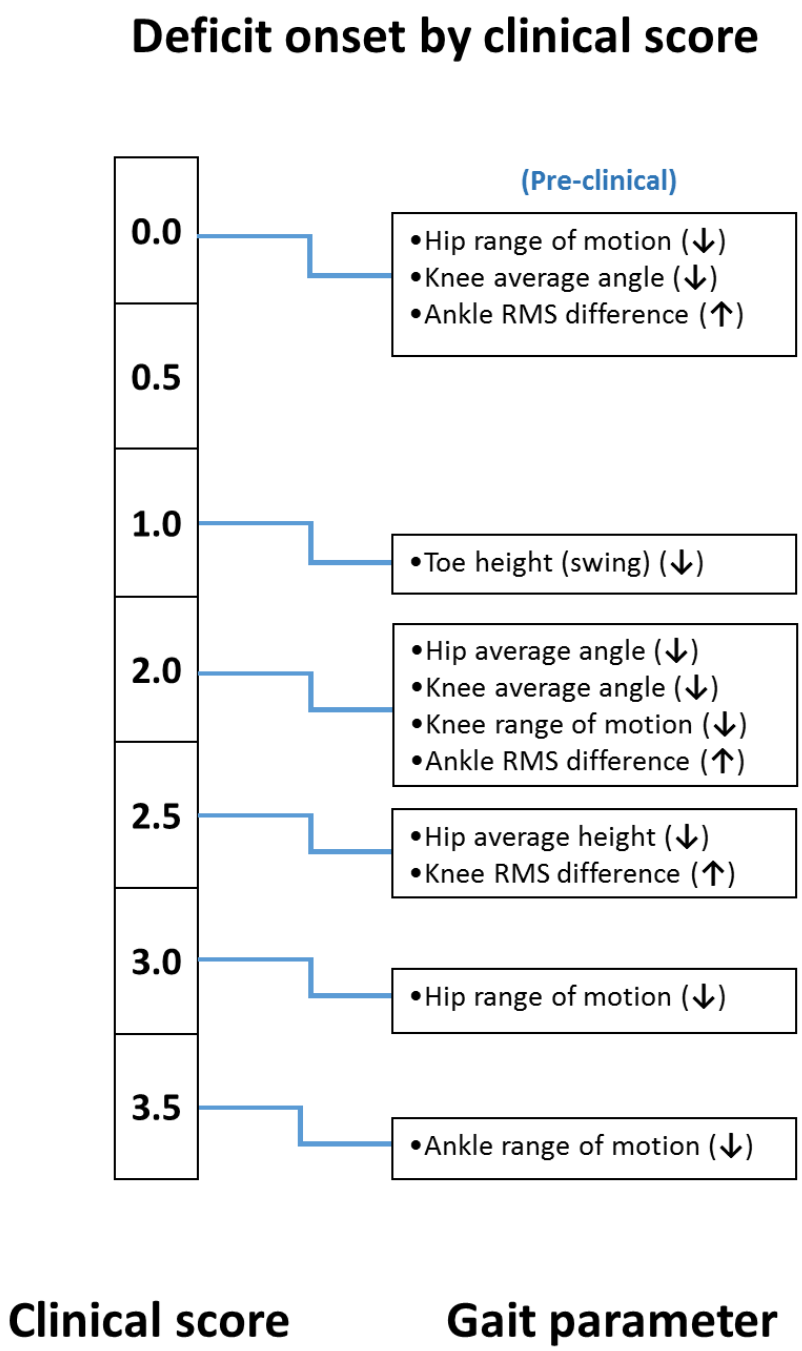

Figure 22: Summary of gait deficit onsets by clinical score. The earliest appearance of gait deficits with respect to clinical scores. All gait parameters examined are included except those that did not change at all or were not correlated with clinical score. Parameters that changed pre-clinically were included twice, for their pre-clinical and clinical onsets, respectively. ↓ or ↑ were used to indicate that a measure decreased or increased, respectively.

Table 5: The defining kinematic changes of each clinical score relative to the last.

CS [a]	Difference from previous CS Kinematic parameters
0.0	NA
0.5	None
1.0	• Avg [b] toe height during swing (↓)
2.0	• Knee range of motion (↓)
2.5	• Avg hip height (↓) • Knee range of motion (↓)
3.0	• Hip height (↓) • Avg toe height during swing (↓) • Avg knee angle (↓) • Hip range of motion (↓) • Knee range of motion (↓) • Knee RMS [c] difference (↑)
3.5	• Avg ankle angle (↑) • Ankle range of motion (↓)

[a] clinical score
[b] average
[c] root mean square

3.5 CORRELATING ROTAROD AND KINEMATIC PARAMETERS WITH WHITE MATTER LESION AREA

Finally, to determine which behavioural parameters best predicted the underlying pathology in EAE, clinical scores, rotarod latency measure and RMS differences for the hip, knee and ankle joints at the chronic time points (DPI 44 for standard EAE and DPI 37 for mild EAE) were compared with white matter lesion area in the spinal cord (L2-L5). Representative images of the lumbar spinal cord show the relationships between white matter loss, ankle RMS difference, rotarod performance and clinical score for increasing disease severity (Figure 23A-D). Clinical scores ($\rho = -0.8426$, $n = 16$, $p = <0.0001$) and rotarod performance ($r = -0.7467$, $n = 16$, $p = 0.0009$) were strongly correlated with white matter loss (Figure24A,B). The hip RMS difference at DPI 44 was not significantly correlated with white matter damage ($r = 0.1483$, $n = 16$, $p = 0.5836$) (Figure 25A). The knee RMS differences strongly correlated with white matter loss ($r = 0.6713$, $n = 16$, $p = 0.0044$) (Figure 25B). Lastly, the ankle RMS difference values showed an almost perfect relationship with white matter loss ($r = 0.9558$, $n = 16$, $p = <0.0001$) (Figure 25C).

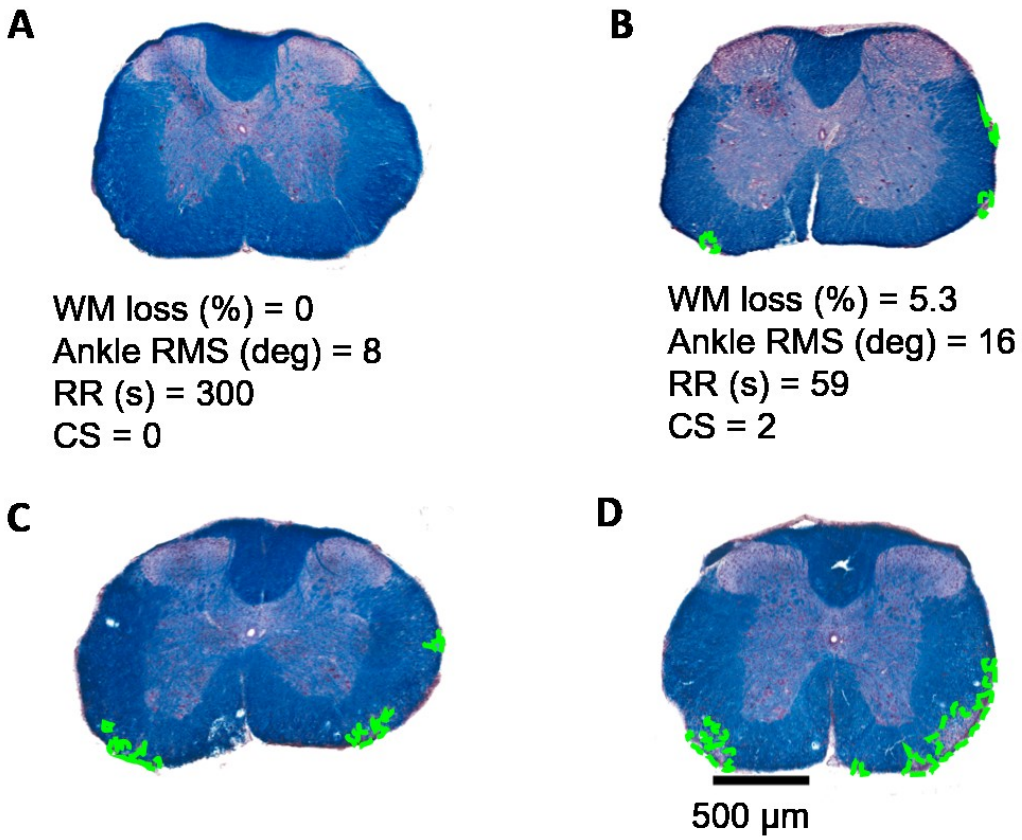

Figure 23: Measurement of white matter damage and correlation with behavioural parameters. **(A-D)** Representative sections from **(A)** CFA and **(B-D)** EAE animals with varying degrees of white matter damage and corresponding behavioural outcomes. White matter (WM), rotarod (RR), clinical score (CS).

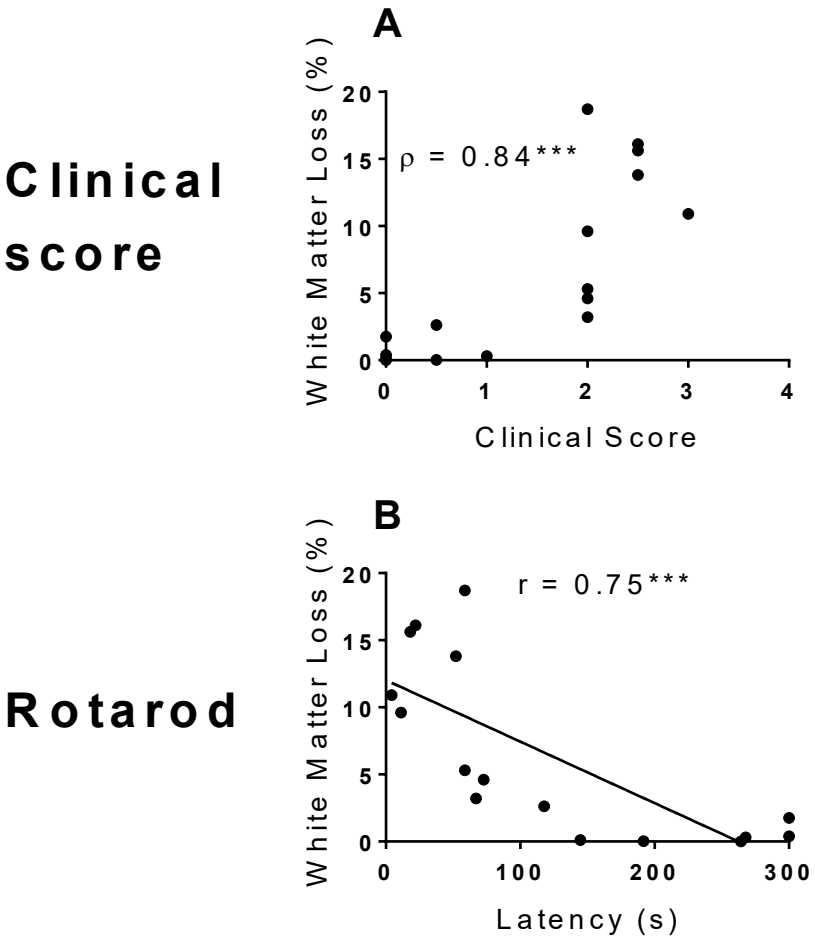

Figure 24: Clinical scores and rotarod performance correlated strongly with white matter loss in the lumbar spinal cord. **(A,B)** Scatterplots of **(A)** clinical scores and **(B)** rotarod latency at chronic time points against white matter loss, with Spearman's rho (ρ) **(A)**, and Pearson's r and linear regression **(B)** shown. * $p < 0.05$, ** $p < 0.01$, *** $p < 0.001$.

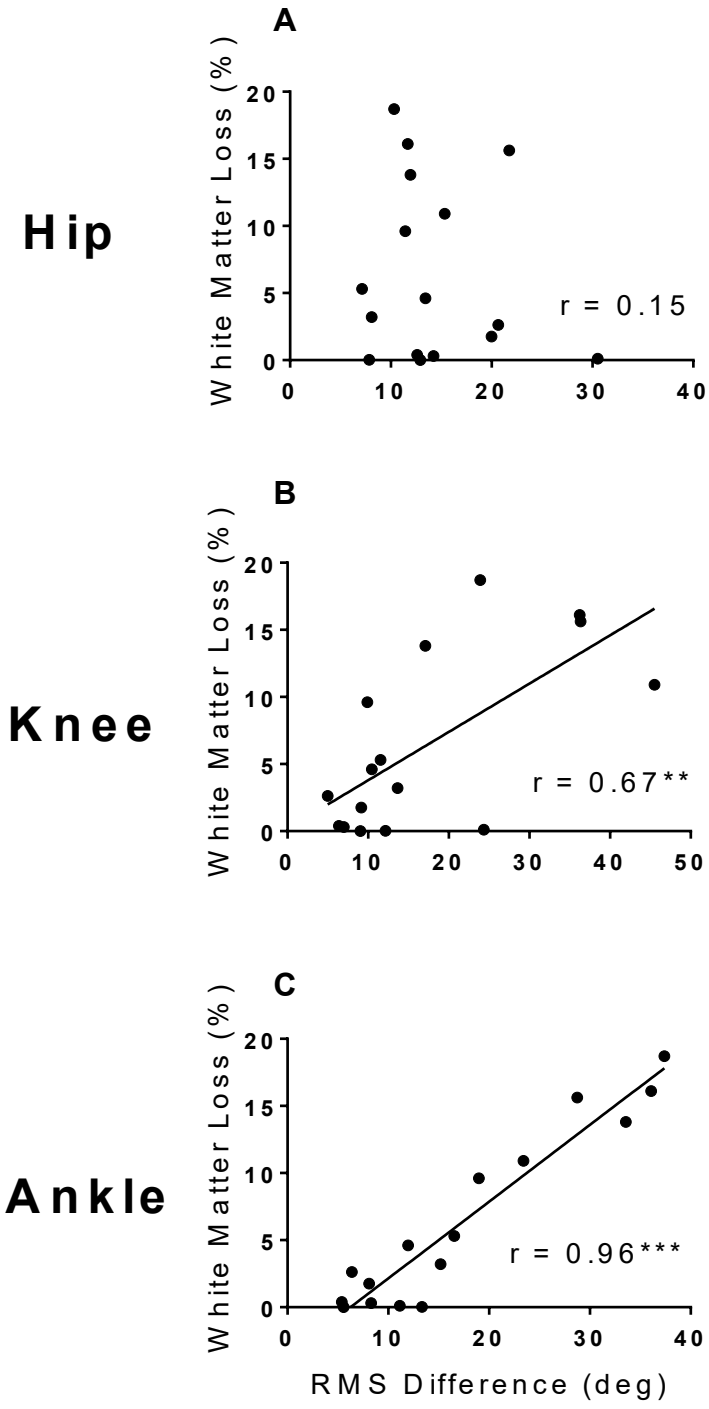

Figure 25: White matter damage in the lumbar spinal cord was highly correlated with ankle RMS difference. **(A-C)** Scatterplots of **(A)** hip, **(B)** knee, and **(C)** ankle RMS difference against white matter loss at time points, with linear regression and Pearson's r shown. **(A)** Hip RMS difference does not correlate with white matter loss. **(B)** Knee RMS correlates strongly with white matter loss. **(C)** Ankle RMS difference correlates very strongly with white matter loss. * $p < 0.05$, ** $p < 0.01$, *** $p < 0.001$.

CHAPTER 4: DISCUSSION

4.1 THE RELATIONSHIP BETWEEN CLINICAL SCORES AND ROTAROD PERFORMANCE

The present experiments revealed that clinical scores and rotarod performance in EAE mice were highly correlated in a negative manner at peak disease severity (DPI 16) (Figure 2C). However, clinical scores correlated weakly to moderately with rotarod performance in the later disease stages associated with recovery (DPI 23 and DPI 30; Figure 2D,E). These results are in agreement with findings reported by Sands et al. (2014) that also showed rotarod performance of SJL mice subjected to myelin proteolipid protein-induced EAE, a relapsing-remitting EAE model, correlated well at peak disease ($r^2 = 0.653$) but not during recovery. Similar to the findings of Sands et al. (2014), I have found that clinical scores during disease remission clustered tightly in the lower-middle range of the scale (1.5-2.5; Figure 2D) while rotarod fall latencies varied more greatly reflecting minor to severe impairments in motor coordination [48].

To determine the predictive values of clinical scores for rotarod performance, EAE animals were classified as asymptomatic, moderately sick or severely sick according to clinical score or rotarod performance as described by van den Berg et al. [4]. This classification scheme revealed that the ability of clinical scores to predict rotarod category was less than 50% for moderately sick animals. Only 37 of the 80 animals that were classified as moderately sick according to clinical scores (0.5-2.5) were also assessed as moderately sick by rotarod (latencies of 150-250 s) (Figure 2F). In contrast, when animals were classified as by clinical score as asymptomatic (0) or severely sick (≤3), the corresponding rotarod-based classifications were in agreement 84

and 100% of the time, respectively. These results are consistent with findings from van den Berg et al. which showed a similar breakdown of the clinical scoring system in predicting the rotarod performance of moderately sick mice [4]. Clinical scores are therefore good predictors of rotarod performance at either extreme of the clinical scale, where animals performed well or poorly, but at the intermediate levels of the scale this relationship was substantially weaker. This suggests that rotarod is providing additional information about motor function of animals in the intermediate levels of the clinical scoring scale that is not captured by clinical scoring alone. However, the high level of agreement between rotarod performance and clinical scores for asymptomatic and severely sick animals suggests that, for these animals, rotarod does not provide additional information beyond what is captured by clinical scoring. Behavioural assays that can provide more information than clinical scores about mice of all levels of disease severity would be much more useful in assessing motor dysfunction.

4.2 KINEMATIC GAIT ANALYSIS OF EAE MICE

4.2.1 PREVIOUS GAIT ANALYSIS IN EAE

Gait changes in Lewis rats subjected to EAE have been studied previously by footprint measurements [56;57]. These studies reported decreased stride length as a characteristic of EAE that normalized with improved clinical scores [56]. Silva et al. (2014) used the CatWalk System to analyze gait in the ventral plane (from underneath the animal) of C57BL/6 mice subjected to MOG_{35-55}-induced EAE. This group observed decreases in both the contact area of paws on the ground and gait regularity [60]. Mitra et al. (2015) found comparable reductions in hindlimb stride length in the same EAE model [67]. These previous studies that have analyzed gait from the ventral plane

provided limited information about walking deficits in EAE mice. Analysis of the footprints from animals whose paws have been dipped in ink yields only spatial information about paw placement, while the Catwalk System records videos of the animals walking from beneath, which solely provides temporal and spatial information about paw placements. Ventral plane analysis of gait is limited by poor sensitivity and high variability that reduce reproducibility [49]. Furthermore, measuring just foot placements provides no information about how movement of the limbs and body have occurred to obtain each foot placement. This markedly restricts the information that can be derived from such measurements about behavioural compensations which potentially confounds interpretation of functional recovery. For example, in two other mouse models of neurodegenerative disease, Huntington's disease and amyotrophic lateral sclerosis (ALS), most gait changes occur in the sagittal plane, indicating the marginal value of ventral plane analyses [49].

There has been only one study that employed sagittal plane kinematics to the study of movement by EAE mice. De Bruin et al. (2016) reported using kinematic gait analysis as part of a detailed behavioural analysis of the effects of two clinically approved therapeutics for MS, fingolimod and dimethyl fumarate, in SJL-PLP mice [58]. The only parameters found to be affected were tail distance from the ground and hindlimb stride length [42;58]. Unfortunately, interpretation of these results is limited to changes measured only at disease remission. Without comparisons between measurements at baseline, peak disease and remission, it is unclear how these therapeutics influenced gait characteristics in animals with varying motor impairments during the disease course. In order to better understand motor changes across the whole spectrum of EAE disease severity, kinematic gait analysis was used to characterize locomotor changes produced by EAE. This is the first study to characterize

gait changes in EAE mice from the perspective of joint kinematics. This study is therefore highly novel in that it achieved the following: (1) First characterization of gait changes in EAE mice using kinematic gait analysis and (2) reported changes in joint angle kinematics in EAE, and (3) the only study to correlate kinematic parameters with spinal cord pathology.

4.2.2 BARRIERS TO USING BETTER BEHAVIOURAL ASSAYS IN EAE

Detailed behavioural analyses of motor function, including kinematic analyses have been performed in various mouse models of CNS injury and neurodegeneration, including spinal cord injury, ALS, traumatic cortical injuries and stroke, Huntington's disease and Parkinson's disease [27;31;49-52;61;68]. In contrast, behavioural analyses of EAE mice beyond clinical scoring is rare with few studies using rotarod or other behavioural measures. Only recently has there been modest growth in the number of studies using behavioural tests other than clinical scoring to assess locomotor deficits in EAE mice.

The heterogeneous nature of motor deficits in EAE requires extensive studies with sophisticated behavioural assays to obtain the necessary statistical power and information required to accurately characterize the sources of these variations. For instance, the random temporal and spatial distributions of inflammatory lesions in the spinal cord that occur in EAE have varied effects on motor symptoms [4]. Differences in the degree to which these lesions are repaired may also impact recovery from EAE in complex ways. These complexities have been cited as the reason for infrequent use of sophisticated behavioural analyses in the EAE field [69]. In response to this problem, one group has created a localized EAE model were the lesion can be targeted to specific

spinal cord tracts via stereotactic injection of pro-inflammatory cytokines at a precise location in mice sensitized with a sub-clinical immunization procedure [70]. This focal model has been used to gain an understanding of how inflammatory lesions at discrete locations within the CNS manifest from a functional perspective and how functional recovery occurs [71]. However, this model is of limited clinical value because like MS, EAE is characterized by sporadic demyelinating lesions in the CNS [4].

Some investigators have questioned whether there is much to be gained by using more sophisticated behavioural assays, citing the correlations between clinical scores and other measures such as impaired rotarod performance and grip strength as being of little value beyond the use of clinical scores to assess functional deficits resulting from EAE [34]. This conclusion is flawed by a failure to consider the confounding impacts of observer subjectivity, lack of sensitivity and the ordinal level of data obtained from clinical scoring. The ordinal level of data derived from clinical scoring is particularly problematic because it does not reflect a continuous scale of measurement. As a result, differences between each level of clinical scoring do not necessarily correspond to the same degree of motor impairment. My demonstration that clinical scores within the low-middle range fail to accurately predict rotarod performance supports these limitations.

4.2.3 GAIT CHANGES IN CFA MICE

Kinematic analyses were performed on CFA animals to account for the possibility that the immunization procedure itself rather than EAE may change gait. It seemed possible that sham immunization with just CFA might induce gait changes because injection of CFA can cause painful focal ulcerative skin lesions while injections of CFA

into or around joints in the hindlimbs can induce monoarthritis [72;73]. As the injection sites were relatively close to the hip joint, both of these occurrences could potentially alter gait. CFA-induced monoarthritis can be achieved by either intra-articular injection into the knee or ankle joint, or by s.c. injection around the desired joint, leading to a variety of gait changes [72;74]. In C57Bl/6 mice, intra-articular injection of CFA into the right ankle joint resulted in decreased gait regularity, decreased stance duration coupled with increased swing duration, and reduced paw pressure while walking relative to the left hindlimb. To the best of my knowledge, the effects of CFA injections at the hip joints on gait have not been previously described. Potential gait changes resulting from this procedure are therefore unknown. Relative to the baseline recording at DPI -2, I only observed a slight increase in the range of motion at the knee joint of less than 20 % at DPI 16 and 30 in CFA mice (Figure 12B). This may be the result of pain or discomfort from the CFA injections, but the changes were small and were in the opposite direction of what was seen in EAE mice. It is therefore unlikely that gait deficits observed in EAE mice are caused by the CFA injections. However, these findings also suggest that sagittal kinematic analysis of the hindlimb joint angles in mouse models of arthritis may reveal the effects of more severe inflammatory joint damage and pain on gait.

4.2.4 PRE-CLINICAL CHANGES IN EAE MICE

Kinematic gait analysis on DPI 9, 2-3 days before clinical onset, revealed minor changes towards differences in four kinematic parameters: The average angles of the hip and knee joints, the range of motion of the hip and the ankle RMS difference (Figure 21A-D). The decrease in hip range of motion observed at DPI 9 persisted throughout the course of EAE but did not worsen with clinical onset or change in a consistent manner (Figure9 D,F).

It is well established that there is axonal loss and spinal cord inflammation prior to the onset of clinical symptoms in EAE [34;75]. In contrast, there have been few descriptions of behavioural changes prior to the onset of clinical symptoms (before the detection of tail weakness). Two groups have reported early decreases in spontaneous home cage and open field activity respectively, but it is unclear whether these differences reflected actual motor deficits or reduced locomotion because of cognitive/emotional changes in the mice [75;76]. When handling EAE mice, I observed that these animals often seemed slightly weaker several days (around DPI 9) prior to disease onset (DPI 10-11). My finding of pre-clinical changes in gait support this observation and suggests that the decrease in hip range of motion is an early sign of hindlimb weakness.

4.2.5 CHANGES IN BODY HEIGHT AND TOE HEIGHT DURING GAIT

Based on most clinical scoring scales, including my own, EAE is characterized by an ascending paralysis that eventually involves the hindlimbs resulting in an inability to support body weight (CS = 3, dropped pelvis). This was reflected by a 30% decrease in hip height for mice with severe EAE relative to baseline at both the early (DPI 16), peak (DPI 23) and chronic time points (DPI 30, 37 and 44) (Figure 3E,F). The absence of full recovery of this measure by DPI 44 indicates long-lasting paralysis in EAE animals. As shown in Figure 5, the first reduction in hip height occurred at CS = 2.5, and was followed by a further decrease at CS = 3.0. Since reduced hip height was not detected in animals with clinical scores less than 2.5 (i.e. less than major walking deficits) in hip height are indicative of greater disease severity.

The average toe height during the swing phase was also measured. It was expected that this would also decrease in EAE animals as they became weaker. As predicted, a decrease was observed at peak disease in both mild (DPI 16) and severe EAE (DPI 23) mice (Figure 4C-F). In animals with mild EAE, the decrease in toe height was transient, occurring only at peak disease while this kinematic measure did not recover until DPI 44 in severe EAE mice. Deficits in toe height during swing were one of the earliest changes detected, decreasing at CS = 1.0, which represents a flaccid tail or tail weakness accompanied by hindlimb splay (Figure 6). The fact that recovery was seen in EAE mice whose clinical scores were still above 1.0 indicates that behavioural compensations in gait enable improved toe clearance during the swing phase. Unsurprisingly, toe height is further decreased at CS = 3.0 when animals had dropped pelvises, meaning that decreases in toe height are characteristic of both mild and severe motor impairment due to EAE. Reduced toe height characterized by a dragging of the toe is a common feature of spinal cord injury in rats and mice. However, the small size and rapid movements of mice make accurate toe height measurements nearly impossible to accurately quantify without the use of high speed image analysis [77-79]. In contrast to EAE mice, SOD1 G93A mice that suffer a progressive loss of motor neurons resulting in hindlimb paralysis showed increased maximal toe height that diminished over time as gait abnormalities accumulated [49]. These finding suggest that changes in toe height are subject to compensation for hindlimb paralysis. Like the *ho15J* genetic mouse model of cerebellar degeneration, EAE mice often display ataxic gait (clinical scores of 2.0-2.5). However, unlike EAE animals, maximal toe height is increased in *ho15J* mice suggesting that different mechanisms contribute to gait deficits in these two models [80].

4.2.6 CHANGES IN HIP KINEMATICS

In both mild and severe EAE mice, impaired hip range of motion was first detected at the preclinical stage of disease. Interestingly, these changes persisted in mild EAE but disappeared at DPI 30-44 in mice with severe EAE (Figure 9 C,E). In addition, average angle was also persistently reduced in mild EAE mice beginning at DPI 9 (Figure 9D). However, in mice with severe EAE, there were small elevations in average hip angle DPI 16 and 37 (Figure 9F). It therefore appears that hip average angle changes differently depending on the severity of disease. Indeed, when looking at the relationship between hip kinematic parameters and clinical scores, there are weak to moderate correlations between hip average angle and range of motion with clinical scores (Figure 10A,B).

4.2.7 CHANGES IN KNEE KINEMATICS

Differences between the average angle and range of motion of the knee joint for mild and severe EAE mice were also detected. In mild EAE, a reduction in the average knee angle was observed before the onset of clinical signs (Figure 12C). However, by comparison to mice with severe EAE that displayed marked reductions in average angle of the knee, these changes were modest (Figure 12E). Range of motion at the knee joint was also dramatically reduced in severe EAE, but not in mild EAE. Both parameters were strongly correlated with clinical scores (Figure 13A,B). Taken together, these results indicate that changes in knee kinematics are a robust feature of EAE but they occur only at intermediate to severe levels of disease severity, first appearing at CS = 2.0. The decreased average angle and range of motion of the knee in EAE mice are

consistent with a failure to support body weight resulting in knee hyper-flexion in EAE mice.

4.2.8 CHANGES IN ANKLE KINEMATICS

Mice with mild EAE failed to show changes in average angle for the knee and only minor reduction in the range of motion for this joint (Figure 15C,D). In comparison, mice with severe EAE displayed no consistent changes in these two kinematic measures. Interestingly, however, there were large increases in variability for both of these parameters in the case of severe EAE (Figure 15E,F). This indicates that changes were occurring, but in opposite directions producing highly variable results between animals with similar clinical scores. Similar to the hip this high variability masked the detection of statistical differences. Examining ankle kinematic parameters in relationship to clinical scores supports this conclusion, as average ankle angle is not correlated with clinical scores and ankle range of motion is only weakly correlated (Figure 16A,B). The only robust change observed for either parameter occurred in mice with CS = 3.5, when a hindlimb was paralyzed. At this clinical score the average angle increased dramatically and the range of motion decreases to near 0 as the leg drags limply behind the mouse.

4.3 ROOT MEAN SQUARE DIFFERENCE

4.3.1 ROOT MEAN SQUARE DIFFERENCE AS A USEFUL MEASURE OF DEVIATION FROM NORMAL GAIT

The gait profile score (GPS) has been developed to overcome limitations imposed by the volume and complexity of kinematic data in human studies [62]. It has recently been employed to characterize gait deficits in people with MS [81]. The GPS is a single number that represents the average deviation across nine kinematic variables from three dimensional gait analysis, and therefore is an overall measure of gait pathology in humans. For each of these kinematic variables a gait variable score (GVS) is calculated. The GVS is the root mean square (RMS) of the difference between the individual's data over an average step cycle and a normal reference step cycle. For example, in the context of these experiments,if the gait variable being assessed is ankle dorsi- and plantar flexion (i.e. ankle angle), the angle of the ankle at each point of the step cycle in an individual with gait pathology (DPI 30) is compared to the angle of the ankle at each point of the step cycle in a non-pathological gait (Baseline) (Figure 17A). This yields a difference in degrees between pathological and normal gaits at each point of the step cycle (Figure 17B). The difference at each point of the step cycle is then condensed into a single number that represents the average distance between the two gaits (Figure 17Cii). Therefore, RMS difference does not describe *how* each variable changes, but rather *how much* each variable changes. This approach therefore precluded the possibility that differences in opposite directions will cancel each other out, as illustrated in Figure 9. The value of calculating RMS difference is that all of the values are squared thereby removing the directionality (all values are now positive) of the differences (Figure 17B). The RMS difference is based on joint position at each part of the step cycle, thereby yielding a single value that represents the complexities of joint angle movement during pathological gait [82]. Moreover, my studies show that RMS difference accurately quantifies the degree to which pathological gait is changed from

normal gait, independent of the way gait changes, making it a highly useful measure for assessing complex gait deficits in EAE mice.

4.3.2 EAE PROGRESSION IS CHARACTERIZED BY INCREASING RMS DIFFERENCES

The RMS was calculated for hip flexion-extension, knee flexion-extension and ankle dorsi- and plantar flexion or, as referred, to herein, hip, knee and ankle angles. The RMS differences for the hip, knee and ankle angles, recorded a week apart in naïve animals, revealed small inter-session variabilities for each joint (hip, 11 degrees; knee, 7.5 degrees; ankle, 9 degrees) that were used as the threshold or normal level of variability (Figure 17D). The RMS differences between post-immunization measurements and baseline measurements (DPI -2) for each of these joints in CFA, mild and severe EAE animals were then compared. As expected, CFA animals did not display differences from baseline at DPI 16 or DPI 30 (Figure 18A-C). Mild EAE was characterized by small increases in the RMS differences from baseline for the knee and ankle only at DPI 37 or DPI 16, respectively (Figure 19A,C). By contrast, robust increases in RMS difference were found at both the knee and ankle joints for DPI 16-44 of severe EAE mice indicating that movements of these joints were most disturbed (Figure 19D,F). Additionally, both knee and ankle RMS differences were strongly correlated with clinical scores and showed increases at clinical scores of 2.0 and 2.5, which are indicative of walking deficits (Figure 20B,C). The increased RMS difference in the knee is not surprising because my previous analyses revealed substantially reductions in range of motion and average angle that were highly correlated with clinical scores. However, the finding of increased ankle RMS differences is remarkable

considering that no differences in average ankle angle or range of motion were observed relative to baseline.

These findings confirm that ankle movements are highly perturbed in EAE but also that the changes are complex and not easily described using basic kinematic parameters. The increase in RMS difference for the hip joint at DPI 37 for mild EAE is interesting because no changes in hip RMS difference were observed in mice with severe EAE. This is consistent with the other kinematic measures of the hip joint which show that in mild EAE there are more robust changes in hip kinematics than in severe EAE mice. This discrepancy is puzzling because one would not expect mild EAE mice to exhibit deficits that are not present in more severely sick mice. This suggests that changes in hip kinematics mostly occur in mildly sick animals and that in more impaired EAE animals,increased variability at the hip joint or larger gait changes in other joints may mask alterations at the hip joint.

4.4 CORRELATING WHITE MATTER LOSS WITH BEHAVIOURAL PARAMETERS

4.4.1 WHITE MATTER LESION AREA WAS VERY STRONGLY CORRELATED WITH ANKLE RMS DIFFERENCE

As a final measure, the percent white matter loss in the lumbar spinal cord was correlated with several behavioural parameters. Clinical scores ($\rho = 0.84$) and rotarod ($r = -0.75$) performance at the last time point were strongly correlated with white matter loss, but the relationship was not perfect, as evidenced by the wide range of white matter damage found in the spinal cords of animals with CS = 2.0 (Figure 24A,B). These correlations are similar in strength to those reported previously [83]. The hip RMS ($r =$

0.15) did not correlate at all with white matter loss (Figure 25A). This result corroborates the finding that hip RMS was relatively unchanged by EAE. The correlation between knee RMS and white matter loss (r=0.67) was comparable in strength to the correlations of both clinical score and rotarod latency with white matter loss (Figure 25B). This is consistent with changes in knee kinematics as being highly correlated with clinical score severity. Finally, there was a striking correlation between ankle RMS difference and white matter loss (r = 0.96), with an almost perfect linear relationship being observed between the two variables (Figure 25C). Correlations as strong as this between behavioural parameters and histopathology are very rarely observed.

4.4.2 CLINICAL IMPLICATION OF THE EXCEPTIONAL STRONG CORRELATION BETWEEN ANKLE RMS DIFFERENCES AND WHITE MATTER LOSS IN THE SPINAL CORD

One of the classic unresolved issues in the field of MS research is the weak relationship between clinical disability and MRI measures of disease burden. The source of the problem is that the rate of disease progression according to MRI is greater than the progression of clinical disability [84]. The traditional explanation of this has been that the traditional MRI measures of T2-weighted and T1 lesions loads are not able to differentiate between differences in the underlying histopathology of these lesions and therefore are unable to provide information about which types of lesions are related to clinical disability [84]. Because of this, a large amount of work has been done to improve MRI techniques and to develop novel measures of disease activity. However, the other possibility is that clinical measures of disability are not sensitive enough to reflect changes in MRI lesion load. So perhaps the question could be rephrased from “what types of changes in the CNS produce clinical disability?”, to “are there more sensitive

clinical tools that better reflect CNS damage?" Although kinematic gait analysis is used as a clinical tool, there have not been any reports of correlations between kinematic changes with MRI lesion load.

Given the extremely tight relationship between changes in kinematics at the ankle joint and white matter loss in the spinal cord, this kinematic measure could be an extremely useful tool for clinical assessment in people with MS and in animal models. Although further experiments are needed to discern whether ankle RMS difference correlates well with white matter loss at all phases of disease, these findings raise the possibility that ankle RMS difference may be representative of the amount of white matter damage at all time points. If this were the case, this behavioural readout could provide detailed temporal information about the time course of demyelination and remyelination in EAE mice by performing repeated testing. One of the classic challenges of measuring recovery, whether it be assessing remyelination or resolution of inflammation in the CNS of EAE mice, is that histological or biochemical analyses can only be performed when tissue is harvested from the mice. This obviously restricts these analyses to a single time point per mouse. Behavioural analysis cannot replace the information gained from morphological and biochemical analyses, but could offer insights into the nature of neurological deficits and functional recovery within the same animal. This would improve the detection of putative therapeutics that reduce disease progression or promote CNS repair.

The histological procedures performed in this study were relatively basic and did not yield detailed information about the neuropathological nature of the white matter lesions measured or the precise anatomical localization of these lesions. The white matter lesions observed after eriochrome cyanine could be the consequence of three

factors alone or in combination: (1) demyelination of intact axons, (2) loss of axons and the subsequent disappearance of myelin, and (3) displacement of axons and myelin by inflammatory infiltrates. Another limitation is that determination of the precise anatomical locations of these lesions was not part of the analysis. This is important because the anatomical location of the lesions could determine their functional impact on the mouse. Hence, a more detailed immunohistochemical analyses of the degree and localization of demyelination, axonal damage and inflammation are warranted.

Another implication of this work is that anatomical localization of spinal cord lesions may not be as important in EAE as has been traditionally assumed. It is well established that, in cases of spinal cord injury, lesions localized to particular spinal tracts give rise to characteristic behavioural changes depending on the neural networks affected [52;68]. The same has often been assumed with EAE, but evidence for this is limited. Kuertan et al. (2007), in a detailed analysis of the kinetics and spatial distribution of histopathology in three different EAE models, described substantial histopathological differences between these models, but also observed nearly identical clinical disease in all of them [83]. These findings may reflect the failure of clinical scores to detect the effects of differences in CNS lesion distribution on motor disability. On the other hand, the near perfect linear relationship between percent white matter area damaged and ankle RMS difference observed herein strongly suggests that lesion burden rather than location is the primary driver of gait changes and motor disability. However, analysis of the anatomical distribution of CNS histopathology in different EAE models coupled with kinematic analysis will be necessary to establish whether this is the case. These studies could yield mechanistic insights into how CNS damage translates into behavioural deficits in the context of inflammatory disease that would enable the development of better therapeutics for MS.

There are a number of reasons why the ankle RMS difference may be so sensitive to white matter lesions in EAE. First, the lower lumbar and sacral segments of the spinal cord have been reported to have the highest density of white matter lesions in C57Bl/6 mice subjected to MOG_{35-55}-induced EAE [4]. As the lower motor neurons of the muscles of the ankle angle are located in these segments, it makes sense that these muscle groups are the most severely affected. Second, because of the interdependence of movements of the segments of leg, changes in the movements of the more proximal hip and knee joints are likely to influence movements of the ankle joint. Increased RMS differences of the ankle may therefore reflect complex compensations or responses to deviations of the muscles of the knee or hip rather than just muscle weakness at the ankle. Finally, the foot-ankle mechanism plays many critical roles in gait including propulsion, balance, weight bearing, shock absorption and adapting to changes in terrain [85]. To perform these various tasks, the ankle is equipped with a large number of proprioceptors that provide the brain with detailed temporal and spatial information about movement [86]. As a consequence, an exceptional amount of neural circuitry is devoted to the precise regulation of ankle movement [85;87-89]. This may explain the remarkable sensitivity of ankle joint movement to stroke or spinal cord injury. Two of the most common gait deficits in these clinical situations are foot drop (decreased ability to clear the foot from the ground during swing) and a decrease in walking speed, which correspond to a pronounced weakness in the distal muscles of the leg, including the ankle dorsi- and plantar flexors [85;90-92].

4.5 RELATING GAIT CHANGES OBSERVED IN EAE TO THOSE SEEN IN PEOPLE WITH MS

Some of the most commonly described changes in walking ability in people with MS are decreases in walking speed and distance [93]. Several clinical measures including the EDSS, the timed 25-foot walk and six-minute walk use these changes to measure disability [93]. As mentioned previously, I observed that animals with EAE could not walk as quickly as naïve or CFA animals. Quantification of these changes in walking speed and ability could be a valuable measure of functional disability. In particular, examining differences in walking speed in freely moving EAE animals and assessing their maximum walking velocities imposed by varying treadmill speeds could be valuable behavioural markers of disease severity.

A number of kinematic changes have been proposed to play a role in the decrease in walking speed of people with MS, including a reduced ability to extend hip, knee and ankle joints of the leg to oppose gravity and propel the body forward during different parts of the step cycle [82]. All three of these changes are part of a progressive flattening of joint angles, or a decrease in angular range of motion due to muscle weakness that occurs with increasing MS disease severity [94]. There are some similarities that can be drawn to the changes occurring in EAE mice. First, there were decreases in the range of motion in both the knee and hip joints of EAE animals. Second, this decrease in range of motion is associated with decreased average angles for those joints over the whole step cycle, indicating an inability to extend the joint and oppose gravity. These changes may contribute to the decreased stride length previously described in EAE animals [56;57;59;60]. On the other hand, in the present experiment, changes in ankle kinematics for severe EAE mice were more complicated and no simple pattern could be deciphered from examining the average angle and range of motion of this joint. However, evidence of a slight decrease in the range of motion of the ankle was

found in mild EAE animals. This corresponds with findings from studies on people with MS with minimal or no clinical impairment which have found reduced range of motion of the ankle joint [95;96]. It has been proposed that this stiffening of the ankle joint is a balance mechanism that is the result of perceived instability in MS patients which may also be the case in EAE mice [82].

One outcome of a stiffening of the ankle joint is foot drop, which is a gait abnormality where the foot is unable to dorsiflex (or lift the toes of the foot upwards) during swing. This results in impaired clearance of the foot from the ground, meaning that the toes of the foot often drag on the ground during the swing phase [82]. This is common in people with MS even at minimally impaired disease stages, and it is clinically significant because it increases the risk of tripping and may also contribute to decreased walking speed. In the present work, the toe height during swing was decreased in both mild and moderate EAE. Toe drag in animals with CS = 3.0 is not surprising because the animal's pelvises were on the ground. However, it is interesting that a decrease in toe height during swing is an early change in EAE, with it being observed starting at CS = 1.0 in animals with no obvious gait deficits. This suggests that EAE may be a useful animal model to study the mechanisms and possible treatment of foot drop in MS.

4.6 LIMITATIONS AND FUTURE DIRECTIONS

There are some limitations to the present study that have been discussed in more detail as they arose throughout this work, but are summarized here. First, EAE mice and healthy mice were not recorded walking at the same speed due to differences in the speed at which optimal recordings could be obtained. The normalization of swing and stance durations for all recordings enabled the comparison of gait kinematics in

mice walking at different speeds, but this approach cannot account for the fact that (1) if mice are walking at different speeds it is impossible to compare parameters that are highly correlated with walking speed, like stance duration and step length, and velocity of leg movements, (2) there may be subtle changes in kinematic parameters that, although less correlated with walking speed, are still affected. Second, the histology done herein is relatively basic and more sophisticated immunohistochemical methods and anatomical analysis methods could better reveal the neuroanatomical substrates of gait impairment in EAE mice. Finally, study of the effects of pharmacological interventions that that promote recovery would be useful to test the utility of this technique in drug discovery. The sensitivity of this technique may enable the detection of subtle improvements in gait that are not detected by clinical scores or rotarod performance and allow the dissociation of functional impairment as a result of inflammatory damage

4.7 CONCLUSION

The present study examined motor and gait impairment in the MOG_{35-55}-induced EAE in C57Bl/6 mice. This study (1) replicated and expanded on the recent descriptions of the relationship between rotarod performance and clinical scores, (2) characterized gait changes in mildly and severely sick EAE animals (3) employed aspects of the GPS (i.e. calculation of RMS difference) for the first time to rodent kinematic gait analysis (4) correlated kinematic parameters and traditional behavioural outcomes with white matter loss in the spinal cord.

This study is the first to report changes in sagittal plane kinematics in an EAE model. The characterization of gait changes reported herein, revealed several gait deficits that are similar between EAE and MS. The identification of similar gait deficits in

both diseases means that improved mechanistic understanding of how cellular and molecular pathological changes in EAE animals result in behavioural abnormalities, could also yield insights into the mechanisms of disability in MS. A better understanding of these mechanisms could aid in the discovery of new targets for treatment of people with MS. Calculating the RMS difference between pathological and normal gait is an approach that was developed for use in human gait research to represent overall quality of gait. To my knowledge it has not been previously applied to rodent models. In this study, the RMS difference was shown to be a useful tool studying gait perturbations in EAE mice that was highly correlated with underlying histopathology. This parameter also likely has utility in studies of other animal models of neurological disorders that involve motor impairment. Because calculating RMS differences in the analysis of kinematic data was developed for human research, its employment in animal studies may facilitate the translation of findings from such studies to humans. Finally, the sensitivity of kinematic gait analysis to subtle changes in gait deficits means that this technique has obvious utility in studies that examine the effects of putative therapeutic interventions.

In conclusion, the application of kinematic gait analysis to mice with EAE yields a tremendous amount of information about the behavioural consequences of auto-immune-mediated demyelination in the CNS and should be employed in future studies. In the field of spinal cord injury, it has been established that measuring the functional outcome of injury and treatment is of the utmost importance, as evidenced by the large body of research devoted to behavioural analyses of these animals. In contrast, the field of EAE research is dominated by clinical scoring, a relatively crude approach to measuring functional outcomes. Although clinical scoring is not without value, the use of more quantitative, sensitive, and informative behavioural measures will enhance the

quality of EAE research and improve our ability to translate findings from animal studies to humans living with this debilitating disease.

Bibliography

[1] A. M. Lavery, L. H. Verhey, and A. T. Waldman, "Outcome measures in relapsing-remitting multiple sclerosis: capturing disability and disease progression in clinical trials," *Mult. Scler. Int.*, vol. 2014, p. 262350, 2014.

[2] C. S. Constantinescu, N. Farooqi, K. O'Brien, and B. Gran, "Experimental autoimmune encephalomyelitis (EAE) as a model for multiple sclerosis (MS)," *Br. J. Pharmacol.*, vol. 164, no. 4, pp. 1079-1106, Oct.2011.

[3] M. R. Emerson, R. J. Gallagher, J. G. Marquis, and S. M. LeVine, "Enhancing the ability of experimental autoimmune encephalomyelitis to serve as a more rigorous model of multiple sclerosis through refinement of the experimental design," *Comp Med.*, vol. 59, no. 2, pp. 112-128, Apr.2009.

[4] R. van den Berg, J. D. Laman, M. M. van, R. Q. Hintzen, and C. C. Hoogenraad, "Rotarod motor performance and advanced spinal cord lesion image analysis refine assessment of neurodegeneration in experimental autoimmune encephalomyelitis," *J. Neurosci. Methods*, vol. 262, pp. 66-76, Mar.2016.

[5] M. H. Cameron and J. M. Wagner, "Gait abnormalities in multiple sclerosis: pathogenesis, evaluation, and advances in treatment," *Curr. Neurol. Neurosci. Rep.*, vol. 11, no. 5, pp. 507-515, Oct.2011.

[6] Multiple Sclerosis International Federation, "Atlas of MS 2013," 2013.

[7] I. Loma and R. Heyman, "Multiple sclerosis: pathogenesis and treatment," *Curr. Neuropharmacol.*, vol. 9, no. 3, pp. 409-416, Sept.2011.

[8] A. Compston and A. Coles, "Multiple sclerosis," *Lancet*, vol. 372, no. 9648, pp. 1502-1517, Oct.2008.

[9] M. Diebold and T. Derfuss, "Immunological treatment of multiple sclerosis," *Semin. Hematol.*, vol. 53 Suppl 1, p. S54-S57, Apr.2016.

[10] A. Signori, F. Gallo, F. Bovis, T. N. Di, I. Maietta, and M. P. Sormani, "Long-term impact of interferon or Glatiramer acetate in multiple sclerosis: A systematic review and meta-analysis," *Mult. Scler. Relat Disord.*, vol. 6, pp. 57-63, Mar.2016.

[11] M. P. Sormani and P. Bruzzi, "Can we measure long-term treatment effects in multiple sclerosis?," *Nat. Rev. Neurol.*, vol. 11, no. 3, pp. 176-182, Mar.2015.

[12] T. Arun, V. Tomassini, E. Sbardella, M. B. de Ruiter, L. Matthews, M. I. Leite, R. Gelineau-Morel, A. Cavey, S. Vergo, M. Craner, L. Fugger, A. Rovira, M. Jenkinson, and J. Palace, "Targeting ASIC1 in primary progressive multiple sclerosis: evidence of neuroprotection with amiloride," *Brain*, vol. 136, no. Pt 1, pp. 106-115, Jan.2013.

[13] **E. C. Tallantyre, L. Bo, O. Al-Rawashdeh, T. Owens, C. H. Polman, J. S. Lowe, and N. Evangelou, "Clinico-pathological evidence that axonal loss underlies disability in progressive multiple sclerosis," *Mult. Scler.*, vol. 16, no. 4, pp. 406-411, Apr.2010.**

[14] **A. Coles, "Newer therapies for multiple sclerosis," *Ann. Indian Acad. Neurol.*, vol. 18, no. Suppl 1, p. S30-S34, Sept.2015.**

[15] **R. Milo and E. Kahana, "Multiple sclerosis: geoepidemiology, genetics and the environment," *Autoimmun. Rev.*, vol. 9, no. 5, p. A387-A394, Mar.2010.**

[16] **A. Eloyan, H. Shou, R. T. Shinohara, E. M. Sweeney, M. B. Nebel, J. L. Cuzzocreo, P. A. Calabresi, D. S. Reich, M. A. Lindquist, and C. M. Crainiceanu, "Health effects of lesion localization in multiple sclerosis: spatial registration and confounding adjustment," *PLoS. One.*, vol. 9, no. 9, p. e107263, 2014.**

[17] **L. Steinman and S. S. Zamvil, "How to successfully apply animal studies in experimental allergic encephalomyelitis to research on multiple sclerosis," *Ann. Neurol.*, vol. 60, no. 1, pp. 12-21, July2006.**

[18] **S. Bittner, A. M. Afzali, H. Wiendl, and S. G. Meuth, "Myelin oligodendrocyte glycoprotein (MOG35-55) induced experimental autoimmune encephalomyelitis (EAE) in C57BL/6 mice," *J. Vis. Exp.*, no. 86 2014.**

[19] **V. Brinkmann, M. D. Davis, C. E. Heise, R. Albert, S. Cottens, R. Hof, C. Bruns, E. Prieschl, T. Baumruker, P. Hiestand, C. A. Foster, M. Zollinger, and K. R. Lynch, "The immune modulator FTY720 targets sphingosine 1-phosphate receptors," *J. Biol. Chem.*, vol. 277, no. 24, pp. 21453-21457, June2002.**

[20] **H. M. Vesterinen, E. S. Sena, C. ffrench-Constant, A. Williams, S. Chandran, and M. R. Macleod, "Improving the translational hit of experimental treatments in multiple sclerosis," *Mult. Scler.*, vol. 16, no. 9, pp. 1044-1055, Sept.2010.**

[21] **W. I. McDonald, A. Compston, G. Edan, D. Goodkin, H. P. Hartung, F. D. Lublin, H. F. McFarland, D. W. Paty, C. H. Polman, S. C. Reingold, M. Sandberg-Wollheim, W. Sibley, A. Thompson, S. van den Noort, B. Y. Weinshenker, and J. S. Wolinsky, "Recommended diagnostic criteria for multiple sclerosis: guidelines from the International Panel on the diagnosis of multiple sclerosis," *Ann. Neurol.*, vol. 50, no. 1, pp. 121-127, July2001.**

[22] **J. F. Kurtzke, "Rating neurologic impairment in multiple sclerosis: an expanded disability status scale (EDSS)," *Neurology*, vol. 33, no. 11, pp. 1444-1452, Nov.1983.**

[23] **C. S. Moore, N. Earl, R. Frenette, A. Styhler, J. A. Mancini, D. W. Nicholson, A. L. Hebb, T. Owens, and G. S. Robertson, "Peripheral phosphodiesterase 4 inhibition produced by 4-[2-(3,4-Bis-difluoromethoxyphenyl)-2-[4-(1,1,1,3,3,3-hexafluoro-2-hydroxypropan -2-yl)-phenyl]-ethyl]-3-methylpyridine-1-oxide (L-826,141) prevents experimental autoimmune encephalomyelitis," *J. Pharmacol. Exp. Ther.*, vol. 319, no. 1, pp. 63-72, Oct.2006.**

[24] **C. S. Moore, A. L. Hebb, M. M. Blanchard, C. E. Crocker, P. Liston, R. G. Korneluk, and G. S. Robertson, "Increased X-linked inhibitor of apoptosis protein (XIAP) expression exacerbates experimental autoimmune encephalomyelitis (EAE)," *J. Neuroimmunol.*, vol. 203, no. 1, pp. 79-93, Oct.2008.**

[25] **J. Warford, Q. R. Jones, M. Nichols, V. Sullivan, H. P. Rupasinghe, and G. S. Robertson, "The flavonoid-enriched fraction AF4 suppresses neuroinflammation and promotes restorative gene expression in a mouse model of experimental autoimmune encephalomyelitis," *J. Neuroimmunol.*, vol. 268, no. 1-2, pp. 71-83, Mar.2014.**

[26] **K. K. Fleming, J. A. Bovaird, M. C. Mosier, M. R. Emerson, S. M. LeVine, and J. G. Marquis, "Statistical analysis of data from studies on experimental autoimmune encephalomyelitis," *J. Neuroimmunol.*, vol. 170, no. 1-2, pp. 71-84, Dec.2005.**

[27] **M. Balkaya, J. M. Krober, A. Rex, and M. Endres, "Assessing post-stroke behavior in mouse models of focal ischemia," *J. Cereb. Blood Flow Metab*, vol. 33, no. 3, pp. 330-338, Mar.2013.**

[28] **L. Menalled, B. F. El-Khodor, M. Patry, M. Suarez-Farinas, S. J. Orenstein, B. Zahasky, C. Leahy, V. Wheeler, X. W. Yang, M. MacDonald, A. J. Morton, G. Bates, J. Leeds, L. Park, D. Howland, E. Signer, A. Tobin, and D. Brunner, "Systematic behavioral evaluation of Huntington's disease transgenic and knock-in mouse models," *Neurobiol. Dis.*, vol. 35, no. 3, pp. 319-336, Sept.2009.**

[29] **S. Olivan, A. C. Calvo, A. Rando, M. J. Munoz, P. Zaragoza, and R. Osta, "Comparative study of behavioural tests in the SOD1G93A mouse model of amyotrophic lateral sclerosis," *Exp. Anim*, vol. 64, no. 2, pp. 147-153, 2015.**

[30] **A. Pajoohesh-Ganji, K. R. Byrnes, G. Fatemi, and A. I. Faden, "A combined scoring method to assess behavioral recovery after mouse spinal cord injury," *Neurosci. Res.*, vol. 67, no. 2, pp. 117-125, June2010.**

[31] **T. N. Taylor, J. G. Greene, and G. W. Miller, "Behavioral phenotyping of mouse models of Parkinson's disease," *Behav. Brain Res.*, vol. 211, no. 1, pp. 1-10, July2010.**

[32] **O. Wirths and T. A. Bayer, "Motor impairment in Alzheimer's disease and transgenic Alzheimer's disease mouse models," *Genes Brain Behav.*, vol. 7 Suppl 1, pp. 1-5, Feb.2008.**

[33] **D. M. Basso, "Behavioral testing after spinal cord injury: congruities, complexities, and controversies," *J. Neurotrauma*, vol. 21, no. 4, pp. 395-404, Apr.2004.**

[34] **M. V. Jones, T. T. Nguyen, C. A. Deboy, J. W. Griffin, K. A. Whartenby, D. A. Kerr, and P. A. Calabresi, "Behavioral and pathological outcomes in MOG 35-55 experimental autoimmune encephalomyelitis," *J. Neuroimmunol.*, vol. 199, no. 1-2, pp. 83-93, Aug.2008.**

[35] **S. P. Brooks and S. B. Dunnett, "Tests to assess motor phenotype in mice: a user's guide," *Nat. Rev. Neurosci.*, vol. 10, no. 7, pp. 519-529, July2009.**

[36] **I. Peruga, S. Hartwig, J. Thone, B. Hovemann, R. Gold, G. Juckel, and R. A. Linker, "Inflammation modulates anxiety in an animal model of multiple sclerosis," *Behav. Brain Res.*, vol. 220, no. 1, pp. 20-29, June2011.**

[37] **M. Bohlen, A. Cameron, P. Metten, J. C. Crabbe, and D. Wahlsten, "Calibration of rotational acceleration for the rotarod test of rodent motor coordination," *J. Neurosci. Methods*, vol. 178, no. 1, pp. 10-14, Mar.2009.**

[38] **R. M. Deacon, "Measuring motor coordination in mice," *J. Vis. Exp.*, no. 75, p. e2609, 2013.**

[39] **H. Shiotsuki, K. Yoshimi, Y. Shimo, M. Funayama, Y. Takamatsu, K. Ikeda, R. Takahashi, S. Kitazawa, and N. Hattori, "A rotarod test for evaluation of motor skill learning," *J. Neurosci. Methods*, vol. 189, no. 2, pp. 180-185, June2010.**

[40] **S. Al-Izki, G. Pryce, J. K. O'Neill, C. Butter, G. Giovannoni, S. Amor, and D. Baker, "Practical guide to the induction of relapsing progressive experimental autoimmune encephalomyelitis in the Biozzi ABH mouse," *Mult. Scler. Relat Disord.*, vol. 1, no. 1, pp. 29-38, Jan.2012.**

[41] **C. A. Dayger, J. S. Rosenberg, C. Winkler, S. Foster, E. Witkowski, T. S. Benice, L. S. Sherman, and J. Raber, "Paradoxical effects of apolipoprotein E on cognitive function and clinical progression in mice with experimental autoimmune encephalomyelitis," *Pharmacol. Biochem. Behav.*, vol. 103, no. 4, pp. 860-868, Feb.2013.**

[42] **N. M. de Bruin, K. Schmitz, S. Schiffmann, N. Tafferner, M. Schmidt, H. Jordan, A. Haussler, I. Tegeder, G. Geisslinger, and M. J. Parnham, "Multiple rodent models and behavioral measures reveal unexpected responses to FTY720 and DMF in experimental autoimmune encephalomyelitis," *Behav. Brain Res.*, vol. 300, pp. 160-174, Mar.2016.**

[43] **P. S. Di, E. Merega, M. Lanfranco, S. Casazza, A. Uccelli, and A. Pittaluga, "Acute desipramine restores presynaptic cortical defects in murine experimental autoimmune encephalomyelitis by suppressing central CCL5 overproduction," *Br. J. Pharmacol.*, vol. 171, no. 9, pp. 2457-2467, May2014.**

[44] **A. Gentile, D. Fresegna, M. Federici, A. Musella, F. R. Rizzo, H. Sepman, S. Bullitta, V. F. De, N. Haji, S. Rossi, N. B. Mercuri, A. Usiello, G. Mandolesi, and D. Centonze, "Dopaminergic dysfunction is associated with IL-1beta-dependent mood alterations in experimental autoimmune encephalomyelitis," *Neurobiol. Dis.*, vol. 74, pp. 347-358, Feb.2015.**

[45] **K. Gobel, J. H. Wedell, A. M. Herrmann, L. Wachsmuth, S. Pankratz, S. Bittner, T. Budde, C. Kleinschnitz, C. Faber, H. Wiendl, and S. G. Meuth, "4-Aminopyridine ameliorates mobility but not disease course in an animal model of multiple sclerosis," *Exp. Neurol.*, vol. 248, pp. 62-71, Oct.2013.**

[46] **S. M. Moore, A. J. Khalaj, S. Kumar, Z. Winchester, J. Yoon, T. Yoo, L. Martinez-Torres, N. Yasui, J. A. Katzenellenbogen, and S. K. Tiwari-Woodruff, "Multiple functional therapeutic effects of the estrogen receptor beta agonist indazole-Cl in a mouse model of multiple sclerosis," *Proc. Natl. Acad. Sci. U. S. A*, vol. 111, no. 50, pp. 18061-18066, Dec.2014.**

[47] **T. Musgrave, C. Benson, G. Wong, I. Browne, G. Tenorio, G. Rauw, G. B. Baker, and B. J. Kerr, "The MAO inhibitor phenelzine improves functional outcomes in mice with experimental autoimmune encephalomyelitis (EAE)," *Brain Behav. Immun.*, vol. 25, no. 8, pp. 1677-1688, Nov.2011.**

[48] **S. A. Sands, S. Tsau, T. M. Yankee, B. L. Parker, A. C. Ericsson, and S. M. LeVine, "The effect of omeprazole on the development of experimental autoimmune encephalomyelitis in C57BL/6J and SJL/J mice," *BMC. Res. Notes*, vol. 7, p. 605, 2014.**

[49] **D. F. Preisig, L. Kulic, M. Kruger, F. Wirth, J. McAfoose, C. Spani, P. Gantenbein, R. Derungs, R. M. Nitsch, and T. Welt, "High-speed video gait analysis reveals early and characteristic locomotor phenotypes in mouse models of neurodegenerative movement disorders," *Behav. Brain Res.*, vol. 311, pp. 340-353, May2016.**

[50] **H. Leblond, M. L'Esperance, D. Orsal, and S. Rossignol, "Treadmill locomotion in the intact and spinal mouse," *J. Neurosci.*, vol. 23, no. 36, pp. 11411-11419, Dec.2003.**

[51] **M. Ueno and T. Yamashita, "Kinematic analyses reveal impaired locomotion following injury of the motor cortex in mice," *Exp. Neurol.*, vol. 230, no. 2, pp. 280-290, Aug.2011.**

[52] B. Zorner, L. Filli, M. L. Starkey, R. Gonzenbach, H. Kasper, M. Rothlisberger, M. Bolliger, and M. E. Schwab, "Profiling locomotor recovery: comprehensive quantification of impairments after CNS damage in rodents," *Nat. Methods*, vol. 7, no. 9, pp. 701-708, Sept.2010.

[53] I. Kister, E. Chamot, A. R. Salter, G. R. Cutter, T. E. Bacon, and J. Herbert, "Disability in multiple sclerosis: a reference for patients and clinicians," *Neurology*, vol. 80, no. 11, pp. 1018-1024, Mar.2013.

[54] N. G. Larocca, "Impact of walking impairment in multiple sclerosis: perspectives of patients and care partners," *Patient.*, vol. 4, no. 3, pp. 189-201, 2011.

[55] M. H. Cameron and S. Lord, "Postural control in multiple sclerosis: implications for fall prevention," *Curr. Neurol. Neurosci. Rep.*, vol. 10, no. 5, pp. 407-412, Sept.2010.

[56] X. Liu, D. L. Yao, and H. Webster, "Insulin-like growth factor I treatment reduces clinical deficits and lesion severity in acute demyelinating experimental autoimmune encephalomyelitis," *Mult. Scler.*, vol. 1, no. 1, pp. 2-9, Apr.1995.

[57] D. L. Yao, X. Liu, L. D. Hudson, and H. D. Webster, "Insulin-like growth factor-I given subcutaneously reduces clinical deficits, decreases lesion severity and upregulates synthesis of myelin proteins in experimental autoimmune encephalomyelitis," *Life Sci.*, vol. 58, no. 16, pp. 1301-1306, 1996.

[58] N. M. de Bruin, K. Schmitz, S. Schiffmann, N. Tafferner, M. Schmidt, H. Jordan, A. Haussler, I. Tegeder, G. Geisslinger, and M. J. Parnham, "Multiple rodent models and behavioral measures reveal unexpected responses to FTY720 and DMF in experimental autoimmune encephalomyelitis," *Behav. Brain Res.*, vol. 300, pp. 160-174, Mar.2016.

[59] N. K. Mitra, U. Bindal, H. W. Eng, C. L. Chua, and C. Y. Tan, "Evaluation of locomotor function and microscopic structure of the spinal cord in a mouse model of experimental autoimmune encephalomyelitis following treatment with syngeneic mesenchymal stem cells," *Int. J. Clin. Exp. Pathol.*, vol. 8, no. 10, pp. 12041-12052, 2015.

[60] G. A. Silva, F. Pradella, A. Moraes, A. Farias, L. M. dos Santos, and A. L. de Oliveira, "Impact of pregabalin treatment on synaptic plasticity and glial reactivity during the course of experimental autoimmune encephalomyelitis," *Brain Behav.*, vol. 4, no. 6, pp. 925-935, 2014.

[61] T. Akay, "Long-term measurement of muscle denervation and locomotor behavior in individual wild-type and ALS model mice," *J. Neurophysiol.*, vol. 111, no. 3, pp. 694-703, Feb.2014.

[62] **R. Baker, J. L. McGinley, M. H. Schwartz, S. Beynon, A. Rozumalski, H. K. Graham, and O. Tirosh, "The gait profile score and movement analysis profile," *Gait. Posture.*, vol. 30, no. 3, pp. 265-269, Oct.2009.**

[63] **R. J. Batka, T. J. Brown, K. P. Mcmillan, R. M. Meadows, K. J. Jones, and M. M. Haulcomb, "The need for speed in rodent locomotion analyses," *Anat. Rec. (Hoboken.)*, vol. 297, no. 10, pp. 1839-1864, Oct.2014.**

[64] **C. A. Schneider, W. S. Rasband, and K. W. Eliceiri, "NIH Image to ImageJ: 25 years of image analysis," *Nat. Methods*, vol. 9, no. 7, pp. 671-675, July2012.**

[65] **R Core Team, "R: A language and environment for statistical computing.," Vienna, Austria: R Foundation for Statistical Computing, 2013.**

[66] **J. D. Evans, *Straightforward statistics for the behavioral sciences.* Pacific Grove, California: Brooks/Cole Publishing, 1996.**

[67] **N. K. Mitra, U. Bindal, H. W. Eng, C. L. Chua, and C. Y. Tan, "Evaluation of locomotor function and microscopic structure of the spinal cord in a mouse model of experimental autoimmune encephalomyelitis following treatment with syngeneic mesenchymal stem cells," *Int. J. Clin. Exp. Pathol.*, vol. 8, no. 10, pp. 12041-12052, 2015.**

[68] **K. Chen, J. Liu, P. Assinck, T. Bhatnagar, F. Streijger, Q. Zhu, M. F. Dvorak, B. K. Kwon, W. Tetzlaff, and T. R. Oxland, "Differential Histopathological and Behavioral Outcomes Eight Weeks after Rat Spinal Cord Injury by Contusion, Dislocation, and Distraction Mechanisms," *J. Neurotrauma*, Apr.2016.**

[69] **B. S. Buddeberg, M. Kerschensteiner, D. Merkler, C. Stadelmann, and M. E. Schwab, "Behavioral testing strategies in a localized animal model of multiple sclerosis," *J. Neuroimmunol.*, vol. 153, no. 1-2, pp. 158-170, Aug.2004.**

[70] **M. Kerschensteiner, C. Stadelmann, B. S. Buddeberg, D. Merkler, F. M. Bareyre, D. C. Anthony, C. Linington, W. Bruck, and M. E. Schwab, "Targeting experimental autoimmune encephalomyelitis lesions to a predetermined axonal tract system allows for refined behavioral testing in an animal model of multiple sclerosis," *Am. J. Pathol.*, vol. 164, no. 4, pp. 1455-1469, Apr.2004.**

[71] **M. Kerschensteiner, F. M. Bareyre, B. S. Buddeberg, D. Merkler, C. Stadelmann, W. Bruck, T. Misgeld, and M. E. Schwab, "Remodeling of axonal connections contributes to recovery in an animal model of multiple sclerosis," *J. Exp. Med.*, vol. 200, no. 8, pp. 1027-1038, Oct.2004.**

[72] **E. H. Lakes and K. D. Allen, "Gait analysis methods for rodent models of arthritic disorders: reviews and recommendations," *Osteoarthritis. Cartilage.*, Mar.2016.**

[73] J. R. Broderson, "A retrospective review of lesions associated with the use of Freund's adjuvant," *Lab Anim Sci.*, vol. 39, no. 5, pp. 400-405, Sept.1989.

[74] U. Heilborn, O. G. Berge, L. Arborelius, and E. Brodin, "Spontaneous nociceptive behaviour in female mice with Freund's complete adjuvant- and carrageenan-induced monoarthritis," *Brain Res.*, vol. 1143, pp. 143-149, Apr.2007.

[75] D. Englert and K. Hempel, "Decrease in motor activity - an early symptom in the course of experimental allergic encephalomyelitis (EAE)," *Experientia*, vol. 35, no. 9, pp. 1207-1208, Sept.1979.

[76] T. Takemiya and C. Takeuchi, "Traveled distance is a sensitive and accurate marker of motor dysfunction in a mouse model of multiple sclerosis," *ISRN. Neurosci.*, vol. 2013, p. 170316, 2013.

[77] D. M. Basso, M. S. Beattie, and J. C. Bresnahan, "A sensitive and reliable locomotor rating scale for open field testing in rats," *J. Neurotrauma*, vol. 12, no. 1, pp. 1-21, Feb.1995.

[78] D. M. Basso, L. C. Fisher, A. J. Anderson, L. B. Jakeman, D. M. McTigue, and P. G. Popovich, "Basso Mouse Scale for locomotion detects differences in recovery after spinal cord injury in five common mouse strains," *J. Neurotrauma*, vol. 23, no. 5, pp. 635-659, May2006.

[79] C. Fiore, D. M. Inman, S. Hirose, L. J. Noble, T. Igarashi, and N. A. Compagnone, "Treatment with the neurosteroid dehydroepiandrosterone promotes recovery of motor behavior after moderate contusive spinal cord injury in the mouse," *J. Neurosci. Res.*, vol. 75, no. 3, pp. 391-400, Feb.2004.

[80] E. Takeuchi, Y. Sato, E. Miura, H. Yamaura, M. Yuzaki, and D. Yanagihara, "Characteristics of gait ataxia in delta2 glutamate receptor mutant mice, ho15J," *PLoS. One.*, vol. 7, no. 10, p. e47553, 2012.

[81] M. Pau, G. Coghe, C. Atzeni, F. Corona, G. Pilloni, M. G. Marrosu, E. Cocco, and M. Galli, "Novel characterization of gait impairments in people with multiple sclerosis by means of the gait profile score," *J. Neurol. Sci.*, vol. 345, no. 1-2, pp. 159-163, Oct.2014.

[82] M. L. van der Linden, S. M. Scott, J. E. Hooper, P. Cowan, and T. H. Mercer, "Gait kinematics of people with multiple sclerosis and the acute application of functional electrical stimulation," *Gait. Posture.*, vol. 39, no. 4, pp. 1092-1096, Apr.2014.

[83] S. Kuerten, D. A. Kostova-Bales, L. P. Frenzel, J. T. Tigno, M. Tary-Lehmann, D. N. Angelov, and P. V. Lehmann, "MP4- and MOG:35-55-induced EAE in C57BL/6 mice differentially targets brain, spinal cord and cerebellum," *J. Neuroimmunol.*, vol. 189, no. 1-2, pp. 31-40, Sept.2007.

[84] **F. Barkhof, "The clinico-radiological paradox in multiple sclerosis revisited," *Curr. Opin. Neurol.*, vol. 15, no. 3, pp. 239-245, June2002.**

[85] **T. H. Kim, J. S. Yoon, and J. H. Lee, "The effect of ankle joint muscle strengthening training and static muscle stretching training on stroke patients' C.o.p sway amplitude," *J. Phys. Ther. Sci.*, vol. 25, no. 12, pp. 1613-1616, Dec.2013.**

[86] **G. Di, I, C. N. Maganaris, V. Baltzopoulos, and I. D. Loram, "The proprioceptive and agonist roles of gastrocnemius, soleus and tibialis anterior muscles in maintaining human upright posture," *J. Physiol*, vol. 587, no. Pt 10, pp. 2399-2416, May2009.**

[87] **B. Brouwer and P. Ashby, "Corticospinal projections to lower limb motoneurons in man," *Exp. Brain Res.*, vol. 89, no. 3, pp. 649-654, 1992.**

[88] **C. Hollnagel, M. Brugger, H. Vallery, P. Wolf, V. Dietz, S. Kollias, and R. Riener, "Brain activity during stepping: a novel MRI-compatible device," *J. Neurosci. Methods*, vol. 201, no. 1, pp. 124-130, Sept.2011.**

[89] **D. J. Goble, J. P. Coxon, I. A. Van, M. Geurts, M. Doumas, N. Wenderoth, and S. P. Swinnen, "Brain activity during ankle proprioceptive stimulation predicts balance performance in young and older adults," *J. Neurosci.*, vol. 31, no. 45, pp. 16344-16352, Nov.2011.**

[90] **C. Capaday, B. A. Lavoie, H. Barbeau, C. Schneider, and M. Bonnard, "Studies on the corticospinal control of human walking. I. Responses to focal transcranial magnetic stimulation of the motor cortex," *J. Neurophysiol.*, vol. 81, no. 1, pp. 129-139, Jan.1999.**

[91] **S. Nadeau, D. Gravel, A. B. Arsenault, and D. Bourbonnais, "Plantarflexor weakness as a limiting factor of gait speed in stroke subjects and the compensating role of hip flexors," *Clin. Biomech. (Bristol. , Avon.)*, vol. 14, no. 2, pp. 125-135, Feb.1999.**

[92] **B. Brouwer, J. Bugaresti, and P. Ashby, "Changes in corticospinal facilitation of lower limb spinal motor neurons after spinal cord lesions," *J. Neurol. Neurosurg. Psychiatry*, vol. 55, no. 1, pp. 20-24, Jan.1992.**

[93] **R. W. Motl, "Ambulation and multiple sclerosis," *Phys. Med. Rehabil. Clin. N. Am.*, vol. 24, no. 2, pp. 325-336, May2013.**

[94] **K. J. Kelleher, W. Spence, S. Solomonidis, and D. Apatsidis, "The characterisation of gait patterns of people with multiple sclerosis," *Disabil. Rehabil.*, vol. 32, no. 15, pp. 1242-1250, 2010.**

[95] **M. G. Benedetti, R. Piperno, L. Simoncini, P. Bonato, A. Tonini, and S. Giannini, "Gait abnormalities in minimally impaired multiple sclerosis patients," *Mult. Scler.*, vol. 5, no. 5, pp. 363-368, Oct.1999.**

[96] C. L. Martin, B. A. Phillips, T. J. Kilpatrick, H. Butzkueven, N. Tubridy, E. McDonald, and M. P. Galea, "Gait and balance impairment in early multiple sclerosis in the absence of clinical disability," *Mult. Scler.*, vol. 12, no. 5, pp. 620-628, Oct.2006.